2015 年度博士学位論文

A Brain Informatics-Based Study on Human Cognition, Emotion, and Their Relationship

脳情報学に基づく人間の認知・感情とその相互関係における研究

指導教員　　鍾　寧教授

前橋工科大学大学院

環境・情報工学専攻　博士後期課程

1236502

Yang Yang

楊　陽

審査員

主査　井田　憲一　教授

副査　今村　一之　教授

　　　鍾　寧　　　教授

　　　白尾　智明　教授

　　　関　崇夫　　教授

Acknowledgements

The author would like to express the sincere appreciations to the thesis committee consisting of Professors Kennichi Ida, Kazuyuki Imamura, Ning Zhong, Tomoaki Shirao, and Takao Seki. I am privileged to have such a strong and interdisciplinary committee.

The dissertation has been finished during the last five years. This work could never been done without the kind guidance of my supervisors Professors Zhong and Imamura. Thus, I would like to express my greatest gratitude for their wise advice and encouragements. As a student with the background of psychology, Prof. Zhong led me into the field of engineering and taught me how to think creatively and work effectively. He also demonstrated that the key to success should be greatly attributed to the working attitude, such as the enthusiasm and earnest. His expertise, understanding, guidance and support made it possible for me to work on the cutting-edge researches that were of great interest to me. It was a pleasure working with him. I am highly indebted and thoroughly grateful to Prof. Imamura for his immense interest in my topic of research as well as specialized comments and suggestions. His generous supports enabled me to establish links with other Japanese scholars and academic organizations.

Maebashi Institute of Technology was my academic home for the last years. I am thankful to all members in Zhong's Laboratory, especially Mr. Taihei Kotake, Dr. Shinichi Motomura, and Dr. Muneaki Ohshima who helped me improve my language ability, adapt to the life in Japan, and maintain the laboratorial environment. I would also like to express my special thanks to Dr. Juzhen Dong for her warm supports to many aspects in my life and study.

I would like to thank the teachers and students in the International WIC Institute, Beijing University of Technology, especially to Prof. Shengfu Lu, Dr. Haiyan Zhou, and Dr. Mi Li, who shared their valuable research experiences and discussed with me for several times to handle the technical issues occurred during my study.

My deepest gratitude is owned to my parents and grandparents who raised me and have been giving me continuous encouragements to motivate me to pursue further knowledge. Moreover, owe to my parents' and parents-in-law's understanding, I could focus on my research without being distracted by family trifles.

Finally, and most importantly, I would like to thank my wife Yunfan Li. Her support, encouragement, quiet patience and unwavering love were undeniably the bedrock upon which the past ten years of my life have been built. Her tolerance of my frequent and perennial leaving is a testament of her unyielding devotion and love. Without her support in life and spirit, this thesis could not be finished, either.

Abstract

This dissertation concentrates on the neural substrates underlying the human cognition, emotion, and their interactions. Directed by the systematic methodology of brain informatics (BI), functional magnetic resonance imaging (fMRI) experiments were performed to investigate the information processing of mental arithmetic, self-regulation of aversive emotion, and attention deployment of patients with major depressive disorder (MDD), which were utilized as typical paradigms to study the relationship between cognition and emotion. Four major findings could be concluded: 1) mental addition calculation is naturally automatic while subtraction calculation is complex; 2) both bottom-up suppression and top-down regulation are engaged in the self-recovery from aversive emotion; 3) cognition and emotion influence each other, since some cognitive resources and brain regions are shared by the both brain functions; 4) Abnormal functioning in the joint brain areas is more likely to lead to impairments in both cognitive and emotional functions simultaneously. Our findings demonstrate that human cognition and emotion are not isolated, but compete for cognitive resources for attention and executive control. The present thesis can also be considered as a case study for demonstrating the advances of BI methodology in accelerating progress towards a multi-level understanding of brain structure and function.

Keywords: Brain informatics, systematic investigation, fMRI, mental arithmetic, DCM, emotion regulation, depression.

研究内容要約：
「脳情報学に基づく人間の認知・感情とその相互関係における研究」

　脳情報学は脳を複雑システムとして捉えた上で、人間の脳内情報処理メカニズムと関わる脳ビッグデータの収集・分析・管理・利用を横断的に行う新たな研究領域と考えられる。脳情報学の一つの目標は、まだ明らかになっていない人間の「思考」の基礎にある神経メカニズムの解明である。この目標を達成するために、本研究では「多視点の立場・全過程の研究」という脳情報学の方法論に基づき、機能的磁気共鳴画像法（fMRI）を利用し健常者の基本認知（加減暗算）・感情（調整）機能・それらの機能の相互関係、及びうつ病患者特有の低下した認知と感情機能を研究した。

　　１．暗算時における加減算の認知処理に関する研究
　人間は四則演算を行う時に、それぞれに対して用いるストラテジーが異なる。数字の量を比較して操作をする減算と、記憶に保存された答えを直接取り出す乗算の違いは既に解明されている。しかし、加算と減算の間に本質的な違いが存在するか否かについては、未だ明らかにされていない。そこで、この問題に対して fMRI 実験を実施し解明を試みた。一般線形モデルと機能的連結分析でデータを処理した後の結果、被験者群が減算を行う際に、左脳半球の下前頭回の賦活が加算した時よりも強く見られた。また、この部位は減算時に音韻処理を担当する脳ネットワークとの関連強度を高めることを発見した。更に、動態的因果モデリング（DCM）分析で減算が音韻や運動など複数の認知モジュールの統合を要することを示した。一方で、加算は減算と比べ複雑ではないことが確認できた。減算時は加算時に比べ追加の処理が必要であるため、計算時に更に時間を要し、正答率が低下する。

　　２．嫌悪状態からの感情回復に関する研究
　被験者が嫌悪を感じた後の状態から冷静になるまでの脳の回復過程に注目した。fMRI 実験を利用して、被験者群が嫌悪を感じる画像を見た後と、特に感情に変化を与えない画像を見た後の各反応を比較した結果、脳は異なるストラテジーで自動的に感情の反応を調整することを発見した。感情回復の初期に、脳は左側の尾状核を中心とするネットワークを配置して、受動的な感情抑制を行う。感情回復の後期になると、抑制ネットワークの賦活が次第に弱くなり、反対に背部の注意ネットワークの賦活が次第に強くなる。この遷移の間に被験者が能動的に注意のリソースを配分し、自身の注意を恐怖の体験から遠ざけることが明らかとなった。これらの結果から、無意識下において人間の脳は異なるストラテジーを利用して感情状態を調整でき、感情回復の時にボトムアップの抑制とトップダウンの認知調整の両方が利用されていることが示唆された。また、

この結果を DCM 分析により検証した。

　３．認知と感情の間の相互作用に関する研究

　認知と感情が相互に与える影響を研究するために、注意を逸らすタスクを用意し、被験者の感情に変化が生じた直後に加減暗算を課したときの脳の認知処理過程を調査した。これにより、ネガティブな感情刺激が計算処理に強い妨害を与えることを解明した。ネガティブな画像を見た後の暗算は計算時間が明らかに長く正答率も低下したが、この現象はポジティブな感情刺激では見られなかった。この現象に対し、fMRI の画像分析を用いて検証を行った。ネガティブな状態で計算した場合、認知活動と関連のある前頭－頭頂ネットワークの賦活がさらに強まり、認知と感情の間に交互作用効果が存在することが示唆された。これは、人間の脳にとってネガティブな感情刺激を受けた後に注意の焦点を計算へ移すことがより難しく、計算タスクを完成するために前頭－頭頂ネットワークが大きな労力を要し、賦活が強まった事が原因と考えられる。長い計算時間と低い正答率が焦点遷移の難しさを示している。

　認知と感情の相互作用を多面的に解明するため、低下した認知機能と感情に関する研究も必要である。そこで、うつ病患者に感情に変化を与える画像タスクと暗算の注意を逸らすタスクを用意し、実験の結果を健常者と比較した。「思考が緩慢である」といううつ病患者の症例通り、患者群は健常者より正答率が低い結果となった。この症例の神経メカニズムを解明するために、多様なデータを利用し体系的な調査を行った。初めに、脳の形態データと静止状態の機能データを統合的に分析し、辺縁領域 - 皮質回路と前頭 - 頭頂ネットワークの構造と機能における両方の変化がうつ病の感情調整の機能障害を引き起こすという結果を導いた。次に、タスク状態と静止状態の機能データを統合的に分析し、機能障害の原因となる島皮質が刺激顕著性の検出に影響を与え、正の感情を低下させ、患者の快感の消失を招くという結果を導いた。最後に、拡散テンソル画像法で患者の白質の構造を観察し、前頭葉と辺縁系を繋ぐ鉤状束の異方性から異常を検出した。つまり、前帯状皮質と島皮質の異常な構造と機能が正の感情と負の感情の不適切なコントロールに繋がり、うつ病の「思考が緩慢である」という症例を招くことを発見した。

　複雑な脳科学の問題に対して、単一の実験と分析方法から研究することは困難である。そこで、脳情報学の体系的な方法論に基づき、多面的にこの問題に着手し、人間の認知・感情とその間の関係を調査した。この研究で、認知と感情の機能は独立した存在ではなく、提携する関係であることが判明した。認知と感情を繋ぐ脳の部位が損傷した場合、いずれかの機能を損ねる可能性がある。本研究はうつ病の病理解明のための新しい根拠を示し、診断と治療評価への貢献が期待できる。更に、将来の研究に向けた脳情報学の活用と体系的調査の基盤を構築した。

Contents

List of Figures

List of Tables

Chapter 1

Prologue

1.1 Introduction

One of the greatest scientific challenges is to understand the human brain. Although the flexible use of cognitive and neuroimaging approaches has allowed the measurement of macroscopic features (such as mental states revealed by behavioral experiments), mesoscopic features (such as blood-oxygen-level dependent changes within gray matter and diffusion anisotropy within white matter tracts), and microscopic features (such as the signal transmission among neurons) of the human brain, a comprehensive understanding has not been achieved across the multiple features to unravel the mystery of higher-order brain functions, such as consciousness and intelligence. For decades, some of engineering's best minds have concentrated their thinking skills on how to create thinking machines — computers capable of emulating human intelligence. However, our techniques at this moment are still far away from the target, due to our lack of knowledge about the underpinnings of the intelligence. The major obstacle that hinders our understanding on the brain is the fragmentation of brain researches and the data they bring about. To date, a great body of studies concerning on only single aspects of the brain have been performed separately, while less is known about how different domains of brain higher functions interact, how neural responses vary by cognitive state, and how the data and information across all the brain-related

disciplines can be integrated, such as those from molecular, cellular, synaptic, circuit, systems, computational, and psychological fields. To overcome these challenges, the brain informatics (BI) has been proposed, which regards the brain as a human information processing system and focuses on thinking-centric higher-order functions of the brain with a full perspective ranging from macrostructure to microstructure (Zhong et al., 2011). In the context of brain big data era, BI puts forward a systematic methodology to lead the way how experiments can be designed to investigate the complex brain, how brain big data can be collected by implementation of experiments and integration of shared public data resources, how the collected data can be effectively managed with help of advanced informatics approaches, and how the brain big data can be systematically analyzed, simulated, modeled, and conceptualized. BI aims at disclosing the mechanism of information processing within the human brain, and providing the key technique for implementing such an attempt by offering informatics-enabled brain studies and applications in a social-cyber-physical space, thereby supporting the Web intelligence (WI) (Zhong et al., 2015).

For many years, the relationship between cognition and emotion which are both considered as critical components of human thinking has fascinated plenty of neuroscientists. A traditional notion conceives that there is a considerable degree of functional specialization and that many regions can be conceptualized as either 'affective' or 'cognitive' (Pessoa, 2008). Anatomically, James Papez proposed the well-known Papez circuit connecting the hypothalamus to the limbic lobe as the basis for emotional experiences, which is situated primarily in the subcortical areas involving the hippocampal formation (subiculum), fornix, mammillary bodies, mammillothalamic tract, anterior thalamic nucleus, cingulum, and entorhinal cortex (Shah et al., 2012). By contrast, it has been indicated that the cerebral cortex, apart from the emotion regions, is

the neural foundation underlying the brain cognition, such as memory, attention, perception, awareness, language, and consciousness. Nonetheless, the progress of electrophysiological and neuroimaging studies seems to have brought new enlightenments in the interplays between emotion and cognition. It has been evidenced that emotion and cognition influence each other. As one of examples describing how emotion affects cognition, Shackman et al. (2006) imposed electric shocks randomly on the subjects when they were engaged in N-back tasks for testing their visuospatial and verbal working memory (WM). As a result, the threat-induced anxiety selectively disrupted accuracy of spatial but not verbal WM performance. On the contrary, cognitive strategies mediate the emotion regulation. Kanske et al. (2011) indicated that both distraction (focusing away from an emotional stimulus) and reappraisal (reinterpreting the emotional situation of an emotional stimulus) can be applied to down-regulate emotional intensity, while a stronger decrease in amygdala activity for distraction was observed when compared with reappraisal. Taken together, although the brain regions corresponding to emotion and cognition are spatially distributed, interactions can be found between these two important systems. However, only few neuroscience-based studies have addressed the mechanisms of such intercommunication. Identification of the emotion context is key to furthering our understanding on the core meaning of verbal conversation. Probably, this is one of reasons why human can always grasp the "heart" of ambiguous or incomplete information but machines can't make it.

Therefore, systematic investigations were carried out on human cognition, emotion, and their relationship in this thesis directed by the guidance of BI methodology (see Figure 1.1). Mental arithmetic was selected as the targeted aspect of the wide-ranging human information processing, given that the mental arithmetic is essential to our intact social lives and that it involves phonological, semantic, and syntactic processes that are

similar to the high-level language peculiar to human alone. Chapters about emotion concentrate on the self-regulation of aversive emotion on which few studies have been implemented before. Finally, this thesis concerns on the interplays among mental arithmetic, emotional responses, and the major depressive disorder (MDD) that serves as counterevidence for revealing impaired cognition and emotion functions. Although works depicted in this thesis represent only a small part of BI researches, it can be considered as a case study for demonstrating the advances of BI methodology in accelerating progress towards a multi-level understanding of brain structure and function.
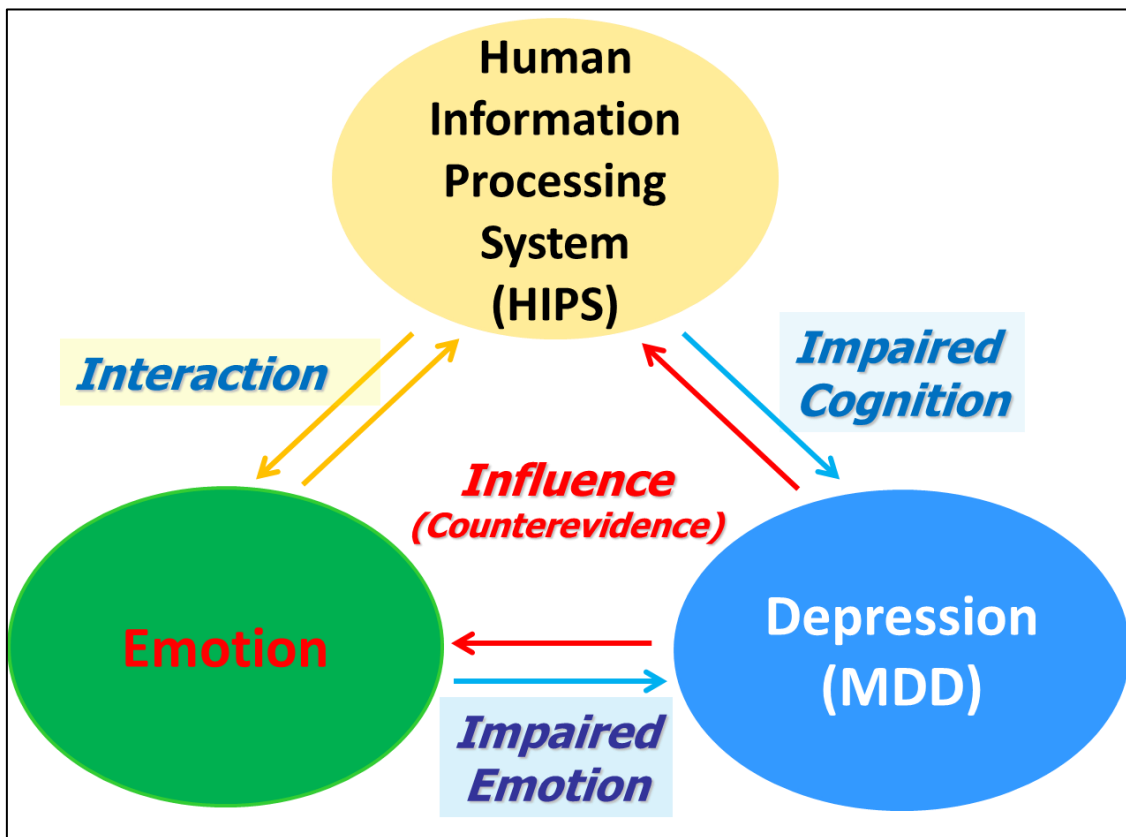
Fig. 1.1: Main contents of this thesis. Systematic investigations were carried out on human cognition, emotion, and their relationship in this thesis directed by the guidance of BI methodology.

1.2 Organization of the Thesis

The main contents of this thesis consist of 7 chapters that are organized as shown in Figure 1.2.
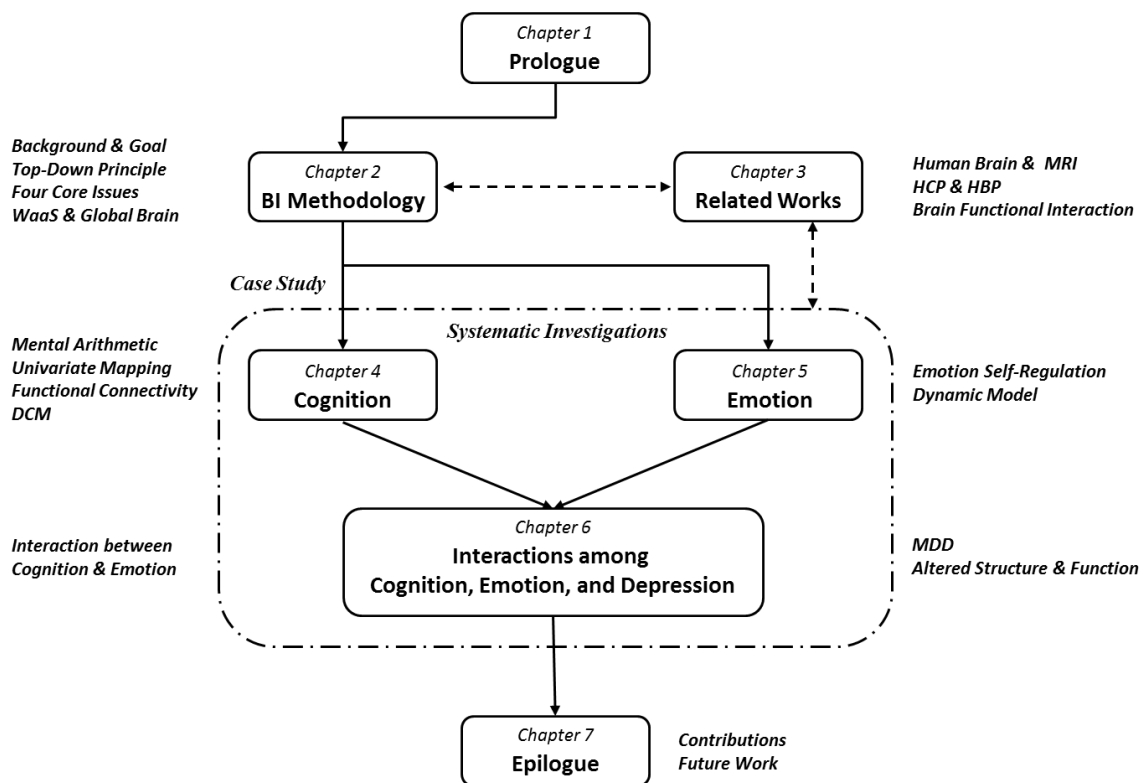
Fig. 1.2: Organization of this thesis. This thesis consists of 7 major chapters.

Chapter 2 describes the BI methodology: its background and goal, top-down principle for cognitive neuroscience research, four core issues, and an overview about the WaaS and Global Brain which serve as a global platform supporting the whole systematic BI research process and its real-world applications.

Chapter 3 introduces related works, including some basic information about the human brain researches and magnetic resonance imaging (MRI) that was employed as

the main approach in this thesis; some information and new progress of the Human Connectome Project (HCP) and the Human Brain Project (HBP); and an overview about cutting-edge studies on the brain functional interaction based on big data.

Chapter 4 elaborates the neural substrates underlying overlaps and differences between mental addition and subtraction processes by using univariate mapping, functional connectivity analysis, and dynamic causal modeling analysis (DCM), respectively.

Chapter 5 focuses on the self-regulation of aversive emotion to investigate the emotion regulation processes underlying the natural recovery period, and proposes a model to explain the dynamic neural activity involved in the regulatory processing.

Chapter 6 delineates interplays between cognition and emotion by using distraction paradigm that contains mental arithmetic tasks and viewing affective pictures. This chapter also describes the systematic investigations on the MDD by combining structural MRI, resting-state MRI, on-task MRI, and diffusion MRI.

Finally, Chapter 7 concludes this thesis. It discusses contributions and some topics for future researches.

<div align="right">**Chapter 2**</div>

The Brain Informatics Methodology

This chapter presents the brain informatics (BI) methodology. The first section gives its background and goal. The second section describes its top-down principle applied in the field of cognitive neuroscience. The third section concerns on its four core issues. Finally, the fourth section outlines an overview about the WaaS and Global Brain which serve as a global platform supporting the whole systematic brain informatics research process and its real-world applications.

2.1   Background and Goal

Brain is the command center and the most complex part of the human body. For centuries, scientists and philosophers have been fascinated by the brain, but for long they viewed this complex system as nearly incomprehensible. However, scientists have learned more about the brain in the last few decades because of the accelerating pace of research in neurological science and the development of new techniques. Histological, neuroimaging, electrophysiological, and behavioral experiments have yielded a great body of results that facilitate our holistic understanding on the brain from microscopic to macroscopic levels. The brain-inspired investigations brought together researchers and practitioners from diverse fields, not only confined in neuroscience and medical fields, but extended to computer science, information technology, AI, Web intelligence,

cognitive science, life science, economics, data mining, data and knowledge science, intelligent agent technology, human computer interaction, complex systems, and system science. Converged interests in the human brain have hastened new kinds of BI methods and global research communities to develop a platform on the intelligent Web and knowledge grids that enable high-speed, distributed, large-scale analysis and computations and radically new ways of data and knowledge sharing (Zhong et al., 2011).

BI is an emerging interdisciplinary and multidisciplinary research field that focuses on studying the mechanisms underlying the human information processing system (HIPS) (Zhong et al., 2011). BI studies the thinking-centric higher-order cognitive functions of the brain, which covers areas such as attention, emotion, memory, language, calculation, heuristic search, reasoning, planning, decision making, problem solving, learning, discovery, creativity, and so forth. BI also focuses on the overall production of the brain big data that are generated when the brain is explored, ranging from experimental design, data collection, to data analysis, management, and utilization. One goal of BI researches is to develop and demonstrate a systematic approach to an integrated understanding of multiple scales of working principles about the brain by means of experimental, computational, and cognitive neuroscience studies, as well as advanced Web-intelligence-centric information technologies. Another goal of BI is to promote new forms of collaborative and interdisciplinary work to contribute to a clearer understanding of the brain. "Brain big data computing" can be summarized as the core conception of BI with double meanings. On one hand, the BI-based empirical studies, such as those based on functional magnetic resonance imaging (fMRI), electroencephalography (EEG), and magnetoencephalography (MEG), shed light on neural mechanisms underlying the information processing (computing) inside the brain

which is driven by various external inputs (stimuli), and offer new insights into the development of human-level intelligence on the wisdom Web and knowledge grids. On the other hand, human brain functions are modeled and conceptualized (computing) based on the notions of information processing systems. Informatics-enabled methods contribute to the computation of brain big data, covering data analysis, curation, mining, and use. Web intelligence-centric information technologies are applied to support brain science studies. For instance, the wisdom Web and knowledge grids enable high-speed, large-scale analysis, simulation, and computation as well as new ways of sharing research data and scientific discoveries.

BI highlights three major aspects that lead different ways to study traditional cognitive science, neuroscience, and AI.

- **Systematic investigations for complex brain science problems**

Understanding the human brain is one of the greatest challenges, since the human brain represents the most complex structure which is capable of generating the kind of higher consciousness and cognition associated with human ingenuity. Moreover, the adult human brain has 86 billion neurons engaging in processing and transmitting information through electrical and chemical signals within brain, and each neuron has between 1000 to 10000 synapses that result in 125 trillion synapses in the cerebral cortex alone (Herculano-Houzel, 2012). The complexity of brain has triggered comprehensive studies with separate concerns on distinct aspects of the brain, such as the morphology, function, connectivity, neuron, and gene. Most of those studies are implemented alone, less attention has been paid on the integration of multiple aspects and relationship between different research objects. In this context, BI proposes a systematic frame for investigating complex brain science problems that is characterized by four features: (1) full scale perspective; (2) multi-modal measurements; (3) whole

process of BI data circle; (4) global brain data resources.

A full scale perspective indicates a holistic consideration about the brain-related researches that advocates an integration of wide-ranging investigations from macro-, meso-, and micro-scales (see Figure 2.1). Firstly, the macro-scale researches examine the behavioral responses to stimuli (i.e., accuracy and reaction time) of human subjects by using cognitive experimental paradigms. Furthermore, other non-physiological information about the subjects is regarded as macro-scale data as well, such as the demographic information of subjects, scores of psychological and mental questionnaires, etc. Macro-scale researches explore the hidden states of human mind indirectly via external phenomena. Secondly, the meso-scale studies emphasize the physiological, electrophysiological, hemodynamic, and endocrine monitoring indicators of the whole brain or some brain regions of interest. Although the importance of structural data of the brain (e.g., voxel-based morphology, white matter tracts) is also stressed, BI puts more emphasis on the brain functions, especially higher cognitive functions presented during both resting-state (task-free) and task-states. The meso-scale studies are dedicated to revealing neural mechanisms of the brain to interpret the external behaviors. Thirdly, the micro-scale studies concentrate on the infrastructural units underlying the brain structure and functions, namely, neuron, synapse, and genome. Studies at this level adopt cellular and molecular approaches to disclose the basic principles of how the brain basic functions proceed. BI does not compete with on-going neuroscience researches, but adds a complementary new strategy to achieve a unified, multi-level understanding of the human brain by integrating multidimensional data. The ultimate objective of brain-centered investigations is to establish integrative, quantitative, and predictive theories of brain structure and function. However, it is difficult to obtain the overview of brain if researches only capture the brain's capabilities but do not show how

the parts of the brain work together. Thus, in the frame of BI, a unified brain atlas, such as the atlas with Montreal Neurological Institute (MNI) coordinates, can provide a reference for building connections between anatomical brain regions and biophysical features of each region observed from different scales.

The explosive growth in the development and use of noninvasive neuroimaging and electrophysiological technologies accelerates the research on human brain under normal and pathological conditions. Multi-modal measurements, using MRI, positron emission tomography (PET), EEG/MEG, eye-tracking, and so forth, have showed the great advantage in visualization and analysis of the brain function and structure in unprecedented detail and transformed the way how studies are conducted on the nervous system under normal and pathological conditions (Kikinis et al., 2014). Multi-modal approaches advances the neuroscience research by overcoming the limits of individual measuring modalities and by identifying the associations of findings from different measuring sources (Liu et al., 2015a). For instance, fMRI combined with EEG enhances the spatiotemporal resolution that cannot be achieved by the single modality alone; joint analyses using the data provided by PET/CT and PET/MRI contributes to the combination of brain structural and functional images. Furthermore, multi-modal approaches can also cross-validate findings from different sources and identify associations and patterns, e.g., causality of brain activity can be deduced by linking dynamics in different imaging readings. Nevertheless, multi-modal neuroimaging computing is a very challenging task due to large inter-modality variations in spatiotemporal resolution, and biophysical/biochemical mechanism. Compared to single modality computing, it requires more sophisticated bias correction, co-registration, segmentation, feature extraction, pattern analysis, and visualization (Liu et al., 2015b). BI proposes a solution which solves these problems by integrating the heterogeneous

data at the metadata level rather than the raw data level (see Figure 2.2). Provenance, which refers to the sources of information, is crucial to making determinations about how to integrate diverse information sources in Semantic Web techniques (Simmhan et al., 2005). By using the BI Provenances, the brain big data center is able to achieve the hybrid upon the heterogeneous data after the somatization.
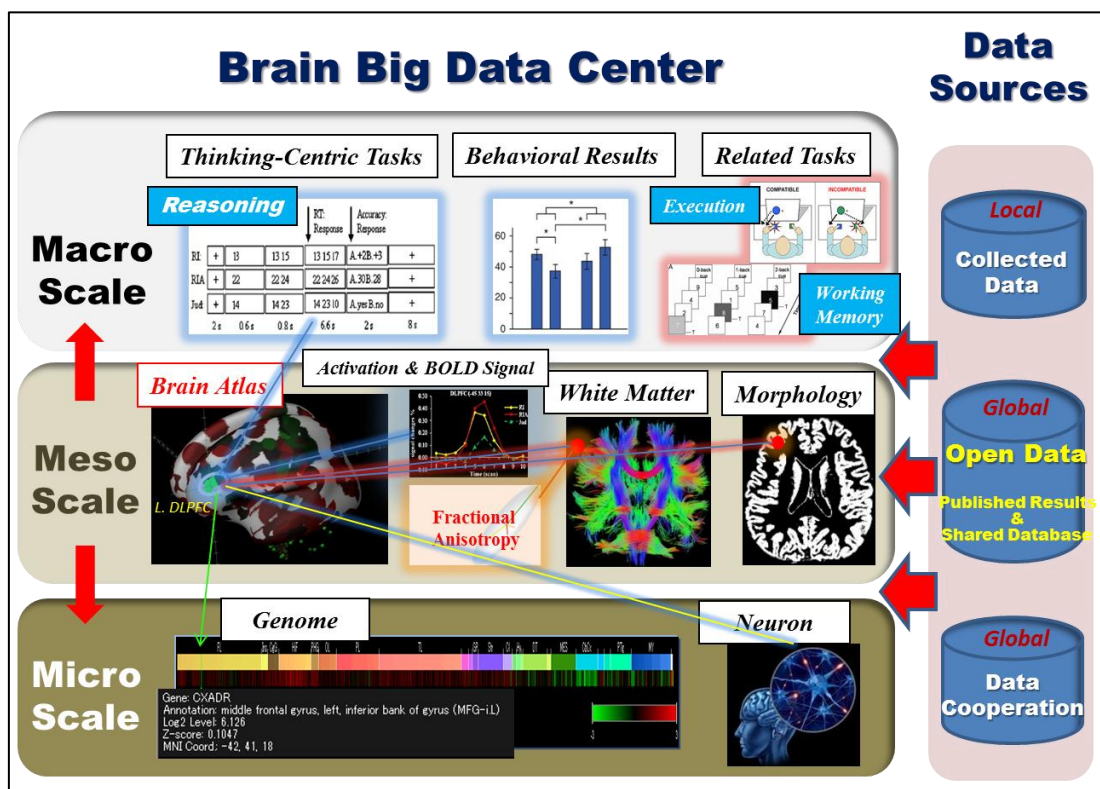
Fig. 2.1: Illustration of brain big data center with full scale data. In the brain big data center, a unified brain atlas (such as the MNI atlas) can provide a reference for building connections between anatomical brain regions and biophysical features of each region observed from different scales. The macro-scale researches explore the hidden states of human mind indirectly via external phenomena. The meso-scale studies emphasize the physiological, electrophysiological, hemodynamic, and endocrine monitoring indicators of the whole brain or some brain regions of interest. The micro-scale studies concentrate on the infrastructural units underlying the brain structure and functions, namely, neuron, synapse, and genome.
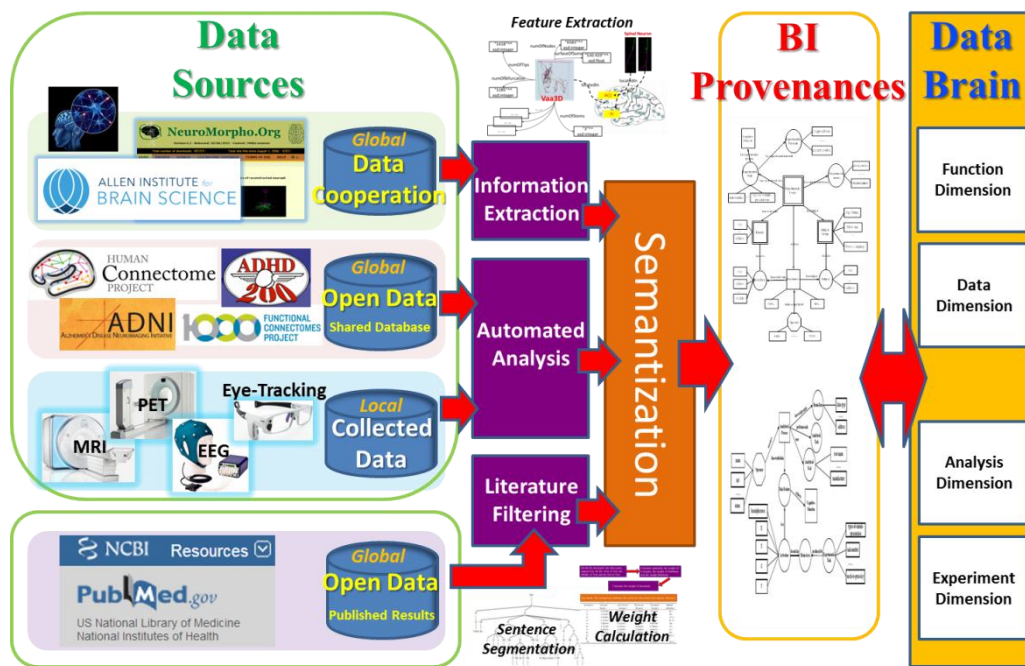
Fig. 2.2: A framework of the BI global data center. BI brain big data center merges global brain data resources, including open data shared by public database, data from cooperative partners, and data collected locally. By using the BI Provenances, the brain big data center is able to achieve the hybrid upon the heterogeneous data after the somatization.

BI researchers use informatics to support brain science studies and attempt to capture new forms of collaborative and interdisciplinary work. The whole BI data process includes measuring, collecting, modeling, transforming, managing, mining, interpreting, and explaining multiple forms of brain data obtained from various sources. During these stages, brain data are processed through a data-cycle system that extracts core values of the data in a hierarchy form to meet needs for different purposes—going through the BI data, information, knowledge, wisdom cycle (or BI data cycle for short)—from the expert-driven and state-of-the-art process to the normative and propagable one (Zhong et al., 2011; Zhong and Motomura, 2009). Systematic BI study produces and absorbs various original data, deriving data and data features, which include a large number of unstructured data, especially multi-modular data. For effectively managing, sharing and

utilizing these data, a transformation from raw data to various metadata is needed. Aiming at different purposes of data sharing and data utilization, the metadata includes different contents. The metadata describing the origin and subsequent processing of biophysical data is often referred to as "provenance" (Simmhan et al., 2005), which can be regarded as a kind of information. Prior knowledge-based four ontological dimensions and their own domain ontologies form a knowledge-base for constructing BI provenances (see Figure 2.2). Thus, these four dimensions can be connected by the relations among dimensions to provide holistic conceptual schemata for various BI provenances. In turn, the newly transformed BI provenances generate new knowledge derived from semantic reasoning and computation to supplement and update the knowledge-base. The evolving knowledge-base provides users the wisdom service, which means the right service, for the right object, at the right time, and in the right context (Zhong et al., 2011). Finally, new data will be produced when users utilize the wisdom service from the BI brain big data center, and become one part of the new round of data cycle.

As shown in Figure 2.2, the BI brain big data center merges global brain data resources. Using biophysical open data shared by public database is an effective way to improve the limited reliability in individual studies on the human brain with small samples caused by the costly acquisition of experimental data. In the last decade, major advances have been made in the availability of shared neuroimaging data, such that there are more than 8,000 shared MRI data sets available online (Poldrack and Gorgolewski, 2014). These data are potential to maximize the contribution of research subjects and enable the availability of large-scale organization on brain big data to get new discoveries hidden in separate data sets. However, existing biophysical databases are almost domain-specific and with particular concerns to construct their datasets. For

instance, the Alzheimer's Disease Neuroimaging Initiative (ADNI, http://adni.loni.usc.edu/) is dedicated to sharing data of patients with Alzheimer's Disease (AD) to facilitate researches on the degenerative disease; The Human Connectome Project (http://www.humanconnectomeproject.org/) is working on typical patterns of structural and functional connectivity in the healthy human brain; the 1000 Functional Connectomes Project (http://fcon_1000.projects.nitrc.org/) focuses only on the resting-state fMRI data. Hence, an informatics-enabled platform, i.e, the BI brain big data center is needed to integrate the data across databases. Nonetheless, the BI brain big data center does not redistribute the collected open data, but provides new information and knowledge obtained via automated analysis on the big data from available databases. On the other hand, although a mass of open data can be acquired, the implementation of BI-based experiments is still necessary. The data collected locally help make up the absent areas that the shared open data failed to cover. More importantly, the local experiments are able to meet the full scale and multi-modular requirements of BI. For example, structural MRI, resting-state functional MRI, task-state functional MRI, and diffusion MRI data can be obtained for each patient of the cohorts with depressive disorder, to corroborate results from different viewpoints (see Chapter 6). Finally, extracting results in published papers is another way to enhance the BI Provenances. The extracted contents of papers are able to support the meta-analysis which has been considered as a powerful method for displaying the common truth behind all conceptually similar studies. By combining the natural language processing (NLP) and semantic web techniques, the BI brain big data center seeks to get the results of papers that most interest users and provide personalized recommendation systems focusing on user preferences to relieve the information overload occurred when researchers retrieve academic information from the Internet.

- **New information technologies for systematic brain science studies**

A systematic BI study cannot be realized using only a traditional expert-driven approach. A powerful brain data center needs to be developed on the Wisdom Web and knowledge grids as the global research platform to support the whole systematic BI research process (Zhong et al., 2011; Zhong and Chen, 2012). Various IT technologies have been applied to brain science studies. Presently, many brain databases have been constructed to effectively store and share multiple levels of brain data. Some distributed analytical platforms of brain data also support the integration of analytical methods. However, these existing information systems cannot effectively support the systematic human brain data analysis needed for BI. These brain databases still require extensive knowledge from investigators because they mainly focus on the description of experiments and data processing, neglecting the relationships among different experiments and data processing. Their data mainly comes from isolated experiments and thus is difficult to describe synthetically. Using those distributed analytical platforms, an expert-driven approach is still required because those analytical platforms mainly focus on the description and performance of analytical work flows. Hence, BI needs to develop a new approach for systematic brain data analysis by using advanced IT technologies (Zhong et al., 2011; Zhong and Chen, 2012).

Researchers have developed expert tools such as the Brain Vision Analyzer, MEDx/SPM, NIS, and AFNI with statistical parametric mapping for cleaning, normalizing, and visualizing event-related potential (ERP)/ EEG and fMRI/DTI data, respectively. They have also studied how to analyze and understand ERP and fMRI data using data mining and statistical learning techniques. To understand human information processing principles and mechanisms relating to higher cognitive functions such as problem solving, reasoning, and learning, as well as clinical diagnosis and pathology of

complex human brain and mind related diseases, we must develop new brain data mining techniques based on the BI methodology. The human brain is too complex for a single data mining algorithm. Agent-enriched brain data mining is thus a key BI methodology for multi-aspect data analysis in multiple data obtained by cognitive experiments, clinical diagnosis, and e-health (Zhong and Motomura, 2009).

- **BI studies based on Web intelligence research needs**

To develop Web-based problem solving and decision making as well as knowledge discovery systems with human-level capabilities, we need to better understand how human beings do complex adaptive, distributed problem solving and reasoning. We also need to understand how intelligence evolves for individuals and societies, over time and place. Ignoring what goes on in the human brain and instead focusing on behavior has been a large impediment to understand complex human adaptive, distributed problem solving, and reasoning. As a result, the relationships between classical problem solving and reasoning and biologically plausible problem solving and reasoning need to be defined and/or elaborated (Zhong et al., 2007c). Current Web intelligence research can be extended from Wisdom Web to Wisdom Web of Things (W2T) (Zhong et al., 2002; Zhong et al., 2007b), which is a novel vision for computing and intelligence in the post-WWW era recently put forward by a group of leading researchers in the Web intelligence, ubiquitous intelligence, BI, and cyber individual fields (Zhong et al., 2013). The W2T is an extension of the wisdom Web in the IoT/WoT (Internet/Web of Things) age. "Wisdom" means that each thing in the IoT/WoT can be aware of both itself and others to provide the right service, for the right object, at the right time, and in the right context. The basic observation is that a new world, called the hyper world, is emerging by coupling and empowering humans in the social world, information and computers in the cyber world, and things in the physical world. There are four fundamental issues for

W2T to address: "*How do we realize the harmonious symbiosis of humans, Web (information), and things in an emerging hyper world? How do we implement the data cycle system as a practical way to realize the harmonious symbiosis of humans, Web (information), and things in the hyper world? How do we holistically investigate intelligence in the hyper world? How do we unify studies of humans, networks, and information granularity in the hyper world?*" A new holistic intelligence methodology can be developed by integrating Web intelligence, ubiquitous intelligence, BI, and cyber-individuals in order to realize the harmonious symbiosis of humans, computers, and things in the hyper world (Zhong et al., 2013).

2.2 Top-Down Principle Applied in Cognitive Neuroscience

To understand the brain, we have to know what the brain does: its high level emergent activities. BI is interested in the full scale data of human brain, covering the field of brain function, anatomy, neuron, even the proteins (see Figure 2.3). Investigation on the detailed mechanics is helpful to enlarge our understanding on the human higher cognitions and intelligence. For instance, we want to understand how a genetic mutation or the wrong positioning of a protein in a cell affects behavior; how a drug acting on a specific molecule can produce changes in cognition. For this, we need multi-scale models detailed enough to represent mutations and the positioning of molecules. Although remarkable progresses have been made in recent years in the field of neuroscience, e.g., the mouse brain connectome has been mapped (Oh et al., 2014) and the genome-wide maps of adult human brain has been generated (Hawrylycz et al., 2012), a huge gap still exist between our existing knowledge about the animal's brain or the infrastructure of human brain and our ultimate goal about the brain that seeks the

complete comprehension of the human consciousness and intelligence. Therefore, BI proposes a top-down principle which insists the priority of direct investigations on the highest order — human information processing system (i.e., the meso-scale of the brain) when conducting the full scale neurological studies, to promptly apply the findings of thinking-centric investigations in enlightening the development of human-level intelligence on the wisdom Web and knowledge grids. Meanwhile, the macro- and micro-scale studies proceed as well. BI aims to bring both high-level and low-level functions of the brain together, by making it finally possible to understand basic principles of cognition, together with the underlying mechanics. At the same time, the multi-scale modeling approach will help settle historical arguments about the level of biological detail necessary to explain specific cognitive capabilities.
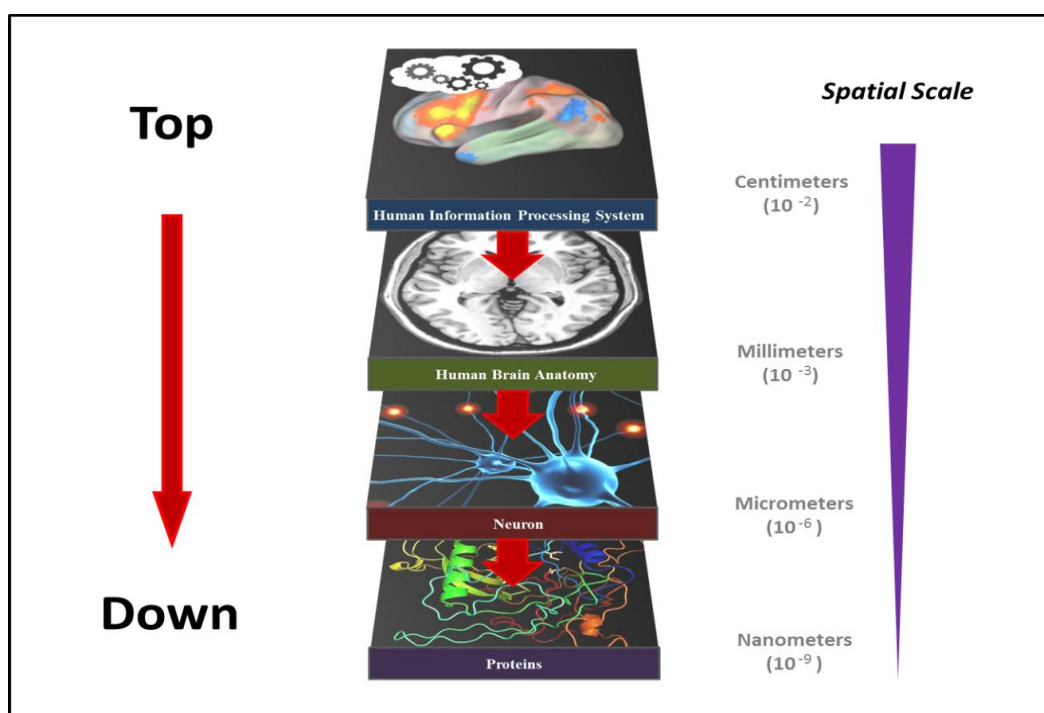
Fig. 2.3: Illustration of BI top-down research principle. BI is interested in the full scale data of human brain, covering the field of brain function, anatomy, neuron, even the proteins. Meanwhile, BI advocates the priority of study on the human information processing system.
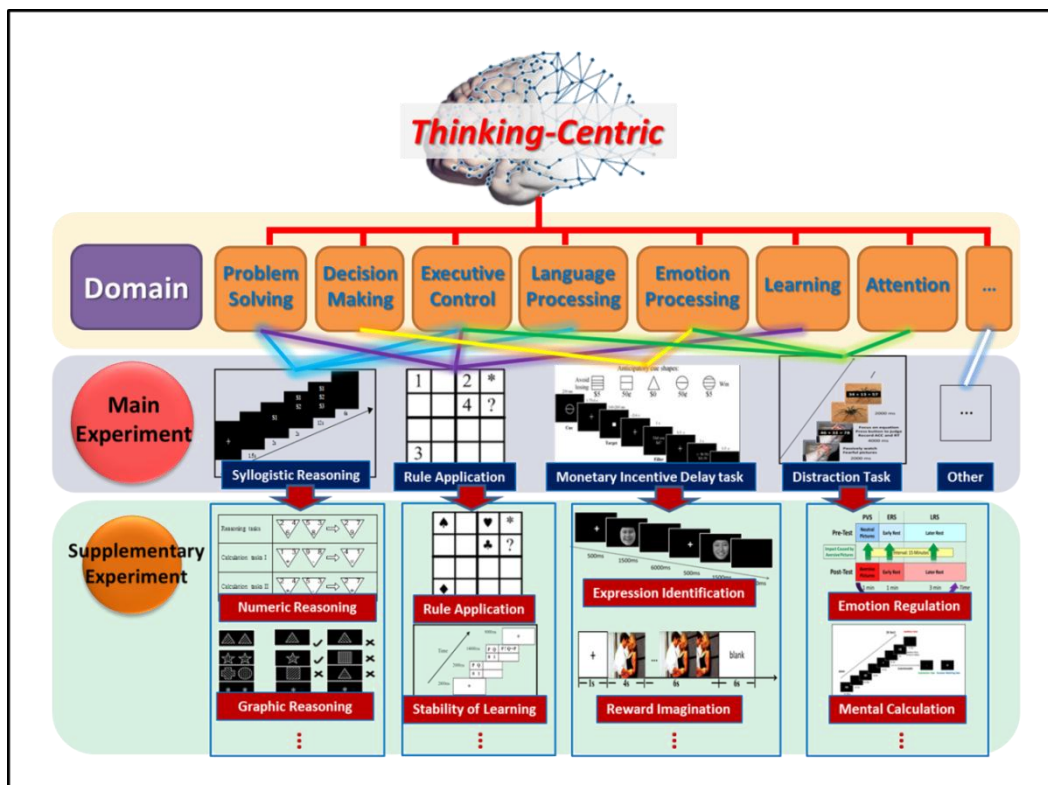
Fig. 2.4: Illustration of thinking-centric experimental design. BI instructs a coarse-to-fine investigation on the thinking-centric brain functions based on top-down principle.

In order to make clear the human information processing system, the top-down principle also instructs the implementation of thinking-centric experiments (see Figure 2.4). The thinking-centric experiments can be carried out based on distinct domains of cognitive functions, such as problem solving, decision making, executive control, language processing, emotion processing, learning, attention, etc., and then finally realize a complete coverage of all higher-order brain functions. Under domains, some classic experimental paradigms are utilized as main experiments which play critical roles in the preliminary exploration of the validity and limitations of each paradigm, as well as getting inspirations for indicating the directions how the subsequent experiments can be designed to be specific enough to induce the brain activity of interest and acquire

more possible scientific values. After the main experiments, inspiring results prompt following experiments which are called supplementary experiments with modified designs based on the classic ones can be performed to fulfill the more precise research objectives. Taken together, the top-down principle of BI instructs a coarse-to-fine strategy to conduct the thinking-centric investigations. The merit of doing this is that the schematized experimental designs make it easier to organize and integrate data and results from different experiments. Because of the top-down consideration, the subsequent experiments serve as supports and extensions to the preceding experiments. Bottom-up strategy is prone to give rise to unstructured datasets which are weak in corroborating each other. Therefore, when the ultimate goal is to achieve a complete view of all higher cognitive functions as BI aims, a top-down modeling approach will be more effective and high-efficiency.

2.3   Four Core Issues of BI

The complexity of brain science determines that BI is systematic. That is, BI adopts a systematic methodology to investigate human information processing mechanisms, which includes four core issues as follows.

(1) Systematic investigations of complex brain science problems.

Besides the full scale and multi-modular investigations of thinking-centric complex brain science problems, BI also concerns on different cohorts of human subjects, including healthy ones as well as the diseased ones (see Figure 2.5). Brain big data indicates the large scale and complexity of the brain-related data sets. However, this term means more than a large quantity. Only accumulation of monotonous data does not contribute to expanding our understanding on the data. The feature of variety of big data,

compared with the volume, is more likely to enable a different view on the data and allow us to learn something new. In a similar way, studies on subjects with brain injuries and mental disorders are effective to show the consequences if certain brain functions are lost or impaired, to explore and validate effects that the monotonous data are inadequate. To increase the variety of brain big data, the systematic studies should give thought to subjects with different genders, ages, health states, education backgrounds, and so forth.
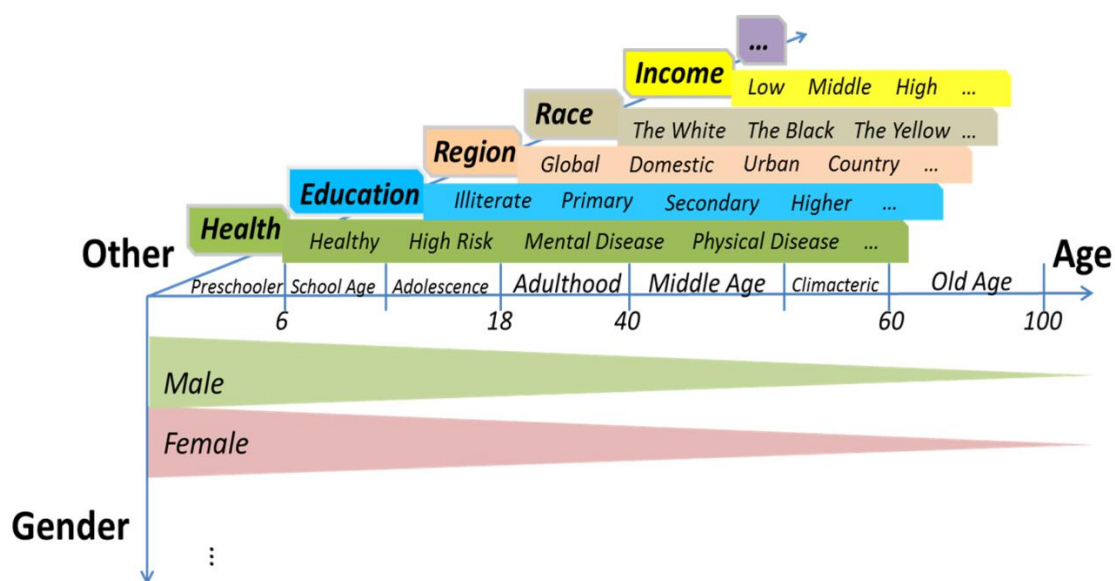
Fig. 2.5: Systematic investigations with different types of subjects. The feature of variety of big data is more likely to further our understanding on the data. Thus, systematic studies should give thought to subjects with different genders, ages, health states, education backgrounds, and so forth.

(2) Systematic design of cognitive experiments.

Besides the top-down principle for constructing the intact brain big data sets, BI asks for a systematic consideration on the design of single experiment as well. To reduce the cost for conducting the experiments and maximize each subject's contribution, BI investigations collect as many as possible data for each time. For instance, it is necessary to involve behavior assessment, structural images, and functional images

during the implementation of fMRI experiment for each time (see Figure 2.6). Functional image is the primary target of the data collection. The underlying neural correlates of the "thinking" in which the subject is engaged can be exhibited by the well-designed cognitive tasks. Meanwhile, the resting-state fMRI (rs-fMRI) has been pervasively employed to investigate the spontaneous neural fluctuations of human brain in the past few years. It has been suggested that spatial patterns and nodal graph properties in the major brain functional networks, e.g., the default mode network (DMN), might vary across the rest period before an on-task state, the on-task state, and the rest period after the on-task state (Wang et al., 2012). Thus, fMRI data over three sequential periods are measured as the routine, including pre-task resting, task-on with active and passive tasks, and post-task resting. Behavioral assessment displays the behavioral responses of subjects which provide the explicit reference for interpreting causality between internal underpinnings and external expressions. Structural images for each subject taken in fMRI experiments consist of a T1 weighted 3D image taken by the magnetization prepared rapid gradient echo (MPRAGE) sequence and a diffusion image based on diffusion tensor imaging (DTI) technique. The T1 image is supplied as a reference for the co-registration of the local structural space and the functional images. Another use of T1 image is to enable the voxel-based morphological (VBM) analysis which is reliable to uncover the structural alterations in the brains of patients with psychiatric disorders (Ashburner and Friston, 2000). In brief, the collection of all types of available data in the fMRI experiments (especially the experiments with patients) allows the multi-angle mining of valuable information to explain the complex brain activities.

(3) Systematic human brain data management.

The development of brain science has led to a vast increase of brain data. To meet

requirements of a systematic methodology of BI, a new conceptual model of brain data was proposed, namely Data-Brain, which explicitly represents various relationships among multiple human brain data sources, with respect to all major aspects and capabilities of human information processing systems (HIPS) (Zhong and Chen, 2012). A multi-dimension framework and a BI methodology based ontological modeling approach have been developed to implement a Data-Brain (see Figure 2.7). The Data-Brain, Data-Brain based BI provenances, and heterogeneous brain data can be used to construct a Data-Brain based brain data center which provides a global framework to integrate data, information and knowledge coming from the whole research process for systematic BI study. Such a Data-Brain modeling approach represents a radically new way for domain-driven conceptual modeling of brain data, which models a whole process of systematically investigating human information processing mechanisms.
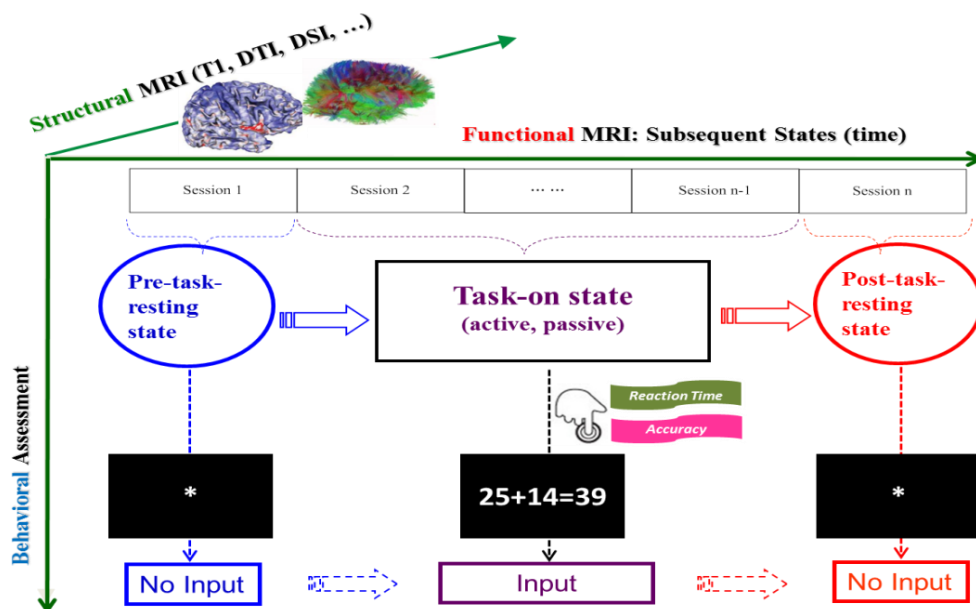
Fig. 2.6: Systematic consideration on the design of single fMRI experiment. It is necessary to involve behavior assessment, structural images, and functional images during the implementation of fMRI experiment for each time.
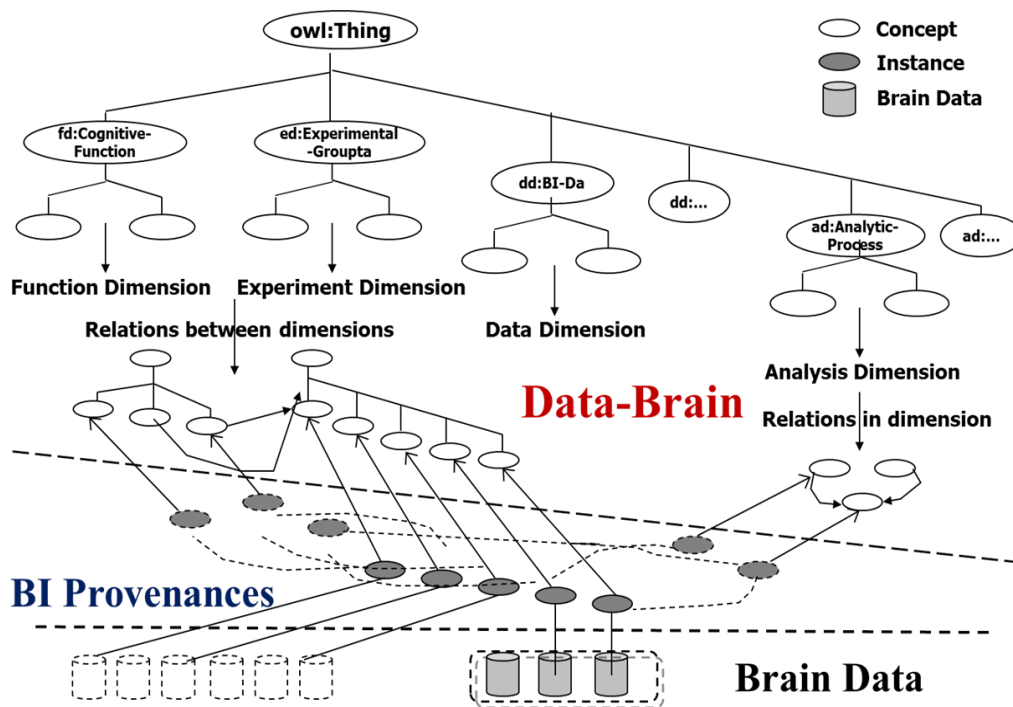
Fig. 2.7: Illustration of the Data-Brain. The Data-Brain that is a conceptual model of brain data provides a global framework to integrate data, information and knowledge coming from the whole research process for systematic BI study.

(4) Systematic human brain data analysis and simulation.

With respect to the human brain, recent neuroimaging techniques, including fMRI, EEG, and MEG, now allow us to probe the brain at unprecedentedly high temporal or spatial resolution without the use of invasive techniques. Multiple advanced computational methods are used to investigate and solve algorithmic image computing problems in basic and applied neuroscience. Some common grounds can be found across the data analyzing techniques: statistical analysis of neuroimages is commonly approached with intragroup or intergroup comparisons made by repeated application of univariate or multivariate tests performed on the global brain or set of the regions of interest sampled in the acquired images (Turkheimer et al., 2000); standard group analyses of fMRI data rely on spatial and temporal averaging of individuals. However, particular approaches are also necessary to refine characteristic information from each

modality of data. The heterogeneity of brain big data sources determines the complexity in the choice of suitable analyzing approaches. BI has proposed a frame of analysis for the systematic purpose. Taking the analysis of fMRI data as an example (see Figure 2.8), behavioral data, structural data, resting-state functional data, and on-task functional data are acquired corresponding to the systematic design of experiments. First of all, separate analyses can be carried out for each type of data. Regarding the behavioral data, subjects are divided into different groups based on the demographic information in intergroup studies to allow the further contrasts between groups (this stage is skipped in intragroup studies). Averages and deviations can be calculated across all subjects over the scores of questionnaires, as well as the accuracy and reaction time of behavioral responses (e.g., button pressing) recorded when the experiment was performed. For the structural data, the VBM analysis can be employed on the T1 images to check whether altered volume of brain regions (mainly for gray matter) occurred. DTI data can be used for tracing the white matter tracts via both deterministic and probabilistic methods, as well as computing the global fractional anisotropy, to examine the possible abnormalities in microcircuit and impairments in data transmission inside the brain. In regard to the on-task functional data, brain regions with both increased and decreased activities during specific task can be identified relative to the baseline. The blood-oxygen-level dependent (BOLD) signals of regions of interest (ROI) can be used for the ROI analysis, e.g., observation and comparison on the shape of BOLD signals extracted from different ROIs, or from the same set of ROIs but during different experimental conditions. Another purpose of extracting BOLD signals is to fulfill the comparisons between observed data and simulated data. The simulation of neuroimaging data is helpful to enhance our strength in verifying the brain dynamics with a tinier temporal resolution, and provide an approach to analyze the neural

mechanisms when there are no available data to use. The fMRI data can be simulated by the Adaptive Control of Thought—Rational (ACT-R) which is a cognitive architecture aiming to define the basic and irreducible cognitive and perceptual operations that enable the human mind (http://act-r.psy.cmu.edu/). If the global analysis is necessary, functional connectivity (FC) and effective connectivity (EC) analyses are selectable, though such methods meet the requirements for both global and regional analyses. Some features can be obtained specific to the resting-state functional data, such as the amplitude of low frequency fluctuations (ALFF) and regional homogeneity (ReHo). Moreover, the resting-state functional data are also appropriate for the FC and EC analyses. At last, integrating multiple types of data from single subject overcomes the limits of individual imaging modalities. Correlation analysis can be used to reveal the interactions among different types of data. In addition, fusion analyses can be performed on the integrated data with help of clustering, pattern recognition, machine leaning, etc.

2.4   WaaS and Global Brain

A huge number of sensors, embedded appliances, actuators, and the portable brain and mental health-monitoring systems have been widely utilized, foreboding that the future researches on human brain will break away from the traditional model of measurements confined at fixed place and moment. The Internet, the mobile Internet (MI), the Internet of Things (IoT), and the Web of Things (WoT) connect humans, computers, and other devices to form an immense network by which various information technologies (IT) and their applications permeate into every aspect of our daily lives. The Wisdom Web of Things (W2T) provides a social-cyber-physical space for all human communications and activities, and creates a hyper world with big data

connecting humans, computers, and things (Zhong et al., 2013). The "Wisdom" means that each of things in the WoT can be aware of both itself and others to provide the right service for the right object at a right time and context. Based on the DIKW (data-information-knowledge-wisdom) hierarchy, the wisdom as a service (WaaS) architecture of IT applications has been proposed (Chen et al., 2014). In a narrow sense, WaaS provides various intelligent IT applications, including software and u-Things, as "wisdom" services. Intelligent technologies are core to WaaS and involve personalization, context awareness, affective/emotion, interaction, autoperception, active services, and so on. By using these intelligent technologies on data, information, and knowledge, those software and u-Things can make correct judgments, decisions, and actions to provide the wisdom service (Chen et al., 2014).
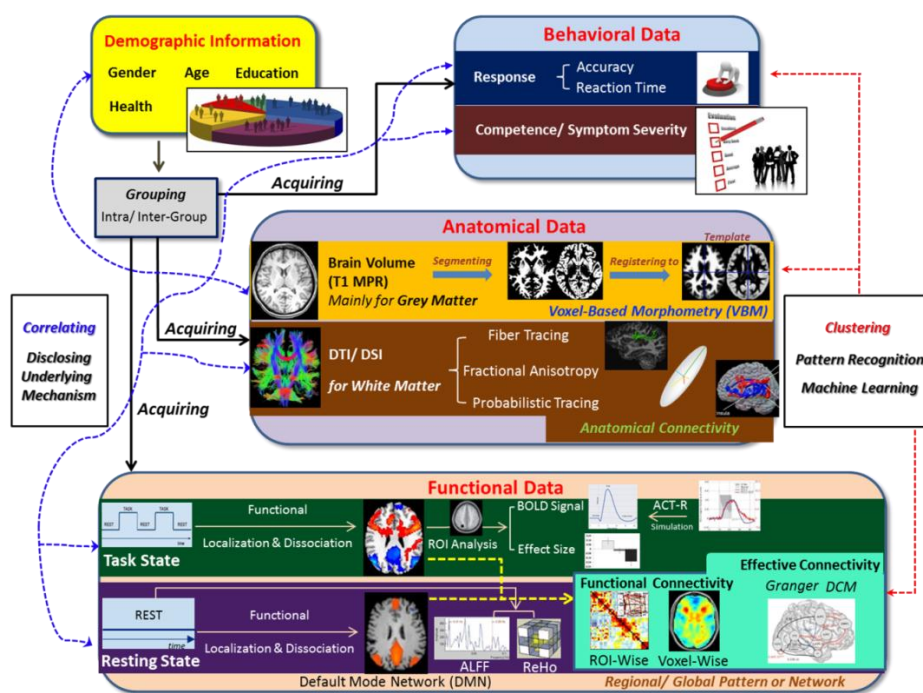
Fig. 2.8: Illustration of systematic human brain data analysis and simulation. In the case of fMRI data analysis, results can be acquired from behavioral data, structural data, resting-state functional data, and on-task functional data, respectively, as well as from the integration of all the data.

A powerful brain data center is the key to constructing the WaaS platform. The BI brain big data center is just the one that supports the whole systematic brain informatics research process and its real-world applications (Chen et al., 2014; Zhong and Chen, 2012). As the core of the brain big data cycle system, the Data-Brain represents a radically new way of storing and sharing the full scale and multi-modular data, information, and knowledge obtained by both local measurements and absorption from global sharing; it also enables high speed, distributed, large-scale, multi-granular, and multimodal analysis and computation on the W2T.

Wearable sensors attached to a person continuously send health information, such as heart rate, blood pressure, blood glucose levels, and so on, to hospitals or doctors. On the other side, the emotional robotic individual as a novel u-thing views emotion and cognition as a starting point for the development of robotic information processing and personalized human-robot interaction on the social-cyber-physical space of the W2T with brain big data (Anzai, 2013; Zhong et al., 2015). A cyber individual model is created by collecting brain data and social behavior data from a specific user, along with basic robotic emotional and cognitive capabilities, such as perception processing, attention allocation, anticipation, planning, complex motor coordination, reasoning about other agents, and perhaps even reasoning about its own mental state (Anzai, 2013; Ma et al., 2011). The emotional robotic individual embodies the user's behavior in the physical world (or the cyber world, in the case of simulated cognitive robotics). Ultimately, the robot must be able to act in the real world and interact with a specific user (such as a patient with depression) at a hospital or at home, to help the person with psychological treatment and rehabilitation (Zhong et al., 2015). Consequently, the W2T increasingly ties its users together into a single information processing system that functions as the hypothetical nervous system of the planet, namely, Global Brain.

A Global Brain is the projected product of the next metasystem transition of life on planet earth and possibly beyond (Heylighen, 2007). This term is a metaphor for the planetary information and communication technology (ICT) network that interconnects all humans and their technological artifacts. As this network stores ever more information, takes over ever more functions of coordination and communication from traditional organizations, and becomes increasingly intelligent, it starts to resemble a brain for the planet Earth. Although the Global Brain will not be achieved in a short time, it is the ultimate aim of BI.

In conclusion, BI regards the human brain as an information processing system, and investigates the essential higher-order cognitive functions of the brain. It provides opportunities for improvement by helping us understand and apply how the brain identifies the "heart" of a piece of information, as well as helping us develop the brain-inspired W2T technology required for communicating only true information—namely, sending only what we need to send and receiving only what we need to receive (Zhong et al., 2015). Implementing neuroimaging experiments and decoding the brain is one of many processing steps for setting up the dynamic and self-organized Global Brain which is capable of offering individualized brain service to each unique user.

Chapter 3

Related Works

This chapter concentrates on the related work, where an overview of researches on human brain with magnetic resonance imaging (MRI) approaches is given by surveying the most well-known brain projects at present, including the Human Connectome Project (HCP) and the Human Brain Project (HBP).

3.1 Brain, Cognition, and Emotion

The human brain is the main organ of the human nervous system. Much of the size of it comes from the cerebral cortex, especially the frontal lobe, which is associated with a set of higher-order mental abilities and processes, collectively known as, cognition. One widely accepted principle is modularity in mind and brain, with dedicated cognitive systems undertaking different kinds of mental activities (Duncan, 2013), related to knowledge, attention, memory and working memory, judgment and evaluation, reasoning and computation, problem solving and decision making, comprehension and production of language, etc. Within psychology and philosophy, the concept of cognition is closely related to abstract concepts such as mind and intelligence. In cognitive science and cognitive engineering, cognition is typically assumed to be information processing in a participant's or operator's mind and brain (Blomberg, 2011), and is treated as essentially computational in nature, with mind being the software and

the brain being the hardware. Similar to the generalized information processing, the whole processes of human thinking contains data input (sensory perception), short-term maintenance and analysis of data and information (working memory), long-term store of information (long-term memory), and output (brain or body response). Because of this background, the perspective of information processing provides a good way to the goal of understanding human thinking in relation to how they process the same kind of information as computers.

On the other side, the neurobiological substrates of human emotion are now attracting increasing interest within the neurosciences motivated by influences that emotion exerts on various domains of cognition, in particularly attention, memory, and decision-making (Dolan, 2002). Emotion is a person's state of feeling in the sense of an affect, typically including a subjective, conscious experience characterized primarily by psychophysiological expressions, biological reactions, and mental states. The annotation and representation of emotion is considerable complex (Shaver et al., 1987). To simplify the description, emotions can be roughly categorized as positive emotions (e.g., joy, trust, optimism, love, etc.) and negative emotions (anger, fear, sadness, anxiety, disappointment, etc.). Normally, emotions are elicited by environmental stimuli. It also is influenced by hormones and neurotransmitters such as dopamine, noradrenaline, serotonin, oxytocin, cortisol and GABA. In addition, the capacity to control emotion by cognitive regulation is important for human adaptation to intact social functioning which impacts on both well-being and psychopathology (Kohn et al., 2014). Emotions can be regulated by cognitive approaches such as attention deployment and reappraisal of stimuli, to amplify or attenuate the arousal intensity (Davidson et al., 2000).

3.2   Magnetic Resonance Imaging

Neuroimaging is a relatively new discipline within medicine, neuroscience, and cognitive science, applying various techniques to either directly or indirectly image the structure, function / pharmacology of the nervous system (Filler, 2009). The advanced neuroimaging techniques, e.g., MRI, PET, EEG, and MEG, have enabled the visualization and analysis of the brain function and structure in unprecedented detail (Kikinis et al., 2014). Among these methods, the MRI has become the most powerful tool with flexibility to allow the measurement of macrostructural features (such as regional thickness of the cortex or volume of specific structures), microstructural features (such as diffusion anisotropy within white matter tracts), and a host of functional characteristics (from task-driven activation to resting functional connectivity) (Poldrack and Gorgolewski, 2014). The technique uses magnetic fields and radio waves to form images of the body, and is a non-invasive way available to examine neural activities in vivo human. For this reason, all the researches on neural mechanisms of human cognition and emotion in the present thesis were completed with help of MRI techniques.

Depending on specific purposes and concerns of biophysical / biochemical features, the following modalities of MRI with varying imaging capabilities can be adopted:

1. *Structural MRI (sMRI)*. The sMRI provides detailed information of brain structure with spatial resolution up to 0.32mm (isotropic), and therefore is critical for the identification of niduses and neuropsychiatric disorders (Shah et al., 2013). A range of sequences can be used to perform sMRI, such as T1, T2, MP-RAGE, FLAIR, proton density (Rydberg et al., 1994). Relatively thin slice of sMRI increases the spatial resolution but also increases scan time, so that it is not suitable for measuring

the dynamic functions of human brain and body. The sMRI computing workflows usually involve artifact correction, segmentation, registration, surface reconstruction (Shokouhi et al., 2011), and can include brain morphometry analysis, such as voxel-based morphometry (VBM) and tensor-based morphometry (TBM) (Ashburner and Friston, 2000).

2. Functional MRI (fMRI). The fMRI can be used to record the brain activity by detecting the associated changes in brain hemodynamics by measuring the hemodynamic response to transient neural activity resulting from a change in the ratio of oxyhemoglobin and deoxyhemoglobin. Blood-oxygen-level dependent (BOLD) contrast is detected, which is closely related to cerebral blood flow (CBF), as brain function requires blood flow to supply oxygen for energy consumption by neurons. The fMRI takes images with relatively high spatial resolution (2mm isotropic) and medium temporal resolution (seconds) for a set of successive scans. Particular strengths of fMRI are reflected in its ability to capture brain activation induced by a task or the spontaneous neural oscillation at resting-state, and to provide the functional connectivity between populations of neurons based on their co-activation (Liu et al., 2015a).

3. Diffusion MRI (dMRI). The dMRI is a MRI sequence that encodes molecular diffusion effects in the nuclear magnetic resonance signal by using bipolar magnetic field gradient pulses (Le Bihan et al., 2001). It allows the mapping of the diffusion process of molecules, mainly water, in biological tissues (i.e., white matter), in vivo and non-invasively. Molecular diffusion in tissues is not free, but reflects interactions with many obstacles, such as macromolecules, fibers, and membranes. Therefore, water molecule diffusion patterns can display details about tissue architecture, either

normal or in a diseased state. By probing at many different orientations, dMRI is able to estimate the orientation of brain white matter fiber bundles, based on the fact that water diffuses most rapidly along the length of axons. Many indicators can be calculated on the dMRI data, such as fractional anisotropy (FA), mean diffusivity (MD), radial diffusivity (RD), and axial diffusivity (AXD). Tractography enables the quantitative analysis of fiber tract morphometry, i.e., orientation and dispersion, as well as the connectome (Durrleman et al., 2009).

3.3   Human Connectome Project (HCP)

The Human Connectome Project (HCP) is a five-year project sponsored by sixteen components of the National Institutes of Health in the United States. The primary goal of the Human Connectome Project (HCP) is to delineate the patterns of structural and functional connectivity in the healthy adult human brain and to provide these data as public resource for biomedical research. The project is being carried out in two phases by a consortium of 36 investigators at 11 institutions. In Phase I (years 1-2, fall 2010 - spring 2012), data acquisition and analysis methods were optimized for 16 major project components. In Phase II (years 3-5, summer 2012 - summer 2015), data were acquired from a cohort of 1200 healthy adults, with primary data acquisition at three of these institutions.

The HCP consists of two major cooperative consortia named "The Harvard / MGH-UCLA Project" and "The WU-Minn Project", which are taking complementary approaches to deciphering the brain's complex wiring diagram. "The Harvard / MGH-UCLA Project" was established by the Massachusetts General Hospital (MGH) and the University of California at Los Angeles (UCLA). They have built a

next-generation 3T magnetic resonance imaging (MRI) scanner, and intend to develop more efficient data acquisition protocols and scanner pulse sequences, as well as novel algorithms and graphical means, to improve the quality and spatial resolution of acquired images and enable the interactive navigation of brain connectivity. "The WU-Minn Project" is led by Washington University in St. Louis and the University of Minnesota with a 10-institution consortium, aiming to comprehensively map long-distance brain connections and their variability through cutting-edge neuroimaging of 1200 healthy adults (including twins and their non-twin siblings).

To obtain brain connectivity maps of the highest quality, HCP is using advanced MR hardware, including new 3T and 7T MR scanners and customized head coils. MR data acquisition has been optimized through refinements with newly developed pulse sequences and key pre-processing steps.

Information about brain connectivity is being obtained using two powerful and complementary MR imaging modalities: diffusion imaging and resting-state fMRI.

- Diffusion imaging is used to chart the trajectories of fiber bundles coursing throughout the brain's white matter. This is being done using HARDI (High Angular Resolution Diffusion Imaging) to acquire the data and probabilistic tractography to estimate fiber trajectories and generate maps of structural connectivity between gray matter regions.

- Resting-state fMRI (R-fMRI) is providing comprehensive descriptions of functional connectivity between different gray matter regions, based on correlations in the fMRI BOLD signal among functionally interacting brain regions.

Additional information about brain function is being obtained using Task-fMRI, in which subjects carry out a variety of behavioral tasks regarding: 1) working memory/category specific representations; 2) recognition memory; 3) incentive processing; 4) motor; 5) language processing; 6) social cognition (theory of mind); 7) relational processing; 8) emotion processing (Barch et al., 2013). In addition, some subjects are being studied using MEG combined with EEG, yielding information about brain function on a millisecond time scale. Behavioral testing using a battery of tests to assess sensory, motor, and cognitive function is enabling assessment of brain circuits associated with particular behavioral features or traits.

The HCP is expected to greatly advance the capabilities for imaging and analyzing brain connections, resulting in improved sensitivity, resolution, and utility, thereby accelerating progress in the emerging field of human connectomics; and provide the neuroscience research community with a novel resource for connectomics that will have a significant impact for enhancing the understanding of the rich neuroanatomical connectedness of the human brain. Successful charting of the human connectome in healthy adults helps pave the way for future studies of brain circuitry during development and aging and in numerous brain disorders.

3.4   Human Brain Project (HBP)

The HBP is a large 10-year scientific research project that is largely funded by the European Union initiated from 2013, aiming to provide a collaborative informatics infrastructure and first draft rodent and human whole brain models within its 10 year funding period. It is directed by scientists at the École Polytechnique Fédérale de Lausanne (neuroinformatics and brain simulation) and co-directed by scientists from the

University of Heidelberg (computer), the University Hospital of Lausanne, and the University of Lausanne (medical). The project involves hundreds of researchers, from 135 partner institutions in 26 countries.

For the first two and a half years (the "ramp-up" phase), the HBP concentrates on setting up the initial versions of the ICT platforms and on seeding them with strategically selected data. For the following four and a half years (the "operational phase"), the project should intensify work to generate strategic data and to add new capabilities to the platforms. In the last three years (the "sustainability phase"), the project should continue these activities while simultaneously moving towards financial self-sustainability – ensuring that the capabilities and knowledge it has created become a permanent asset for European science and industry.

During the 10-year period, the HBP will achieve three objectives:

1. Future Neuroscience. Achieve a unified, multi-level understanding of the human brain that integrates data and knowledge about the healthy and diseased brain across all levels of biological organization, from genes to behavior.

2. Future Computing. Develop novel neuromorphic and neurorobotic technologies based on the brain's circuitry and computing principles; develop supercomputing technologies for brain simulation, robot and autonomous systems control and other data intensive applications.

3. Future Medicine. Develop an objective, biologically grounded map of neurological and psychiatric diseases based on multilevel clinical data; use the map to classify and diagnose brain diseases and to configure models of these diseases; use *in silico* experimentation to understand the causes of brain diseases and develop new drugs

and other treatments; establish personalized medicine for neurology and psychiatry.

The HBP pursues four goals, each building on existing work, and acting as a catalyst for new research.

1. Data: generate strategically selected data essential to seed brain atlases, build brain models and catalyse contributions from other groups.

2. Theory: identify mathematical principles underlying the relationships between different levels of brain organization and their role in the brain's ability to acquire, represent and store information.

3. ICT platforms: provide an integrated system of ICT platforms providing services to neuroscientists, clinical researchers and technology developers that accelerate the pace of their research.

4. Applications: develop first draft models and prototype technologies demonstrating how the platforms can be used to produce results with immediate value for basic neuroscience, medicine and computing technology.

In order to achieve the objectives and goals, the HBP is developing six information and communications technology (ICT) Platforms. These Platforms will enable large-scale collaboration and data sharing, reconstruction of the brain at different biological scales, federated analysis of clinical data to map diseases of the brain, and development of brain-inspired computing systems.

The HBP's ICT Platforms are:

- Neuroinformatics: a data repository, including brain atlases

- Brain Simulation: building ICT models and simulations of brains and brain components

- Medical Informatics: bringing together information on brain diseases

- Neuromorphic Computing: ICT that mimics the functioning of the brain

- Neurorobotics: testing brain models and simulations in virtual environments

- High Performance Computing: hardware and software to support the other Platforms

Finally, the HBP is organized in thirteen subprojects (SP), spanning strategic neuroscience data, cognitive architectures, theory, ethics and society, management and the development of six new informatics-based platforms including: 1) Strategic Mouse Brain Data; 2) Strategic Human Brain Data; 3) Cognitive Architectures; 4) Theoretical Neuroscience; 5) Neuroinformatics; 6) Brain Simulation; 7) High Performance Computing; 8) Medical Informatics; 9) Neuromorphic Computing; 10) Neurorobotics; 11) Applications; 12) Ethics and Society; 13) Management.

The Human Brain Project is expected to enormously accelerate progress towards a multi-level understanding of brain structure and function, towards better diagnosis, better understanding, and better treatment of brain diseases and towards new brain-inspired Information and Communications Technologies. The impact on European science, European industry, the European economy and European society is potentially very large.

3.5 Conclusion

The human brain is a considerably complex information processing system that is involved in every human emotion, feeling, thought, and decision. In recent years the field of neuroimaging has seen a revolution in the development of several large projects that are increasing the amount of available data (Poldrack and Gorgolewski, 2014), such as the HCP and HBP. One feature in common between the two well-known projects is the stress on the collection of massive brain data with multiple modalities. The complexity of human brain makes it necessary to perform the large-scale computations upon brain big data, as more kinds and amount of data are likely to provide more explicit clues for unraveling the mysteries that single data sets cannot help. Another similarity of the two projects is the concerns on the development of ICT and informatics-enabled new technologies for supporting the data acquisition, analysis, and visualization. At last, both the projects bring the higher cognition into their research scopes. The cognitive functions are unavoidable questions, although the two projects have other emphases.

It is not to be denied that both the projects offer several possibilities to strengthen the devices and techniques for studying human brain, and will create a better understanding of the brain structure and functions, as well as facilitate medical research related to healing and brain development. However, some limitations do exist within each project. For the HCP, relatively narrow research interests in the functional and structural connectivity within healthy adults' brains determine the difficulty in extending research findings to other relevant fields, e.g., psychiatry and molecular biology, unless subsequent projects are initiated. The HBP gives all-sided concentrations on the brain researches, ranging from techniques and theories to management and ethics, and also

involving comparisons between rodent animal's brain and human brain. It might be a potential trouble to integrate the diverging results obtained from distributed 135 partner institutions of the project in 26 countries. In addition, the project is inclined to bet on the brain simulation, while some of European researchers argue that the technology of a large-scale simulation of the brain is radically premature.

Studies on Human Cognition Using fMRI

Cognition is a variety of domains of all mental abilities and processes, such as attention, memory and working memory, judgment and evaluation, reasoning and calculation, problem solving and decision making, comprehension and production of language, etc. As one representative, mental calculation (arithmetic) is crucial in our daily life and represents an important part of the children's curriculum at school. Recent data even suggest that poor numeracy is more detrimental to life perspectives than poor literacy (Klein et al., 2013). In Human Connectome Project (HCP), a range of selected cognitive experiments were implemented to allow a comparison of network connectivity in a task context to connectivity results generated using resting-state fMRI, and the math task was also adopted for exploring the language processing (Barch et al., 2013). Consequently, there is increasing interest in revealing the neural substrates of numerical cognition.

We also concentrate on the mental calculation that is conceived as one typical component of human cognition. In this chapter, systematic studies on neural substrates underlying overlaps and differences between mental addition and subtraction processes will be elaborated. The involved investigations on the mental arithmetic using systematic analyzing approaches also serve as a case study for demonstrating advantages of BI methodology in mining latent knowledge hidden in one dataset as far as possible.

4.1 Introduction

Higher cognitive functions, such as reasoning, learning, computation, problem-solving, are realized by cooperation from distributed brain regions. Brain Informatics (BI) is powerful to reveal the complicated interaction between cortical areas by examining the information processes and underlying neural substrates on basis of systematic methodology (Zhong et al., 2007a). Neuroimaging studies in the past decades have revealed that mental arithmetic is not only a basic daily activity but also provides powerful paradigms for investigating fundamental cognitive processes underlying abstract problem solving from a variety of domains, such as magnitude representation, executive control, verbal processes, and sensory-motor-derived concepts (Ansari, 2008; Houde et al., 2010; Nieder and Dehaene, 2009), for a review). Moreover, for practical significance, explicit understanding of the neural mechanisms of arithmetic calculations also provides new insights into mathematical education (De Smedt et al., 2011). With increasing knowledge of the human brain, the core processes of arithmetic calculations that support mental manipulation of numerical quantities (e.g., magnitude comparison) have been associated with the bilateral intraparietal sulci (IPS) (Ansari, 2008; Dehaene et al., 2003). Another breakthrough in mental arithmetic in the field of neuroimaging is the finding of the dissociation of cognitive processes between mental subtraction and multiplication (Yi-Rong et al., 2011; Zhou et al., 2006). Nevertheless, with respect to the two simplest operations we learn early, little has been known regarding whether addition and subtraction employ shared or separate cognitive procedures and strategies. Against this background, we implemented a functional magnetic resonance imaging (fMRI) study and addressed questions of the neural correlates underlying the relationship between addition and subtraction.

Converging evidence has identified the fronto-parietal network including the parietal and prefrontal cortices as the main frame that acts during mental arithmetic tasks (Arsalidou and Taylor, 2011) for a review). The triple-code model of numerical processing put forward by Dehaene and Cohen proposed that numbers are represented in three codes including visual Arabic form, verbal word form and analogue magnitude form, which corresponds to ventral occipitotemporal areas, left perisylvian, and bilateral inferior parietal respectively (Dehaene et al., 2003). However, dissociations in the neural network were ascertained among operations, especially between subtraction and multiplication. Functional neuroimaging data in healthy adults have revealed that the intraparietal sulcus and the posterior superior parietal lobe are more active during subtraction than during multiplication, whereas the left angular and supramarginal gyri are modulated to a stronger degree during multiplication relative to subtraction (Chochon et al., 1999; Ischebeck et al., 2006). Involvement of different strategies was indicated to account for such dissociation (Barrouillet et al., 2008; Campbell and Xue, 2001; Dehaene et al., 2003). Multiplication was attributed to being mainly solved by rote arithmetical fact retrieval, which employs the left perisylvian language areas and modularizes phonological associations between a digit pair and their answer, whereas subtraction requires quantity-based procedural strategies on the basis of an analogue mental number line that have been demonstrated to rely on the intraparietal sulci. This hypothesized recruitment of different neural networks between operations has been supported by lesion studies: lesions in the left perisylvian cortex resulted in impairments in multiplication but not subtraction, whereas lesions to regions of the intraparietal cortex led to difficulties with subtraction but not multiplication (Dehaene and Cohen, 1997; Dehaene et al., 2003).

By contrast, neuroimaging studies focusing on the relationship between addition and

subtraction are relatively scarce. Behavioral studies have shown significantly longer reaction time and lower accuracy in subtraction than in addition processes (Campbell et al., 2006; Klein et al., 2014), but little is known about how the neural activity contributes to these differences. One important reason confining our understanding of the differences can be attributed to the obscure understanding of addition. Relative to the large agreement about the use of quantity-based procedural processes in subtraction, strategies and neural networks involved in addition are still being debated, especially between a retrieval hypothesis and a hybrid hypothesis asserting coexistence of both direct retrieval and procedural manipulations. On the one hand, some studies have suggested addition, just like multiplication, is dependent on a strategy based on retrieval of rote arithmetic fact rather than the "subtraction strategy" (Schmithorst and Brown, 2004). A recent study on fiber tractography supported the shared strategy of fact retrieval in both multiplication and addition in view of the positive correlation observed in both operations between arithmetic competency and the fractional anisotropy in the left anterior portion of the arcuate fasciculus that was considered to subserve phonological processing and link the frontal and inferior parietal cortices (Van Beek et al., 2014). More evidence confirming the retrieval hypothesis also comes from studies on children. (De Smedt et al., 2011) reported a dissociable pattern in children aged 10-12 years who showed reliance on the fronto-parietal network during subtraction processing but only employed the left hippocampus during addition processing, demonstrating reliance on the hippocampus for arithmetic fact retrieval during addition in the early stages of learning arithmetic facts. (Cho et al., 2012) reported a consistent activation of prefrontal and hippocampal regions during mental addition in 7-9-year-old children. However, a few notable questions cannot be well explained by this hypothesis of a common strategy between addition and multiplication. For example, individual

growth and functional maturation might result in a shift from the memory-based frontal activation to the quantity-specific parietal activation in arithmetic processes (Rivera et al., 2005), and studies in adults have shown common activation during both addition and subtraction in the parietal regions associated with procedural calculation (Yi-Rong et al., 2011). Moreover, neural differences suggest that distinct cerebral processes between addition and multiplication have also been identified (Rosenberg-Lee et al., 2011; Zhou et al., 2006; Zhou et al., 2007). On the other hand, the hybrid hypothesis proposes a dual system that can recruit either retrieval or procedural strategies in addition based on the difficulty of the problems, such as the problem size. Problem size manifests an effect that problems with numerically small operands and answers can lead to more accurate and faster responses than problems with comparatively large operands and answers (De Smedt et al., 2011). It has been suggested that small problems are usually solved by means of fact retrieval, whereas large problems are more often solved by more error-prone and time-consuming quantity-based procedural strategies, such as counting or decomposing a problem into smaller problems (Campbell and Xue, 2001). Furthermore, (Klein et al., 2010) investigated addition with different levels of difficulty (larger sum vs. smaller sum, carry vs. non-carry) and proposed a multi-modular processing in addition involving an alterable use of strategies based on the difficulty level. Lower difficulty with smaller sums resulted in increased reliance on a ventral pathway associated with the temporo-parietal areas and subcortical-limbic areas, which appeared to subserve the fact retrieval strategy. Higher difficulty with larger sums resulted in increased reliance on the dorsal pathway associated with the fronto-parietal areas, which appeared to subserve magnitude-related procedural processing. Their recent study (Klein et al., 2013) on the probabilistic fiber tracking supported the dual pathways and indicated the pathways operate as a functionally integrated circuit for

mental calculation. Nevertheless, these studies did not report the differences between addition and subtraction; thus, it is still unclear whether this dual system also exists in subtraction. Consequently, two potential explanations might account for the differences between addition and subtraction. If only retrieval of rote arithmetic memory is used for solving addition problems, the differences might be attributed to a double dissociation. Dissociated neural substrates might be discovered for the two operations, with more activation elicited by addition in subcortical and left perisylvian language areas that were proposed to be responsible for storage and retrieval of arithmetic facts (Dehaene and Cohen, 1995, 1997) compared with more activation induced by subtraction in the IPS that underlies quantity representation (Ansari, 2008) because of the double dissociation of calculation strategies. However, if mental addition is reliant on the hybrid strategy, partially overlapping brain networks might be observed in addition and subtraction processes, and the differences between the two operations might result from partially different cognitive strategies and some other mental processes.

Taken together, I carried out an fMRI experiment to investigate both the common and different aspects between mental addition and subtraction processes. Healthy subjects were invited to solve 2-digit simple addition and subtraction problems without carrying and borrowing during the fMRI scanning. Blood-oxygen-level-dependent (BOLD) changes were measured during addition and subtraction processing followed by a conjunction analysis for exploring overlaps of activated brain regions elicited by mental addition and subtraction, respectively, and a functional connectivity analysis for detecting differences in brain networks employed during different calculation, and a dynamic causal modeling analysis (DCM) for investigating causal relationships between distributed nodes in the networks during mental calculations.

In this chapter, a BI methodology-based systematic investigation on mental arithmetic will be introduced. The second section depicts the multi-aspect analysis based on BI methodology. The third section introduces common and different patterns of brain activation during mental addition and subtraction processes. The fourth section describes the common and different brain networks underlying mental addition and subtraction. The fifth section presents the dynamic causal differences between mental addition and subtraction.

4.2   Multi-Aspect Analysis Based on BI Methodology

BI methodology appeals a systematic analysis on the human brain data. In this chapter, we focus on the task-based fMRI data, and aim to uncovering the neural mechanisms of mental addition, subtraction, as well as their common and distinct aspects. To realize this goal, series of analyzing approaches were used for exploring the same data set from phenomenon to essence (see Figure 4.1): mean reaction time and accuracy of subjects under different types of calculations were compared to reflect indirectly the differences in information processes between operations by behaviors; conjunction analysis was applied to show the joint regions with common brain activation during both addition and subtraction calculations; differences between activation pattern of the two operations were revealed by cognitive subtraction (Price et al., 1997); brain networks based on the temporal co-activation were studied by functional connectivity analysis; causality of network nodes (regions) were examined by dynamic causal modeling (DCM). A systematic use of multiple analyzing techniques has helped further our understanding on the thinking-centric human brain.
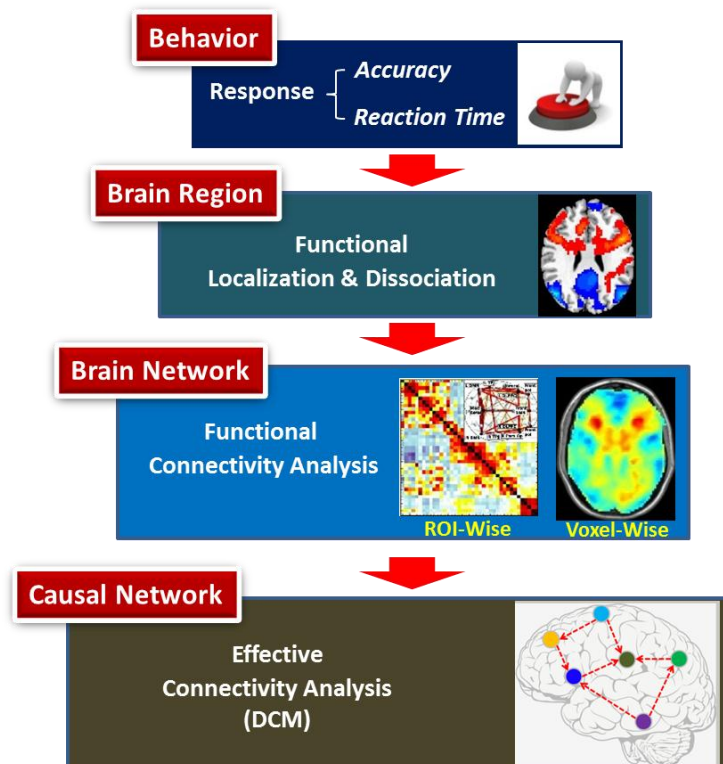
Fig. 4.1: Multi-aspect analysis based on BI methodology. The same data set was analyzed systematically from phenomenon to essence.

4.3   Common and Different Brain Regions for Mental Addition and Subtraction

In this section, we focus on common and different patterns of brain activation induced by 2-digit addition and subtraction problems without carrying and borrowing. We implemented an fMRI experiment including three types of tasks: the addition task (AT), subtraction task (ST), and number matching task (NT) that served as the baseline. We assumed that addition and subtraction exploit some overlapped calculation strategies by sharing some common brain regions; nonetheless some intrinsic differences also exist between the two calculation processes.

4.3.1 Materials and Methods

Participants

Data from 20 Chinese college graduates (9 females) with a mean age of 25.76 (SD = 3.76) years were included in the final analysis. Data from 3 participants had previously been excluded due to unacceptable head movements within the scanning sessions. All of the participants were right-handed, educated with identical techniques, had normal or corrected-to-normal vision, and reported no history of neurological or psychiatric disorders. Prior to their participation in the study, written informed consent was obtained from each participant after the nature and possible consequences of the studies were explained. This study was approved by the Ethics committee of Xuanwu Hospital, Capital Medical University, Beijing.

Stimuli and Procedure

A block-designed fMRI experiment involving 2-digit simple addition and subtraction problems was performed in the current study. Participants were shown three types of tasks in a unified sequential pattern during scanning, including an addition task (AT), a subtraction task (ST), and a number matching task (NT) that served as the baseline (see Figure 4.2). Signs of "+", "-", and "#" corresponded to the three conditions, respectively. All of the visual stimuli were presented in a partitioned format and in the sequential order of "first operand", "second operand", "operation sign", and "proposed solution" within each trial. Units and tens in the first operand were always larger than the corresponding ones in the second operand for all three conditions to control the "unit-decade compatibility effect" observed in number comparison tasks (e.g., faster and more accurate response to 56 vs. 32, which is compatible because 5 > 3 and 6 > 2;

slower and less accurate response to 43 vs. 34, which is incompatible because 4 > 3 but

3 < 4) (Nuerk et al., 2001, 2004). Participants were required to compute "first operand

plus the second" in the AT, or "first operand minus the second" in the ST, or judge

whether the "proposed solution" was the same as one of the two previous operands in

the NT, and then press two response keys using the left and right thumbs to evaluate the

validity of the "proposed solution" as quickly and accurately as possible. Reaction times

and accuracy were obtained for each trial. The difficulty of mental arithmetic was found

to be associated with the involvement of carrying or borrowing manipulations.

Whenever such operations were required, response latencies, error rates, and functional

brain activation increased considerably (Imbo et al., 2007a; Imbo et al., 2007b).

Therefore, carrying and borrowing were excluded to ensure that all of the problems

were simple. So far, few studies have tried to examine the arithmetic processes with

2-digit simple problems. In fact, 2-digit stimuli can provide some advantages: (1) they

are more likely to activate the prefrontal cortex than small single-digit addition

problems (De Pisapia et al., 2007; Rosenberg-Lee et al., 2011; Zhou et al., 2007), and (2)

they enable neural activity in wider brain areas in both hemispheres (Ratinckx et al.,

2006). In this way, an impartial comparison can be implemented by using simple

problems to test whether addition and subtraction differ when both the operations can

elicit activation in the bilateral frontal and parietal cortices. Consequently, in

consideration of the parallel processes on the units and tens separately for 2-digit

numbers (Nuerk et al., 2001, 2004), number size and distance for each digit of a

problem varied from 1 to 9 and 1 to 8, respectively. The frequency of occurrence of

each number was balanced across three conditions. Neither "tie" problems (e.g., 32 + 32,

67 - 67) that involved different operand encoding (Blankenberger, 2001; Zhou et al.,

2007) nor repeated problems were recruited. Incorrect proposed solutions deviated by ± 1

or ± 10 from the correct solutions in 50% of all the trials. Each trial lasted for 6 s, resulting in an exposure time of 250 ms for the first operand, 250 ms for the second operand, 500 ms for operation sign, and 2000 ms for the proposed answer. Every two stimuli were separated by a 500-ms mask (only background). The inter-trial interval was 1500 ms. Four successive trials of the same condition were presented in one block that lasted for 24 s. Blocks of three conditions were mixed and counterbalanced, and every two task blocks were separated by a 24-second rest block. Data were acquired in two functional runs with a total of 32 trials for each type of task.
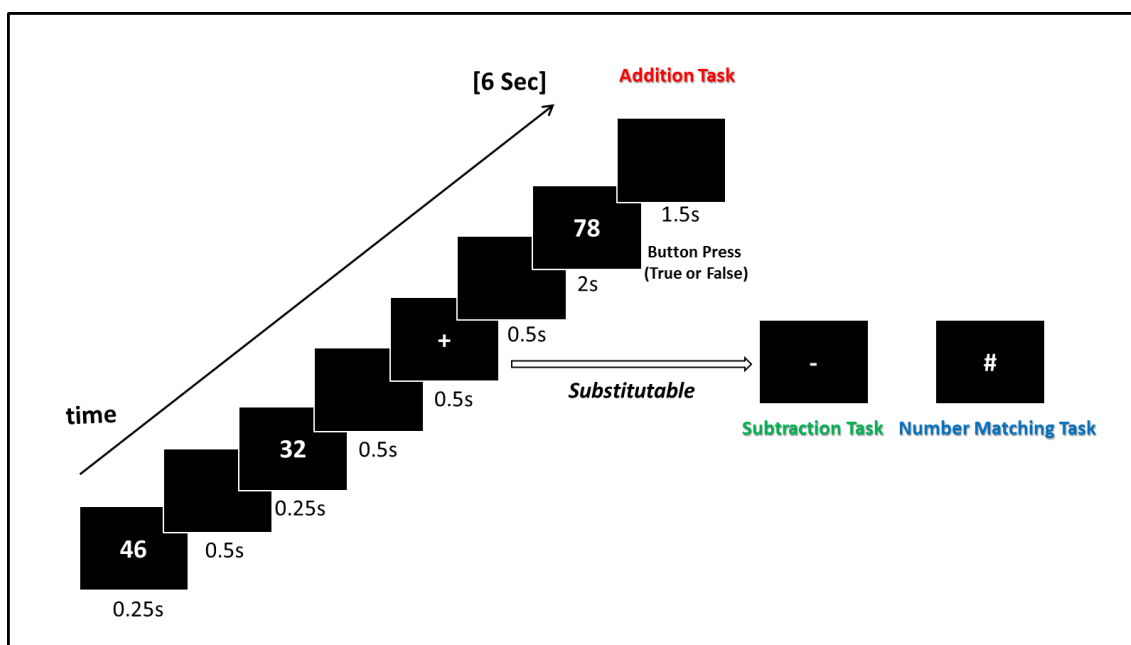
Fig. 4.2: Paradigm of stimuli presentation. Participants were shown three types of tasks in a unified sequential pattern during scanning, including an addition task (AT), a subtraction task (ST), and a number matching task (NT) that served as the baseline.

MR Data Acquisition

The fMRI data were acquired with a 3.0 Tesla MRI scanner (Siemens Trio Tim; Siemens Medical System, Erlanger, Germany) using a 12-channel phased array head coil. Foam padding and headphones were used to limit head motion and reduce scanning noise. One hundred ninety two slices of anatomical images with a thickness of

1 mm were obtained using a T1 weighted 3D magnetization prepared rapid gradient echo (MPRAGE) sequence (TR = 1600 ms, TE = 3.28 ms, TI = 800 ms, FOV = 256 mm, flip angle = 9°, voxel size = 1 × 1 × 1 mm3). Functional images were collected through an echo-planar imaging (EPI) sequence (TR = 2000 ms, TE = 31 ms, flip angle = 90°, FOV = 240 × 240 mm^2, matrix size = 64 × 64). Thirty axial slices with a thickness of 4 mm and an interslice gap of 0.8 mm were acquired.

Data Preprocessing

The preprocessing of fMRI data was performed with SPM8 software (Wellcome Trust Centre for Neuroimaging, London, UK, http://www.fil.ion.ucl.ac.uk) implemented on a MATLAB platform (MathWorks, Natick, MA). The first two images were discarded to allow the magnetization to approach dynamic equilibrium. The data format was converted to make the fMRI data available for the SPM software. Functional images were corrected for slice-timing differences and realigned to the median image to correct rigid body motion. Cases with head movement exceeding 2 mm or 2 degrees were rejected. The high resolution anatomical image was co-registered with the mean image of the EPI series and then spatially normalized to the MNI template. After applying the normalization parameters to the EPI images, all volumes were resampled into 3 × 3 × 3 mm^3 and smoothed with an 8-mm FWHM isotropic Gaussian kernel.

fMRI Analysis

Data were statistically analyzed using SPM8. After specifying the design matrix, each participant's hemodynamic responses induced by the trials were modeled with a box-car function convolved with a hemodynamic function. The parameters for the effects of the addition task (AT), subtraction task (ST), and number matching task (NT) were estimated. Contrast images were constructed individually based on the general linear

model (GLM). At the group-level (i.e., random-effects analysis), one-sample t-tests were implemented for each voxel of the contrast images. Considering the involvement of the common cognitive processes across the three conditions on basic visual encoding, digit maintenance, matching judgment, and button pressing, the calculation-specific neural correlates underlying addition and subtraction were revealed by contrasts of AT > NT and ST > NT separately ($p < 0.05$, FDR corrected, with a minimum cluster size of $k > 10$). The results for how subtraction differed from addition were identified by the contrast of ST > AT ($p < 0.05$, corrected for AlphaSim, with a minimum cluster size of $k > 22$; $p < 0.001$ before correction). Regions of activation originally obtained in MNI coordinates were converted into Talairach coordinates with the WFU PickAtlas toolbox (Lancaster et al., 2000; Maldjian et al., 2003).

4.3.2   Results

Behavioral Results

The behavioral results are shown in Table 4.1. We performed one-way repeated-measures analyses of variance on the accuracy (ACC) and reaction time (RT) using AT, ST and NT as the conditions. The average ACC was $94.47 \pm 4.59\%$ (mean $\pm$ SD) for the addition task, $90.67 \pm 6.33\%$ for the subtraction task, and $95.51 \pm 5.98\%$ for the number matching task. The main effect of condition was significant, $F_{(2, 57)} = 4.009$, $p = 0.024$. Post-hoc paired t-tests indicated that the ACCs of AT and NT were significantly higher than that of ST after a Bonferroni correction ($p=0.039$, and $p=0.009$, respectively). The difference between AT and NT did not reach significance.

The average RT was 1216.04 ± 105.34 ms for the addition task, 1259.51 ± 140.17 ms for the subtraction task, and 1244.99 ± 115.21 ms for the number matching task. No

significant differences were found for the RT among the three conditions ($F_{(2, 57)} = 0.667$, $p = 0.517$).

Common Regions Activated in Both Addition and Subtraction Processes

All task conditions (addition task, subtraction task, and number matching task) were compared with no task (Rest) condition, and then conjunction analyses were implemented for comparisons of AT > Rest and ST > Rest, to obtain the overlapped regions of activation between addition and subtraction (see Figure 4.3). Significant brain activation ($p < 0.05$, FDR corrected, with a minimum cluster size of $k > 10$) was observed in visual cortex and frontoparietal network including bilateral cuneus and fusiform, lingual gyrus on the right hemisphere; bilateral inferior parietal lobule, right superior parietal lobule, bilateral insula and superior frontal gyrus, precentral gyrus, inferior frontal gyrus, and medial frontal gyrus on the left hemisphere. Only increased activation was found (see Table 4.2).
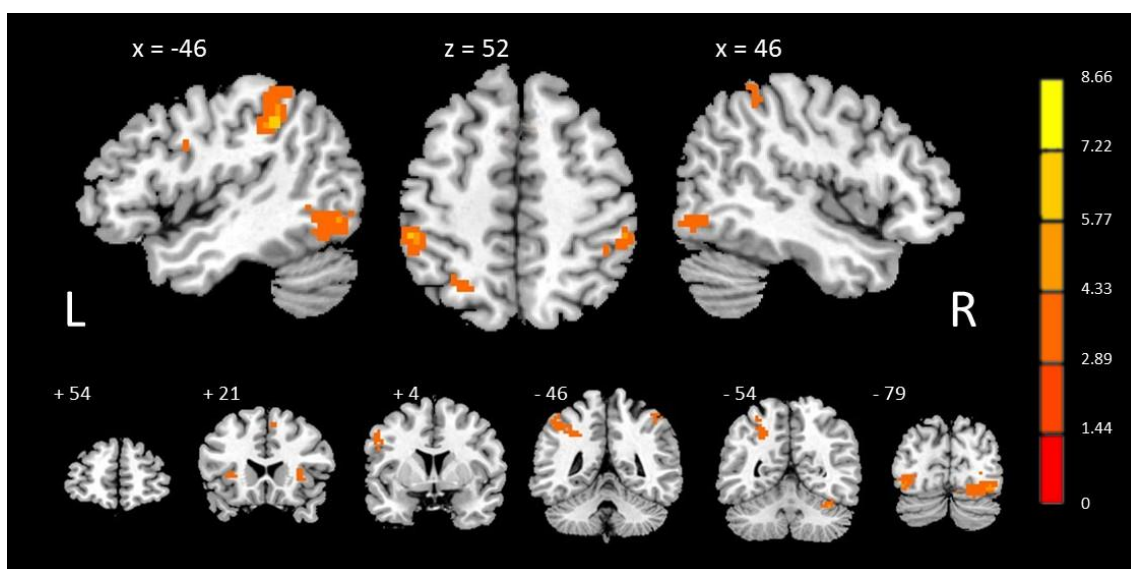
Fig. 4.3: Results of conjunction analysis. Common regions activated in both addition and subtraction processes are shown in MNI coordinates. Color bar indicates the t-score.

Table 4.1: In-scanner behavioral results. One-way repeated-measures analyses of variance was performed on the accuracy (ACC) and reaction time (RT) using addition task, subtraction task, and number matching task as conditions.

	Accuracy (% correct)				Reaction Time (ms)			
	M	SD	F (2,57)	P	M	SD	F (2,57)	p
Addition	94.47	4.59	4.009	0.024	1216.04	105.34	0.667	0.517
Subtraction	90.67	6.33			1259.51	140.17		
Number Matching	95.51	5.98			1244.99	115.21		

Table 4.2: Common regions activated in both addition and subtraction processes. Loci of maxima are in Talairach coordinates in millimeters. Abbreviations: LinG, lingual gyrus; FuG, fusiform gyrus; IPL, inferior parietal lobule; PrecG, precentral gyrus; IFG, inferior frontal gyrus; SPL, superior parietal lobule; mFG, medial frontal gyrus; SFG, superior frontal gyrus; L, left; R, right, BA, Brodmann area.

Region	BA	Cluster	Talairach Coordinates			T-score
			x	y	z	
R. Cuneus	17	624	18	-93	-1	8.66
R. LinG	17		21	-84	0	7.78
R. FuG	19		27	-83	-10	6.61
L. IPL	40	250	-43	-45	38	6.85
			-49	-41	46	5.98
L. Cuneus	17	601	-15	-95	-1	5.79
L. FuG	19		-23	-86	-11	5.75
L. PrecG	6	38	-51	3	37	4.57
			-46	0	31	4.01
L. IFG	9		-54	6	29	4.08
R. IPL	40	33	48	-41	48	4.49
			40	-49	47	3.60
R. SPL	7		34	-55	52	3.31
L. Insula	13	18	-32	14	9	3.71
R. Insula	13	17	30	16	13	3.57
L. mFG	6	17	-4	1	48	3.49
L. SFG	6		-2	10	49	3.31
R. SFG	6		7	10	52	3.23

Differences between Addition and Subtraction Processes

Specific neural substrates underlying addition and subtraction processes were revealed by the contrasts of AT > NT and ST > NT, respectively (see Table 4.3). As shown in Figure 4.4A and 4.4B, regions that showed increased activation during addition processes were found in the bilateral intraparietal sulci (IPS), bilateral caudate nuclei, left insula, as well as posterior portion of dorsolateral prefrontal cortex (pDLPFC, BA9) in the left hemisphere. Regions that showed increased activation during subtraction processes were found in the left frontal cortex covering dorsolateral and inferior portions, left supplementary motor area (SMA, BA 6/32), left fusiform gyrus (FFG, BA37), right pDLPFC, right precentral gyrus/middle frontal gyrus (frontal eye field, FEF, BA 6), and bilateral insula, in addition to the common areas shared with addition in the bilateral IPS, and bilateral caudate nuclei. Regions with decreased activation were also revealed by the contrasts in both addition and subtraction processes, which were located in the areas that overlapped with the default mode network (DMN) (Fox et al., 2005), including the bilateral inferior temporal gyri (ITG), bilateral angular gyri (AG), medial portions of the prefrontal cortex (mPFC), and posterior cingulate cortex (PCC).

Differences between addition and subtraction were disclosed by the contrast of ST > AT, as shown in Figure 4.4C. Compared with addition, subtraction induced greater activation in the left inferior frontal gyrus (IFG, BA45/44) and left SMA (see Table 4.4). No significant differences resulted from the contrast of AT > ST.
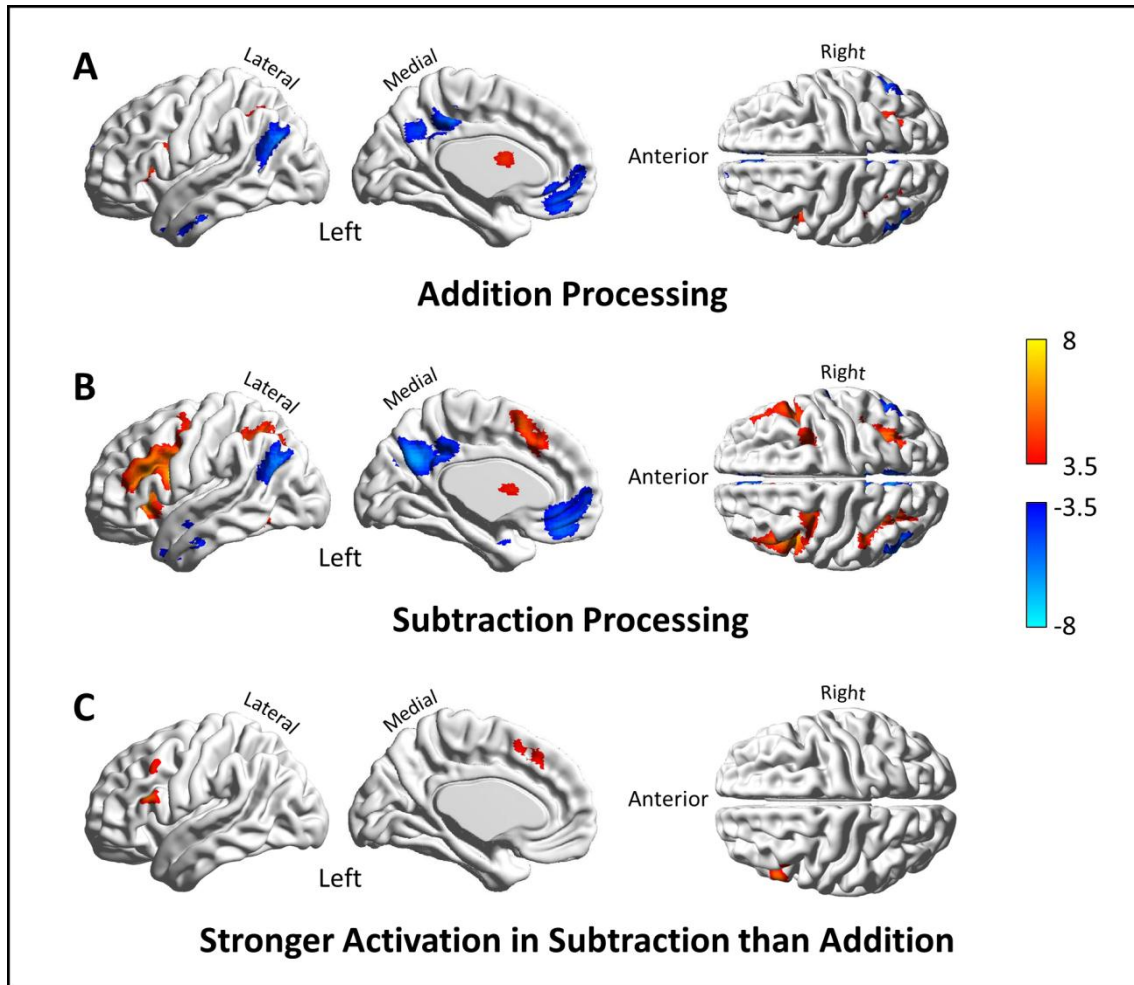
Fig. 4.4: Operation-specific brain regions. Regions with significant activation are elicited by contrasts of AT > NT, ST > NT, and ST > AT. Warm color bars indicate the t-scores specific to increased activation, whereas cold color bars indicate the t-scores specific to decreased activation.

4.3.3 Discussion

The regions activated in the present study corroborate some parts of results in relevant researches (Lucchelli and De Renzi, 1993; Rickard et al., 2000; Whalen et al., 1997). In general, the frontoparietal network is critical for both subtraction and addition. Furthermore, subcortical regions play an important part as well. The relationship between the two operations is complex because both the similarities and differences can be identified between the two operations.

Table 4.3: Regions with significant activation and deactivation elicited by contrasts. Abbreviation: AT, addition task; ST, subtraction task; NT, number matching task; IPS, intraparietal sulcus; pDLPFC, posterior portion of dorsolateral prefrontal cortex; FFG, fusiform gyrus; FEF, frontal eye field; SMA, supplementary motor area; AG, angular gyrus; ITG, inferior temporal gyrus; PCC, posterior cingulate cortex; mPFC, medial portions of the prefrontal cortex; L, left; R, right; BA, Brodmann area.

Contrast	Region	BA	Cluster	Talairach Coordinates			T-score
				x	y	z	
Activation							
AT > NT	L. IPS	7	28	-27	-54	50	4.72
	R. IPS	7	33	27	-51	44	5.45
	L. pDLPFC	9	11	-45	7	27	5.15
	L. Caudate		19	-9	2	16	5.94
	R. Caudate		32	9	9	13	4.81
	L. Insula	13	35	-30	22	4	5.90
ST > NT	L. FFG	37	18	-48	-51	-13	4.04
	L. IPS	40	144	-27	-54	47	6.76
	R. IPS	7	151	27	-60	44	6.05
	L. pDLPFC	9	354	-42	7	27	6.66
	R. pDLPFC	46	225	48	5	27	6.23
	R. FEF	6	26	33	2	50	4.75
	L. SMA	6/32	106	-3	11	50	5.82
	L. Caudate		115	-6	8	11	4.58
	R. Caudate		151	15	-14	20	4.83
	L. Insula	13	85	-30	22	2	7.11
	R. Insula	13	47	33	22	2	6.31
Deactivation							
AT > NT	L. AG	39	409	-53	-69	23	8.85
	R. AG	39	360	50	-62	25	6.06
	L. ITG	20	181	-53	1	-20	7.74
	R. ITG	20	246	45	5	-38	7.05
	L. PCC	31	495	-3	-32	40	7.15
	L. mPFC	11	389	-9	52	-3	6.68
ST > NT	L. AG	39	238	-50	-66	31	6.83
	R. AG	39	186	45	-56	25	6.73
	L. ITG	21	75	-56	-5	-20	5.36
	R. ITG	20	83	50	-7	-27	6.68
	R. PCC	31	535	12	-43	35	7.36
	L. mPFC	11	363	-6	38	-17	5.88

Table 4.4: Regions with significant activation elicited by ST > AT. Abbreviation: AT, addition task; ST, subtraction task; IFG, inferior frontal gyrus; SMA, supplementary motor area; L, left; R, right; BA, Brodmann area.

Contrast	Region	BA	Cluster	Talairach Coordinates			T-score
				x	y	z	
ST > AT	L. IFG	45/44	28	-56	21	18	4.82
	L. SMA	8		-6	20	43	3.78

Common Activation of IPS in Addition and Subtraction

Although researchers have come to an agreement on the involvement of IPS in calculation tasks, conflicts still exist regarding whether mental addition would activate the IPS. For instance, Rosenberg-Lee et al. reported no activation in parietal cortex during addition processing when they compared the processes between four basic operations (Rosenberg-Lee et al., 2011). However, Fehr and colleagues reported the activation in left inferior parietal lobule during addition in a similar experiment in which they compared the common brain regions of the four operations (Fehr et al., 2007). One difference between the two studies is the method for presenting visual stimuli. The paradigm in the former experiment presented the whole equation of an arithmetic problem in which stimuli on the screen were remained for a while. The later experiment showed the stimuli separately like sequential series so that subjects had to retain each stimulus after interpreting it into verbal form rather than calculating automatically on basis of visual Arabic form depending on visual-spatial processing. Based on BI methodology that advocates systematic investigation on human information processing, strategies of problem-solving can also be referred. Subjects will be inclined to pick the easier and faster approach and avoid the regular number manipulation with IPS if it is allowed. Nevertheless, mental calculations are always performed without visual reference in the everyday life. Thus, we required subjects to solve arithmetic problems

relying on information in verbal form in the present study, and induced activation in the surface of bilateral parietal areas as well as the intra part of left parietal sulcus (IPS) during both addition and subtraction calculations (as shown in Figure 4.3). Collectively, although the difficulty of arithmetic problems selected in the current experiment was simple and without carrying and borrowing, common activations found in IPS for the both operations suggested the magnitude processing during both calculations. It can be proved that strategies adopted for the two calculations are not double dissociated. Thus the hypothesis of strategic difference is insufficient to explain why subtraction differs from addition.

Differences in Activation Patterns between Mental Addition and Subtraction

Simple mental arithmetic problems induced increased activation in a wide range of brain regions that was consistent with most previous studies on mental arithmetic (Arsalidou and Taylor, 2011), such as the bilateral IPS and insula, the left DLPFC, IFG, SMA, FFG, and subcortical regions, and induced decreased activation located in the regions of the default mode network (DMN) (Fox et al., 2005), including the bilateral ITG, AG, mPFC, and PCC. Many of these regions were specific to subtraction calculation (see Figure 4.4). Compared with addition, subtraction provoked significantly greater activation in the left IFG (BA45/44) and SMA as shown in Figure 4.4C. The left IFG is well known as one part of Broca's area that has been certified as an important locus for linguistic processing and working memory (D'Esposito et al., 1999; Gabrieli et al., 1998; Mainy et al., 2007; Poldrack et al., 1999). Subdivisions of Broca's area have been specified and implied to correspond to disparate functions. It has been proposed that the superior and posterior portions of the IFG (BA45/44) are related to phonological and syntactic processing, while the ventral and anterior portions of the

IFG (BA47/45) are more dedicated to semantic processing (Hagoort, 2005; Poldrack et al., 1999). Studies on the relationship between working memory and arithmetic with dual tasks have suggested the involvement of phonological processes in procedural strategies-based calculations as phonological load interfered with performance on arithmetic trials (Hecht, 2002); Imbo and Vandierendonck, 2007c). Hence, the activation in the left IFG during subtraction, especially in the superior and posterior part disclosed in this study, is more likely to correspond to extra phonological processes that contribute to a temporary storage of verbal information, such as subvocal rehearsal of operands or intermediate results. With regard to the left SMA, this area was proposed to be associated with movement sequencing for a series of mental manipulations during calculations (Clower and Alexander, 1998; Nieder and Dehaene, 2009). However, recent experiments have demonstrated the great reliance on finger-counting-related perception during mental calculation in 8-13 year-old children, particularly during larger subtraction problems requiring numerical quantity processing (Berteletti and Booth, 2015). Investigations with adult subjects also provided evidence on the overlapping brain circuits between arithmetic and finger representation (Andres et al., 2012). Given the crucial role of SMA in representations for finger movements (Diedrichsen et al., 2013), the converging results indicate the possibility that the SMA underlies finger perception when subjects engaged in arithmetic problem solving. Although our results do not allow us to disentangle whether the SMA is involved in goal decomposing/sequencing or finger counting in the present study, it can be affirmed that subtraction employed an auxiliary process of motor representation relative to addition.

4.4   Common and Different Brain Networks for Mental Addition and Subtraction

This section is concerned with common and different brain networks involved in 2-digit addition and subtraction calculations. The fMRI can be used for studying both, functional segregation and functional integration. As an extension of the study on the segregated brain regions specific to addition and subtraction calculations in the previous section, we conducted functional connectivity analyses on the same dataset collected in our fMRI experiment. Functional connectivity is defined as the temporal dependency of neuronal activation patterns of anatomically separated brain regions (van den Heuvel and Hulshoff Pol, 2010). In the past years an increasing body of neuroimaging studies has started to explore functional connectivity by measuring the level of co-activation from distributed brain regions. As the result of fMRI analysis in the last section, significantly increased activation was found in the left IFG and SMA during subtraction calculation relative to addition calculation. We speculated that the subtraction-specific activation in the left IFG was implicated in phonological processing. To verify this assumption, we concentrated on the differences in brain region communications during different mental calculations.

4.4.1   Materials and Methods

Since this part of study is extended from the investigation mentioned in the last section, the information about participants, experimental design, MR data acquisition, and preprocessing steps here is same as that described in Section 4.3.1.

fMRI Analysis

Functional connectivity analyses were applied to elicit the latent association among the activated regions observed in addition and subtraction processes, with help of Resting-State fMRI Data Analysis Toolkit (REST) (Song et al., 2011). In order to test whether the significantly increased activation observed in the left inferior frontal gyrus (L. IFG, BA45) during subtraction processing (see Figure 4.4C) is related to phonological processing, this region (-56, 21, 18) was selected as the seed for further analyses. At first, a seed-centered voxel-wise connectivity analysis was performed voxel-by-voxel all over the brain after the linear trend was removed, to figure out the temporal correlations between the predefined spherical seed (radius = 5 mm) and all the other voxels. The Pearson correlation coefficients were computed between the mean time course extracted across voxels within the seed and time courses from any other voxels outside the seed. Resulting correlation coefficients were mapped onto the brain atlas for each subject after the Fisher's r-to-z transformation, and then followed by a one-sample t-test ($p < 0.05$, corrected for Bonferroni, with a minimum cluster size of $k > 10$) to obtain the significance at group-level. Finally, nine regions of interest (ROIs) were picked out based on the results of seed-centered analysis. For each subject, the mean time courses of the nine spherical ROIs (radius = 5 mm) were extracted and divided into addition section and subtraction sections corresponding to the AT blocks and ST blocks. After that, separate addition- and subtraction-specific networks were established based on the correlation coefficients between each pair of the nine ROIs for each operation, whereby the results were output as correlation matrices. For display purposes, each correlation matrix was then transformed into a binary matrix based on the threshold Z (Z = 0.203, corresponding r = 0.2). In each matrix, the edge between any two regions was 1 if the corresponding correlation coefficient significantly exceeded the threshold and 0

otherwise. At last, paired t-tests were applied to compare the same edges from different matrices.

4.4.2 Results

Results of Seed-Centered Connectivity Analysis

Ten regions including one site next to the seed located in the pars triangularis of the inferior frontal gyrus (IFGtri) on the left revealed high correlation to the seed (see Table 4.5). As shown in the top panel of Figure 4.5, the regions contained left IFGtri, putamen, anterior part of middle temporal gyrus (aMTG), posterior part of middle temporal gyrus (pMTG), supramarginal gyrus (SMG), AG, IPL, middle occipital gyrus (MOG), right IFGtri, and the orbital part of IFG (IFGorb), which generate a moderate left-hemisphere lateralization.

Operation-Specific Networks Revealed by Functional Connectivity Analysis

Nine ROIs were defined based on the aforementioned ten sites involved in the left IFGtri-centered network, thereamong, sites of left putamen and MOG were removed due to the little connection to numeric manipulation. Emerging evidence indicates that the putamen and MOG are more related to emotional response and feature/shape recognition, respectively (Andrews et al., 2015; Koster et al., 2015). On the other hand, the left IFGorb symmetric to its counterpart on the right hemisphere was recruited to replace the original peak of this region covered by the strong activation from the adjacent left IFGtri. The ROIs included left IFGtri (-56, 21,18), IFGorb (-30, 29, -12), aMTG (-50, -27, -9), pMTG (-56, -41, -6), SMG (-65, -37, 27), AG (-36, -59, 36), IPL (-50, -47, 44), right IFGtri (56, 32, 7), and right IFGorb (30, 29, -12). The functional

connectivities for addition and subtraction were calculated respectively based on the time courses between any pair of the ROIs. As shown in the bottom panel of Figure 4.5, it turned out that differences existed between the addition-specific and subtraction-specific networks. In the addition network, a total of 11 edges constituted a simple network. Each ROI connected to at most three neighboring ROIs except the left SMG that showed no connection to any node. For the subtraction network, in addition to the 11 edges involved in addition network, 16 subtraction-specific edges were identified. The 27 edges constituted a highly dense subtraction-specific network in which the striking increase of mutual connections between one ROI and all the others could be found. Most remarkable increase of edges centered at the left SMG, IPL, and right IFGorb.

Differences were uncovered in not only the density but also the intensity between the two networks. Two same edges from different networks were contrasted by using t-tests after the Fisher's r-to-z transformation. As shown in Figure 4.6, the intensity was significantly greater in subtraction network than in addition network for most edges. The left SMG, IPL, and right IFGorb presented stable correlation with the major nodes in the left hemisphere during subtraction processing.

4.4.3 Discussion

The left IFGtri is well known as BA45 and one part of the Broca's area that has been certified as an important locus for language processing. Plenty of studies reported the involvement of Broca's area in the three parallel processes of language: syntax, phonology, and semantics (Hagoort, 2005; Patel, 2003; Poldrack et al., 1999; Rodd et al., 2005). Subdivisions of Broca's area have been specified and implied to correspond to

disparate functions. It was proposed that the posterior aspect of the IFG (BA44/45) was related to phonological and syntactic processing, while the ventral and anterior aspect of the IFG (BA47/45) was more dedicated to semantic processing (Hagoort, 2005; Poldrack et al., 1999). However, prior studies have also emphasized the association between the BA 45 and non-verbal working memory (Rama and Courtney, 2005), response inhibition (Collette et al., 2001), and other cognitive functions (Hugdahl et al., 2006). Therefore, we attempted to verify whether the left IFGtri played a role in phonological processing by examining the other distributed brain regions showing co-activation with the left IFGtri.

Table 4.5: Regions showing significant correlations to the seed. Abbreviation: IFGtri, pars triangularis of the inferior frontal gyrus; aMTG, anterior part of middle temporal gyrus; pMTG, posterior part of middle temporal gyrus; SMG, supramarginal gyrus; MOG, middle occipital gyrus; IFGorb, orbital part of IFG.

Region	BA	Cluster	Talairach Coordinates			T-score
			x	y	z	
L. IFGtri	45	467	-56	21	18	35.58
R. IFGtri	45	160	56	32	7	13.36
R. IFGorb	47	17	30	29	-12	8.32
L. Putamen		55	-3	-26	-4	10.96
L. aMTG	21	70	-50	-27	-9	8.77
L. pMTG	20/21	58	-56	-41	-6	8.09
L. SMG	40	14	-65	-37	27	8.50
L. AG	39	25	-36	-59	36	8.38
L. IPL	40	31	-50	-47	44	8.35
L. MOG	19	43	-24	-81	18	8.00

As the seed, the left IFGtri depicted a moderate left-hemisphere lateralized network with other two frontal nodes in the right hemisphere. The pattern of co-activation with the seed was found in the left IFGorb, MTG, AG, SMG, IPL, right IFGtri, and IFGorb, which are largely overlapped with the left frontoparietal network specialized in

language processing (Smith et al., 2009). Both Broca's and Wernicke's areas are involved in this network in which neural activities strongly correspond to cognition-language paradigms. Among those regions showing co-activation, the left IFGtri and SMG are constantly proven to engage in phonological working memory based on their recruitment during tasks that rely heavily on this process, such as counting the syllables of a pseudo-word (Poldrack et al., 1999), repetition of a word (Price et al., 1996), or syllable identification in the presence of a low signal-to-noise ratio (Sekiyama et al., 2003). Nonetheless, the bilateral IFGorb and AG are more likely to be involved in semantic processing. These regions have been proposed to be dedicated to the online retrieval of semantic information (Demb et al., 1995), word generation (Gurd et al., 2002), and semantic processing of both words and pictures (Vandenberghe et al., 1996). In addition, the left AG and MTG are canonically recognized as the most important loci for language comprehension in the temporal-parietal regions. Although subtle dissociations exist among the regions revealing significant correlations to the left IFGtri, on the whole, co-activation in the cohort of regions that are all specialized in phonological and semantic processes demonstrated the role of the left IFGtri in language processing during subtraction calculation, rather than response inhibition or other cognitions. Especially, the regions of IFG also have been repeatedly found to be devoted in subtraction (Ischebeck et al., 2006; Yi-Rong et al., 2011). Other researchers also attributed their activation to processes in phonological working memory, such as the maintenance of intermediate mental operations (Fehr et al., 2007; Van Beek et al., 2014). Given that our findings are consistent with results of previous studies, we believe that the left IFGtri is specific to extra phonological processing when engaging in mental subtraction, facilitating a temporary storage of verbal information, such as subvocal rehearsal of operands or

intermediate results. With respect to the functional dissociation within the IFGtri-centered network, correlations between phonology-related and semantics-related regions are conceivable because the relevant module-phonological loop has been evidenced to be related to some semantic processes as well, e.g., semantic coding (Baddeley, 2003).
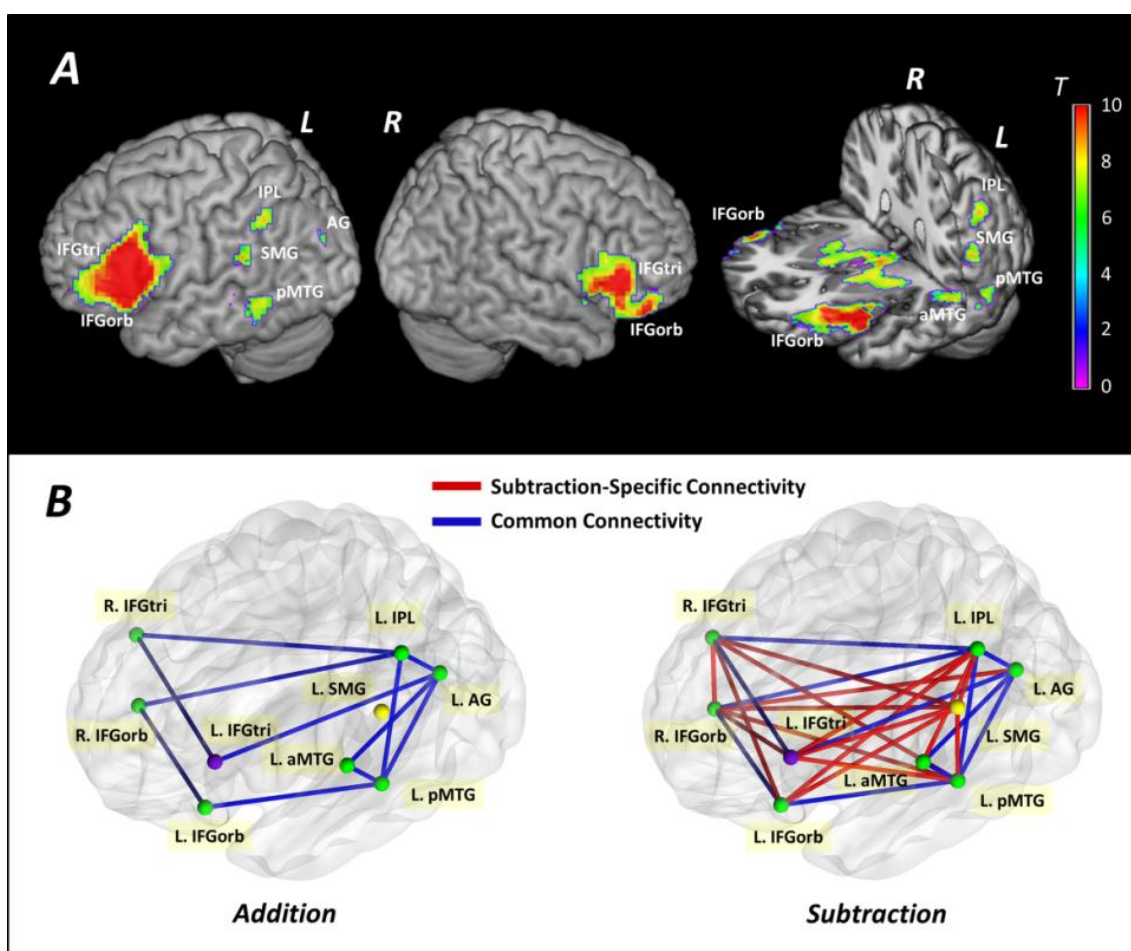
Fig. 4.5: Left IFGtri-centered and operation-specific networks. (A) Voxel-wise connectivity analysis centered at the left IFGtri (-56, 21, 18) generated a network with a moderate left-hemisphere lateralization. (B) Nine ROIs derived from the Left IFGtri-centered network constituted the addition- and subtraction-specific networks.

However, it is also possible that the IFGtri-centered network is pre-existing and thus independent of subtraction. To rule out such possibility, we constructed the addition-specific and subtraction-specific networks, and then compared them. A distinct reliance on the language-related network was shown for subtraction that could account for the differences between the two operations. Compared to addition, subtraction activated a more interactive language system with high internal density and significant intensity. The most important aspect is that the left IPL and its subdivision-SMG corresponding to magnitude processing showed more stable associations with the language-related sites, which implies the more synchronized neural activities between numerical manipulation and language processing during subtraction.

Recent researches attempted to extract the convergence among the language, mathematics, and Broca's area. Friedrich and Friederici (2009) revealed that the neural network underlying syntactic processing of abstract mathematical formulae was partially overlapped with the network subserving rule-based formal languages, with the involvement of BA45 (despite its misregistration with the cytoarchitectonically defined Broca's area). Their latest study indicated that the reason why the abstract algebra formulae appeared more difficult than the concrete arithmetic formulae, although they shared a common underlying structure, could be explained by the additional linguistic interpretation on the abstract formulae recruiting a fronto-parietal network (Friedrich and Friederici, 2013). Obviously, subtraction is not as abstract as the algebra formulae, nevertheless, it is always considered to be more difficult than addition by most people. Thus, we speculate that the activation induced by subtraction in the left IFGtri may be associated with the phonological processing as well. The calculation of subtraction needs to draw extra support from the left IFGtri other than the shared neural substrates underlying fact retrieval and actual calculation that is common with addition.
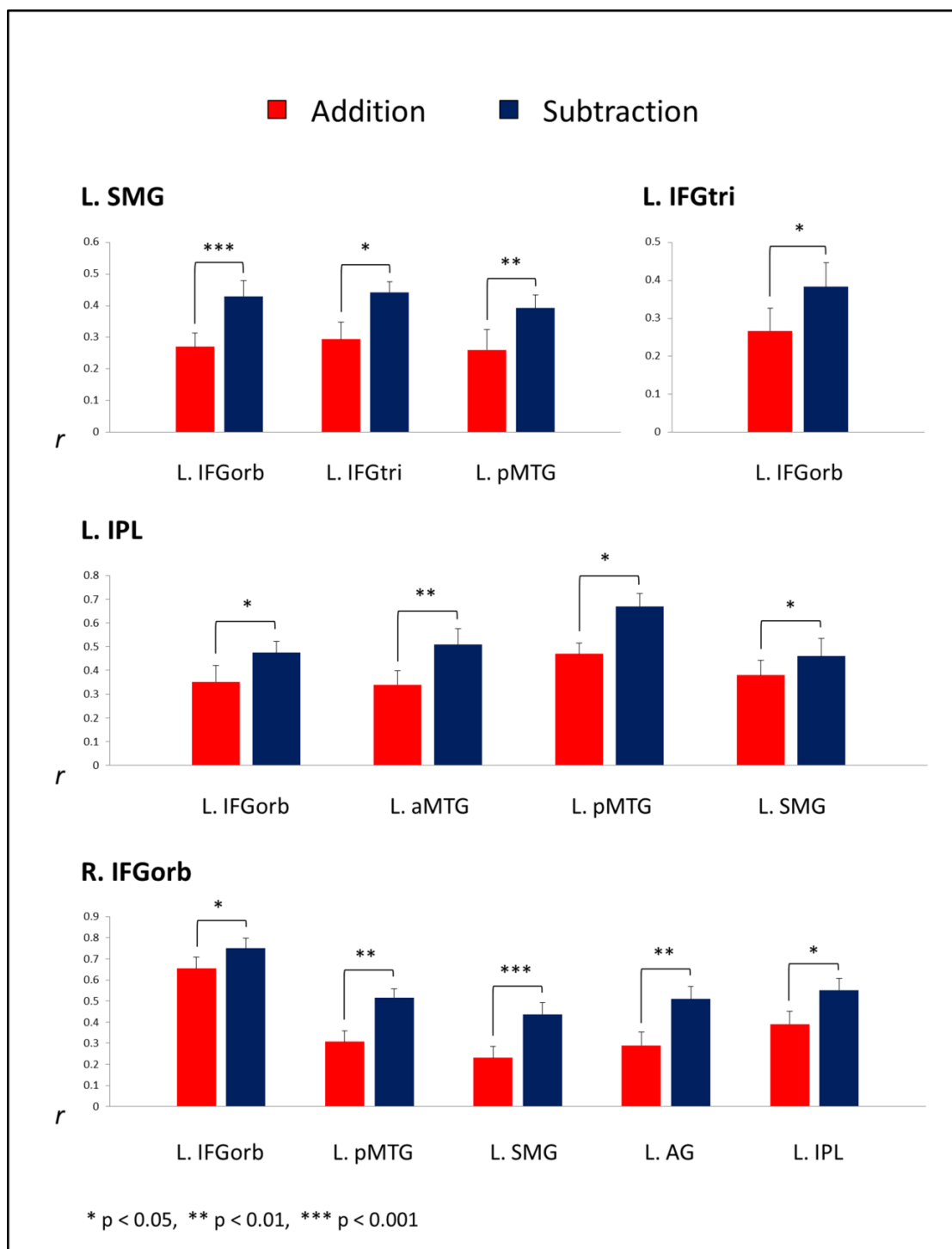
Fig. 4.6: Intensity differences between addition-related and subtraction-related networks. Connectivities in subtraction showed significantly higher intensity than in addition. The three nodes of left SMG, IPL, and right IFGorb presented stable correlation with the major nodes in the left hemisphere during subtraction processing.

As a result, subtraction appears more complicated. However, it has been generally accepted that the human comprehension on the magnitude is resembled to a mental number line primarily localized in the parietal lobe (Dehaene and Cohen, 1997; Dehaene et al., 2003). Thus the left IFGtri perhaps only plays an auxiliary role in the subvocal rehearsal of operands or intermediate results. In line with the previous study, Price et al. (Price et al., 1999) investigated on patients and suggested that the IFG may contribute to semantic processing in the healthy brain but be not absolutely necessary for task completion. The BA45 was proposed to only affect the efficiency aspect but not all of the semantic function (Binder et al., 2009). Historically, the mathematical representation went through a fronto-parietal shift and no longer put strong demands on language area, which looks perhaps similar to second-language acquisition where higher proficiency in past-tense formation leads to a decrease in IFG activation (Maruyama et al., 2012; Tatsuno and Sakai, 2005). As a result, when solving the arithmetic problems, it is more plausible to summarize that the left IFGtri is involved in a partial modulation in the numerical understanding, such as the aspect of efficiency.

4.5 Dynamic Causal Differences between Mental Addition and Subtraction

It is still ambiguous how the differences occur in neuronal mechanism between mental addition and subtraction. In this section, we focused on the dynamic interactions between brain regions activated by mental arithmetic. Using fMRI measurement and a dynamic causal modeling (DCM) approach, this part of study aimed to identify the neural substrates underlying the latent reason for differences between cognitive processes of simple addition and subtraction calculations.

To address the ambiguity about the neuronal processes underlying addition and subtraction, effective connectivity analysis can be used to characterize distributed and context-sensitive neuronal processing by referring explicitly to the influence that one neural system exerts over another at a neuronal level (Friston, 2011). In this study, we examined the directed (effective) connectivity among brain regions during addition and subtraction with dynamic causal modeling (DCM) (Friston et al., 2003). This biophysical model of the underlying neuronal interactions among an a priori selected set of brain regions (nodes) is based on a system of bilinear differential state equations with coupling parameters specified by three matrices (A matrix, B matrix, and C matrix) (Friston et al., 2003). These parameters correspond to the effective connectivity. The purpose of DCM is to estimate the coupling parameters of a model and evaluate how well a particular model explains the observed data. In other words, one first identifies the best model, in terms of which parameters exist − and then one examines the parameter estimates to make inferences about directed coupling among regions. This involves inferring which nodes receive endogenous (or fixed) connections from other nodes (encoded by the A matrix parameters), which specific connections are modulated (i.e., enhanced or reduced transmission between nodes) by experimental conditions (encoded by the B matrix parameters), and which nodes receive driving inputs (stimuli) from experimental manipulations (encoded by the C matrix parameters). Typically, several pre-specified models can be compared, and one model that represents the best explanation for the data among hypothesized models can be identified by Bayesian model selection (BMS) (Penny et al., 2004). Alternatively, one can perform an exhaustive search over all possible combinations of connections to identify the best model − all average the parameter estimates over models to produce the Bayesian parameter average. In this work, we will use Bayesian model reduction to perform

exhaustive searches over all combinations of connections (and how they change between addition and subtraction) to identify the underlying functional architecture. This is known as structure learning or network discovery.

In this analysis, we examined the directive connectivity among the brain regions identified by the whole brain analysis above using dynamic causal modeling (DCM) (Friston et al., 2003). DCM analyses generally focus on a subgraph or limited number of brain regions to reduce the number of extrinsic connections and their conditional dependencies (Daunizeau et al., 2011). Studying a few key regions also reduces computational load (Ma et al., 2015). Although, we used a relatively small number of regions, the number of potential architectures or models entailed by each DCM is potentially enormous. However, recent advances in DCM (Bayesian model reduction) have been introduced that can be used for structure learning or network discovery. This approach searches for an optimum model by identifying the sparsity structure (i.e., absence of connections, or modulatory effects) using an efficient form of model comparison (Friston et al., 2011). In what follows, we described the specification of the regions or nodes and how regional activities were summarized. We then describe the connectivity architectures of two (full) models that were subsequently used to explore (reduced) variants with one or more connections (changes in connections) removed.

Our results revealed significantly greater activation in the left inferior frontal gyrus (IFG) and supplementary motor area (SMA) during subtraction compared with addition processes in Section 4.3, indicating auxiliary processing for phonology (e.g., subvocal rehearsal) and motor representation (e.g., finger counting) in subtraction calculations. Further investigation with the DCM network discovery revealed partially overlapping endogenous networks underpinning the two operations. However, our findings also endorse previous hypotheses about the differences in strategic implementation,

dominant hemisphere, and the neuronal circuits underlying addition and subtraction. Moreover, for simple arithmetic, our connectivity results suggest that subtraction calls on more complex processing than addition: auxiliary phonological, visual, and motor processes, for representing numbers, were needed for subtraction, relative to addition.

4.5.1 Materials and Methods

Since this part of study is extended from the investigation mentioned in the last section, the information about participants, experimental design, MR data acquisition, and preprocessing steps here is same as that described in Section 4.3.1.

Regions of Interest and Time Series Extraction

Three components are necessary for specifying a DCM: (i) a design matrix of external or experimental inputs and (ii) the time series stored in volume-of-interest (VOI) files and (iii) on an adjacency matrix or graph specifying which connections at present (and how they are affected by experimental condition). The design matrix that is optimal for a given DCM is sometimes subtly different than the one used for fMRI univariate analysis, since the regressors of the design matrix need to be recombined to define the explanatory variables and inputs for the DCM. However, this re-combination does not change the underlying general model, simply the way in which the explanatory variables are combined to explain neuronal responses in the DCM.

Here, we used an experimental input that covered all number processing and two distinct inputs for addition and subtraction: in detail, we used three experimental inputs (1) "Number processing" that comprised all conditions with visual number input, i.e., AT, ST, and NT; (2) "Addition" that was exclusively involved in addition-specific blocks and (3) "Subtraction" that model subtraction blocks. Regions or volumes of

interest (VOIs) showing addition and subtraction effects were identified using the group-level random effects in the aforementioned whole brain analysis (see Figure 4.7). The coordinates of midpoints among the voxels showing peak responses for addition and subtraction were selected for time-series extraction. Other common regions with deactivation overlapped the default mode network (DMN) (Fox et al., 2005) and thus were considered as task-negative areas and not included in DCM analysis. Subtraction-specific regions – with activation that could only be observed when comparing subtraction to the control task – were selected to represent subtraction-specific areas. Most of these overlapped the dorsal pathway associated with magnitude or quantitative processing (Klein et al., 2013). With the help of the VOI tool in SPM8, time series were taken from 8 mm spheres centered on each region, using the principal eigenvariate across all suprathreshold voxels for each participant (uncorrected $P < 0.05$), with the mean and other confounds removed from the measured time-series (Stephan et al., 2010). Please see the results section and Figure 4.7 for the (average) location of the ensuing regions.

DCMs Specification and Network Discovery

As implemented in DCM 12 in SPM12b (http://www.fil.ion.ucl.ac.uk/spm), we then specified full connectivity models: all within-node (intrinsic) and between-node (extrinsic) connections for both the endogenous (fixed) connectivity and modulation effects were considered. The term "modulation effect" denotes bilinear modulation effects in the context of a deterministic DCM. These bilinear effects model the change in connectivity attributable to addition or subtraction. The number processing experimental input entered at the hierarchically lowest region above the fusiform gyrus (Dehaene and Cohen, 1997; Schmithorst and Brown, 2004). This driving input was

modeled in terms of the C matrix. The remaining (addition and subtraction) inputs exerted only modulatory effects on intrinsic and extrinsic connections. These modulatory effects were modeled using two B matrices.
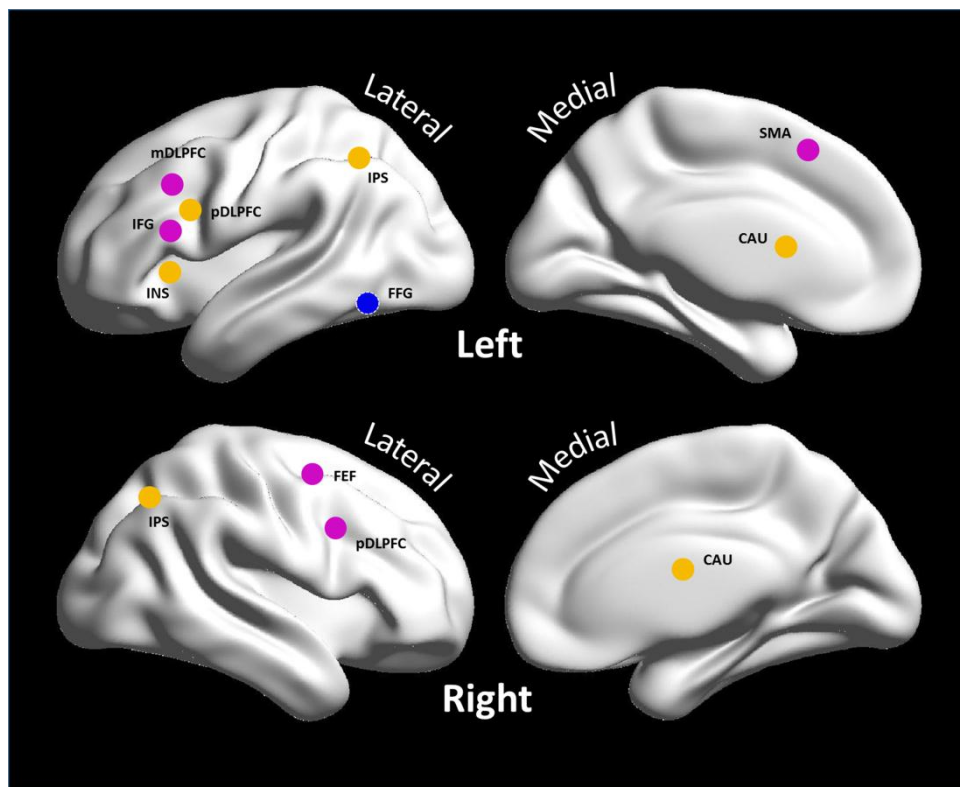
Fig. 4.7: Volumes-of-interest (VOIs) selected for the DCM analysis. Orange spots denote brain regions with common activation during both addition and subtraction processes; purple spots denote brain regions with activation during subtraction only; the blue spot denotes where the number processing experimental input entered the brain. Abbreviation: IFG, inferior frontal gyrus; mDLPFC, middle portion of dorsolateral frontal cortex; pDLPFC, posterior portion of dorsolateral prefrontal cortex; INS, insula; IPS, intraparietal sulcus; FFG, fusiform gyrus; CAU, caudate; SMA, supplementary motor area; FEF, frontal eye field.

We investigated two distinct networks comprising six and eight nodes respectively. The first network comprised nodes that showed both addition and subtraction effects, while the second network focused more on subtraction – comprising nodes that showed significant subtraction effects, relative to the number task. These two networks

correspond to the ventral and dorsal pathway regions implicated in arithmetic computations. We will refer to them as the ventral pathway (first) and dorsal pathway (second) DCMs respectively.

Finally, the resulting models were pruned to discover the most likely model of connections (and their modulation by addition and subtraction). These procedures rely upon Bayesian model reduction (Friston et al., 2011). This reduction searched over all possible reduced models of our fully connected models and returned a discovered network that best explained the observed fMRI data. Changes in connectivity were quantified using Bayesian model averages over the reduced model space. These changes are expressed in hertz – because connection strengths in DCM can be regarded as rate constants, i.e., the rate of change in a target area produced by unit activity in another.

4.5.2   Results

Six regions corresponding to areas activated by both addition and subtraction were included in the first DCM. These comprised the bilateral IPS, bilateral caudate nuclei, left pDLPFC, and left insula. The second DCM corresponded to the dorsal pathway network for subtraction and included eight regions showing subtraction effects, including the right pDLPFC, right FEF, left SMA, left IFG, left mDLPFC, in addition to the bilateral IPS and left pDLPFC that were also included in the common network. The location and coordinates of the ensuing 14 nodes node comprising the two networks are shown in Figure 4.7 and Table 4.6.

The network discovery identified optimal sparse model structures from initial full models (by pooling model evidence over subjects). Redundant connections (and changes) with low posterior probability are effectively eliminated. The remaining

connectivity and modulatory effects with nonzero posterior probability (with a mean of 97.33%) were regarded as the key structure of the discovered networks.

With respect to the six-node (ventral pathway) DCM comprising both addition and subtraction nodes, the connectivity matrix (A matrix) exhibited a highly interconnected (dense) infrastructure (see Figure 4.8A). All nodes were linked by bidirectional connections with the exception of connections from the left IPS to the left caudate, from the right IPS to the right caudate, from the left IPS to the right caudate, and from the left pDLPFC to the left caudate.

Table 4.6: VOIs selected for DCM analysis. Abbreviation: IPS, intraparietal sulcus; pDLPFC, posterior portion of dorsolateral prefrontal cortex; FEF, frontal eye field; SMA, supplementary motor area; IFG, inferior frontal gyrus; mDLPFC, middle portion of dorsolateral frontal cortex; FFG, fusiform gyrus; L, left; R, right; BA, Brodmann area.

Region	BA	Talairach Coordinates		
		x	y	z
Common				
L. IPS	40	-27	-54	49
R. IPS	7	27	-56	44
L. pDLPFC	9	-44	7	27
L. Caudate		-8	5	13
R. Caudate		12	-2	17
L. Insula	13	-30	22	3
Subtraction-Specific				
L. IPS	40	-27	-54	49
R. IPS	7	27	-56	44
L. pDLPFC	9	-44	7	27
R. pDLPFC	9	48	5	27
R. FEF	6	33	2	50
L. SMA	6/32	-3	11	50
L. IFG	45/44	-56	21	18
L.mDLPFC	8/9	-50	18	47
Driving Input				
L. FFG	37	-48	-51	-13
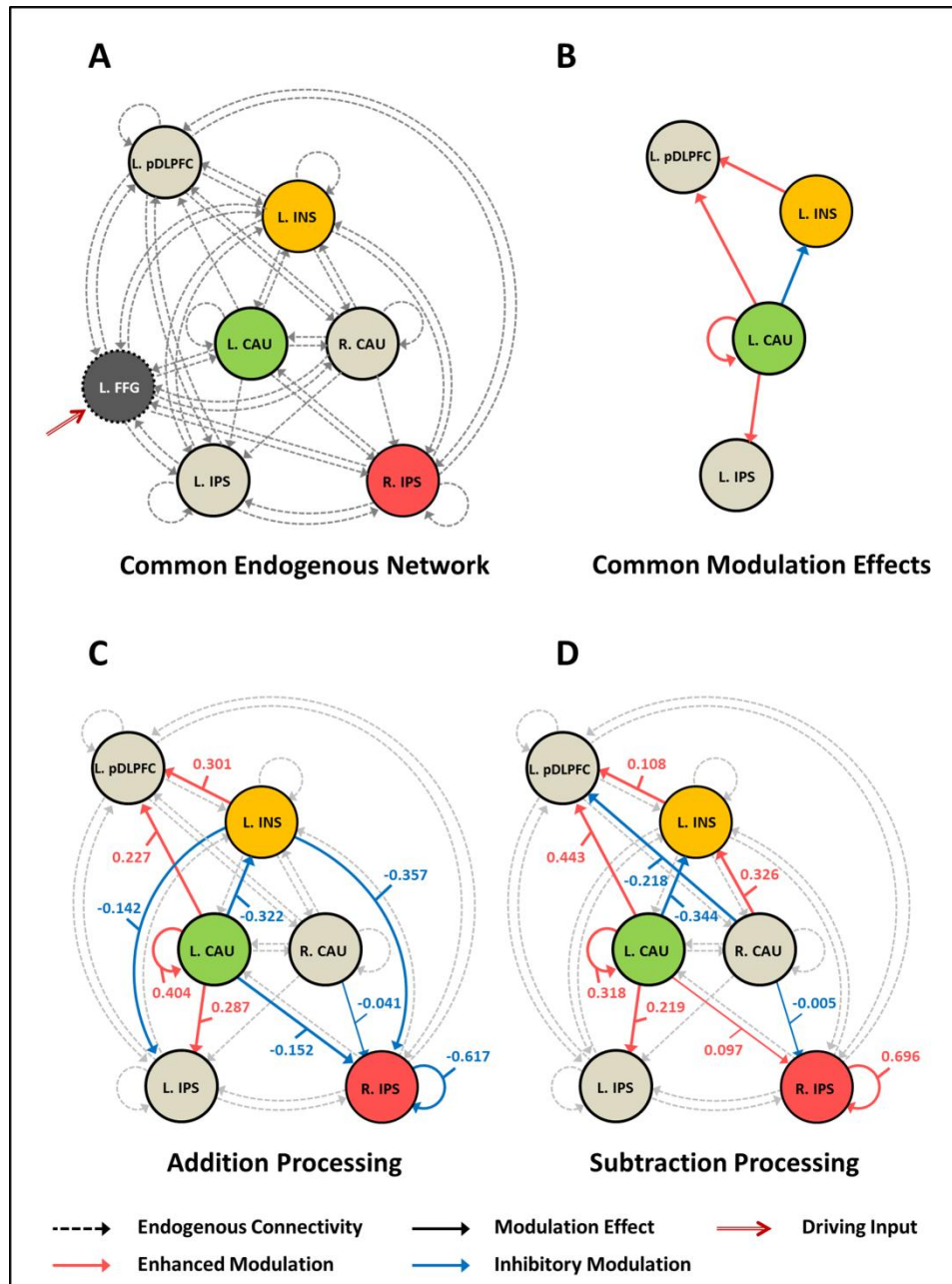
Fig. 4.8: Networks discovered for arithmetic operations based on six (ventral pathway) regions showing addition and subtraction effects. (A) Addition and subtraction processes shared a network with common endogenous (or fixed) connectivity revealed by non-redundant parameters in the A matrix; (B) a core network with identical nodes, connections, and modulatory directions (enhancement or suppression with addition and subtraction) was identified; (C) modulatory effects elicited by addition processing; (D) modulatory effects elicited by subtraction processing; Abbreviation: FFG, fusiform gyrus; IPS, intraparietal sulcus; pDLPFC, posterior portion of dorsolateral prefrontal cortex; INS, insula; CAU, caudate; L, left; R, right.

In terms of the modulatory effects of addition and subtraction, several connections showed enhanced or inhibitory effects to facilitate arithmetic processing. For addition (see Figure 4.8C), enhanced effects were imposed on connections from the left caudate to the left pDLPFC, from the left caudate to the left IPS, from the left insula to the left pDLPFC, and the self-connection in the left caudate. Inhibitory effects were inferred on connections from the left insula to the left IPS, from the left insula to the right IPS, from the left caudate to the left insula, from the left caudate to the right IPS, from the right caudate to the right IPS, and the self-connection in the right IPS. For subtraction (see Figure 4.8D), enhanced connections were found from the left caudate to the left pDLPFC, from the left caudate to the left IPS, from the left caudate to the right IPS, from the left insula to the left pDLPFC, from the right caudate to the left insula, as well as from the left caudate and right IPS to themselves. Inhibitory effects were exerted on connections from the left caudate to the left insula, from the right caudate to the left pDLPFC, and from the right caudate to the right IPS.

As shown in Figure 4.8B, a core component of the network with overlapping nodes, connections, and modulatory effects (enhancement or suppression) between addition and subtraction processes was identified. We compared the changes in connectivity using paired t-tests to examine differences in the ventral pathway (see Table 4.7). Only two connections showed significant differences, which were from the left caudate to the left IPS and from the left caudate to the left pDLPFC, with corrected p values of 0.049 and 0.032, respectively.

With respect to the extended subtraction network used to characterize effective connectivity in the magnitude-related dorsal pathway, most of the eight nodes were bidirectionally connected (see Figure 4.9A). Absences of fixed connections were all afferent connections associated with the left IFG, from the left mDLPFC, right FEF, and

right IPS, respectively. A few of the connections were enhanced by subtraction (see Figure 4.9B), including those from the left IFG to the left SMA, left pDLPFC, and right IPS, respectively, in addition to the connection from the left IPS to the right IPS and self-connections in the left SMA and right IPS. Inhibitory effects of subtraction were seen on connections from the left pDLPFC to the right IPS, from the right FEF to the right IPS, and from the left mDLPFC to itself.

Table 4.7: Directed connections and corresponding modulatory changes in the first (ventral pathway) DCM. Modulatory effects at the group level revealed by Bayesian parameter averaging (BPA) and statistics between networks are presented. Abbreviation: CAU, caudate; IPS, intraparietal sulcus; pDLPFC, posterior portion of dorsolateral prefrontal cortex; L, left.

Connectivity		Modulatory Strengths		*P*
From	*To*	**Addition**	**Subtraction**	
L. CAU	L. IPS	0.287	0.219	0.049[*]
L. CAU	L. pDLPFC	0.227	0.443	0.032[*]
L. CAU	L. CAU	0.404	0.318	0.276
L. CAU	L. INS	-0.321	-0.344	0.292
L. INS	L. pDLPFC	0.301	0.108	0.148

4.5.3 Discussion

In the present study, we compared the neuronal processes involved in mental arithmetic, specifically addition and subtraction, in 20 normal healthy subjects by using simple calculation problems − with a special focus on the differences between addition and subtraction. To examine distributed processing during addition and subtraction, we conducted effective connectivity analysis using DCM (in a structured learning or discovery mode) by identifying optimum architectures. Our results disclosed a ventral-pathway-dependent addition network and a subtraction network comprising both

ventral and dorsal pathways. Moreover, the distributed nature of differences between addition and subtraction – in terms of strategies and laterality were also revealed by examining the connectivity between brain regions.
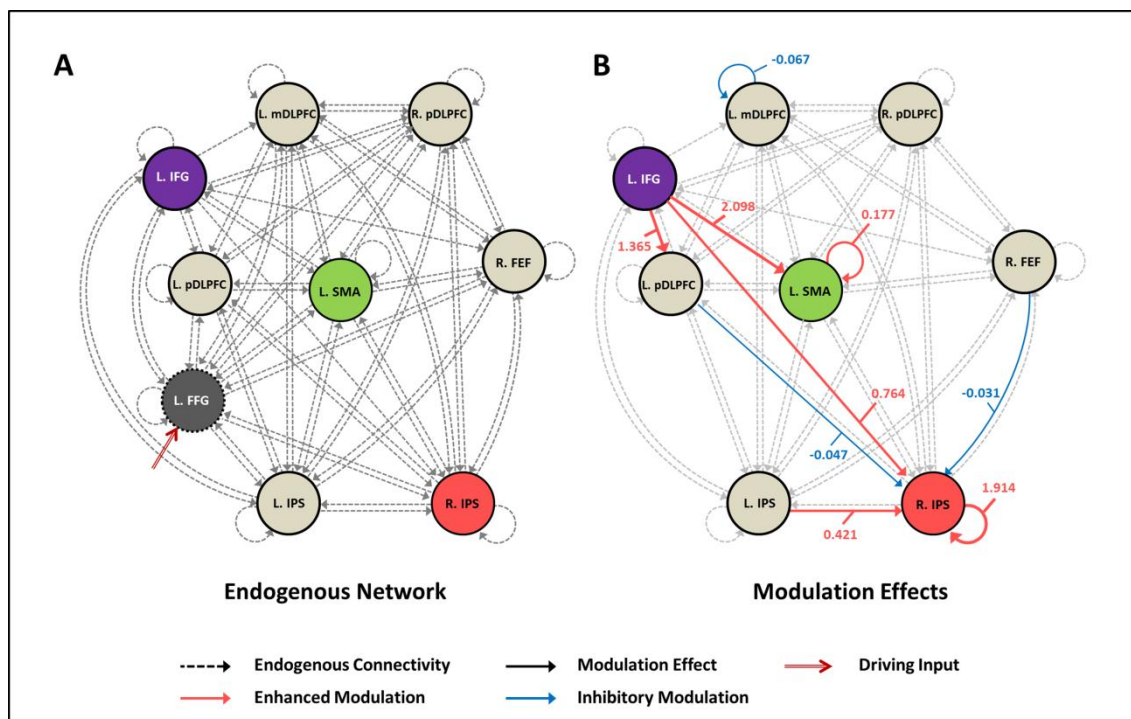
Fig. 4.9: Optimum model for the extended subtraction (dorsal pathway) network. (A) The endogenous (or fixed) connectivity was revealed by non-redundant entries in the A matrix; (B) modulatory effects of subtraction encoded by the B matrix are shown with corresponding changes in connectivity (in hertz). Abbreviation: FFG, fusiform gyrus; IPS, intraparietal sulcus; pDLPFC, posterior portion of dorsolateral prefrontal cortex; IFG, inferior frontal gyrus; FEF, frontal eye field; SMA, supplementary motor area; mDLPFC, middle portion of dorsolateral frontal cortex; L, left; R, right.

Simple mental arithmetic problems induced activation in a wide range of brain regions that were consistent with most previous studies on mental arithmetic (Arsalidou and Taylor, 2011), such as the bilateral IPS and insula, the left DLPFC, IFG, SMA, FFG, and caudate nuclei, and induced decreased activation located in the regions of the default mode network (DMN) (Fox et al., 2005), including the bilateral ITG, AG, mPFC,

and PCC. As Klein et al. (2013) proposed, the bilateral IPS, posterior IPS, SMA, FEF, and the left IFG (BA44, 45, 47) and the right IFG (BA45) constituted the dorsal pathway; whereas the perisylvian, occipito-temporal, and subcortical areas appeared to be connected entirely via the ventral route. Thus, many of resulting regions were specific to subtraction calculation (see Figure 4.7), and demonstrated a recruitment of a network comprising ventral and dorsal areas during subtraction – and only ventral areas during addition.

Subtraction produced significantly greater activation in the inferior frontal areas covering the left IFG (BA45/44) and middle part of DLPFC (mDLPFC), as well as the left SMA than addition (as shown in Figure 4.4C). The left IFG is well known as one part of Broca's area that is an important locus for linguistic processing and working memory (D'Esposito et al., 1999; Gabrieli et al., 1998; Mainy et al., 2007; Poldrack et al., 1999). Subdivisions of Broca's area have been specified and implicated in disparate functions. It has been proposed that the superior and posterior portions of the IFG (BA45/44) are related to phonological and syntactic processing, while the ventral and anterior portions of the IFG (BA47/45) are more dedicated to semantic processing (Hagoort, 2005; Poldrack et al., 1999). Studies of the relationship between working memory and arithmetic (with dual tasks) have suggested the involvement of phonological processes in procedural strategy-based calculations as phonological load interfered with performance on arithmetic trials (Hecht, 2002; Imbo and Vandierendonck, 2007c). Hence, the activation in the left IFG during subtraction, especially in the superior and posterior part detected in this study, is likely to correspond to extra phonological processes that contribute to a temporary storage of verbal information, such as subvocal rehearsal of operands or intermediate results. Another key part of the frontal area is the mDLPFC. A large body of evidence associates this area

with visual working memory (Petrides, 2000; Stern et al., 2000). It has been suggested that the mDLPFC is related to the active monitoring of multiple events in working memory, such as the executive process of monitoring and manipulation of spatial information (Owen et al., 1996), self-ordered processes of visual stimuli (Petrides et al., 1993), and so forth. In the current study, therefore, a putative role of the mDLPFC in active monitoring of operands displayed sequentially can be plausibly inferred, providing a visual support to subserve working memory together with the phonological support contributed by the left IFG. With regard to the left SMA, this area has been associated with movement sequencing for a series of mental manipulations during calculation (Clower and Alexander, 1998; Nieder and Dehaene, 2009). However, recent experiments have demonstrated the great reliance on finger-counting-related perception during mental calculation in 8-13-year-old children, particularly during larger subtraction problems requiring numerical quantity processing (Berteletti and Booth, 2015). Studies of adult subjects also provide evidence for overlapping brain circuits that are shared between arithmetic and finger representation (Andres et al., 2012). Given the crucial role of SMA in representations for finger movements (Diedrichsen et al., 2013), the converging results indicate the possibility that the SMA underlies finger perception when subjects engage in arithmetic problem solving. Although our results do not allow us to ask whether the SMA is involved in goal decomposing/sequencing or finger counting, it is plausible that subtraction calls on an auxiliary process of motor representation, compared to addition. Collectively, significantly greater activation observed in the frontal areas in subtraction, relative to addition processes, is consistent with their specialization for procedural processing that implicates working memory and numeric representations in multiple forms.

To address the question of whether calculation differences exist in strategic

application and cerebral laterality, we performed a DCM analysis of networks based on six regions engaged by addition and subtraction. Our rationale was that addition and subtraction entail differential switching on or off (or modulating) connections within a distributed system. Effective connectivity describes the directed propagation of activity from one neuronal system to another in a context-sensitive fashion.

As suggested in many studies, the bilateral IPS may be the core neural substrate underlying magnitude representation (Ansari, 2008; Dehaene et al., 2003). The left posterior portion of DLPFC (BA 9) is specialized for working memory (Baddeley, 2003; Smith et al., 1998) and related to information segregation and integration (De Pisapia et al., 2007). We speculate that the left pDLPFC subserved the integration of sporadic information received from other nodes within the network, given the multiple afferent connections observed in our data. Compared with the fronto-parietal areas, the left caudate nucleus and left insula – which were categorized as fact-retrieval related ventral areas (Arsalidou and Taylor, 2011; Klein et al., 2013) – also played a crucial part in both addition and subtraction. As part of the basal ganglia, the caudate is implicated in higher-order motor control (Menon et al., 1998) as well as learning and memory (Graybiel, 2005; Nomura and Reber, 2008). The triple-code model suggests that the left caudate is involved in the retrieval of rote arithmetic facts since lesions to this area impair arithmetic fact retrieval from memory, irrespective of the particular arithmetic operation (Dehaene and Cohen, 1995, 1997). Place between information integration and mental representation, the insula may act as a toggle system that switches between outward processes (i.e., integration) and inward processes (i.e., representation) in line with its role as a network hub (i.e., salience network), responsible for switching between the executive control network and the default mode network during information processing (Arsalidou and Taylor, 2011; Sridharan et al., 2008).

Addition and subtraction specific networks were constructed on basis of the regions identified above (see Figure 4.8C and D), in which differential addition and subtraction modulation effects were quantified. Within both networks, connections for propagating signals (i.e., retrieved arithmetic facts) from the left caudate nucleus to the left IPS and pDLPFC were increased, indicating the contribution of fact retrieval to numeric processes and the final stage of information integration, not only in addition but also subtraction processes. However, modulated efferent connections from the left insula to the bilateral IPS distinguished the two networks. In terms of addition effects, connections from the left insula to the bilateral IPS were inhibited. In view of the established co-activation associated with the anterior portion of insula (as activated in this study) and fronto-parietal cognitive processing areas and the causality of salience detection and executive processing (Uddin, 2015), it is possible that observed inhibitory connections suppressed the functioning of the bilateral IPS during addition. Conversely, such inhibition was not seen in the effects of subtraction on network connectivity, suggesting more reliance on magnitude-related processing in subtraction compared to prior selection of retrieved facts in addition. Another apparent difference between subtraction and addition comes from the distinct changes in afferent connections to the right IPS. Dissociations of the modulation effects on self-connections of the right IPS were revealed, reflecting suppression for addition and enhancement for subtraction processes, respectively. Due to the inhibitory properties of the self-connection, the suppression (decreased self-connection) indicates unlocking of neuronal excitability of sensitivity, while the enhancement (increased self-connection) suggests more rigorous limitation of the neural fluctuations. The former is more likely to associate with regions showing reduced activity, e.g., the right IPS in addition network, and the later might be related to regions showing greater activity, e.g., the right IPS in subtraction network and

the left caudate in both networks. In addition to the inhibitory effects received from the left insula, the afferent signal from the left caudate to the right IPS for transferring arithmetic facts was also suppressed in addition network, whereas the same connection was intensified in subtraction network.

The right IPS is considered to play a particularly important role in the quantitative processing of numbers. Although bilateral parietal areas are involved in manipulating magnitude information, number comparison-related task performance has been found to rely more on the right parietal lobule, while numerical processing, requiring access to linguistic code, is more strongly associated with the left hemisphere (Chochon et al., 1999). A right intraparietal lesion creates difficulties in quantitative processing of numbers, even when knowledge about arithmetic facts is unimpaired (Dehaene and Cohen, 1997). Evidence from intraoperative cortical electro-stimulation also demonstrates impaired performance on simple subtraction problems, compared to multiplication problems when receiving stimulation at right parietal areas (Yu et al., 2011).

Cues from dynamic interactions within the networks indicate how the nodes were differentially mobilized in addition and subtraction. We tentatively propose that subtle differences in use of computational strategies, rather than a double dissociation between simple multi-digit addition and subtraction processes. Based on a common frontal-subcortical-parietal circuit (as shown in Figure 4.8B) specialized for basic numeric representation, fact retrieval, and information integration, mental addition is more likely to employ a retrieval-based approach, while mental subtraction is likely to draw on the magnitude processing capabilities in the parietal cortex, especially the right IPS. With respect to the operation-specific laterality, our ventral pathway DCM analysis emphasizes the role of the right IPS and right caudate nucleus. It has been proposed that

the right caudate is involved in assigning priority values or sequence to information that needs to be processed in number tasks (Arsalidou and Taylor, 2011). Enhanced coupling of the right caudate and the left insula during subtraction suggests that this region might take a similar role to the insula in coordinating competing neuronal systems. More active participations of the right IPS and caudate in subtraction network suggest that, unlike the addition processes relying primarily on the left hemisphere, mental subtraction calls on the bilateral neural systems.

To substantiate our hypothesis that subtraction engages bilateral cerebral regions, we optimized an extended fully-connected network based on dorsal pathway (see Figure 4.4B and 4.9). A bilateral architecture is clearly seen. However, only a few fixed connections were modulated, which were largely associated with the right IPS. In line with aforementioned roles, the left IFG may support subtraction by transmitting phonological information to the left SMA, pDLPFC, and the right IPS. Enhancement under subtraction was seen for these connections. Connections from the left IPS to its right counterpart were also increased, suggesting a greater role of the right IPS than the left IPS in selecting the final answers in subtraction tasks. Inhibited afferent connections to the right IPS came from the left pDLPFC and right FEF. The former reduction is plausibly associated with restraints on spontaneous impulses for checking computations undertaken by the left pDLPFC − to ensure efficiency. The latter inhibition is likely to result from the particular saccade direction during multi-digit subtraction processing against the normal rightward reading habits of Chinese subjects. Since the right FEF was responsible for eye movement, and subtraction lead to leftward and downward shifts of spatial attention, which are opposite in addition (Fischer and Shaki, 2014). Regarding modulations of self-connections, the left SMA and right IPS were inhibited, whereas activity in the visual monitoring-related left mDLPFC was disinhibited. Taken

together, the right IPS showed responses to mental subtraction across the ventral and dorsal networks. In short, compared with the left-lateralized addition, subtraction is characterized by recruitment of bilateral circuits.

As for simple multi-digit arithmetic problems, our DCM results disclosed distinctions between mental addition and subtraction in strategic application, laterality, and inclusions of neural circuits. However, we speculate that such differences are not absolute. As the co-activation in both ventral and dorsal regions (that overlap with the subtraction pattern in current study) are also observed in complex addition (Klein et al., 2013; Stanescu-Cosson et al., 2000). It has been suggested that brain activation induced by addition shifts from subcortical and perisylvian language areas into dorsal regions, with the increasing difficulty of the problem (Klein et al., 2013); and previously reported differences between arithmetic operations probably emerged due to differential task complexity but not different types per se (Tschentscher and Hauk, 2014). Our data also support the possibility of context-sensitive neuronal couplings and available circuits in addition, given that addition and subtraction processes shared the same (fixed) network infrastructures. Nevertheless, when solving simple multi-digit arithmetic, we propose that addition presents easy problems that only engage the ventral pathway; whereas subtraction requires difficult mental arithmetic that calls on hybrid pathways. Our findings suggest that, on this occasion, mental subtraction is inherently more complex than mental addition. This perspective can also explain our behavioral results, in which subtraction was performed with significantly lower accuracy than addition ($p < 0.05$). To investigate whether subtraction is always more difficult than addition, further experiments may be necessary.

In our study, significantly greater activation in the frontal cortex (e.g., left IFG) that was related to more general (non-numerical) cognitive processes reflected the higher

task demands of subtraction. Nevertheless, Katzev et al. (2013) suggest that activation in the left IFG is mediated not only by task demands but also by individual ability. In this study, all of the subjects can be considered as skilled in solving simple mental arithmetic – due to their identical experience of at least 16 years of education in China. Further research is necessary to test whether the differences we found can be observed in individuals with low arithmetic ability. In addition, considering that the effect of abacus-based mental calculation training might be to enhance motor and visuospatial processes (Hu et al., 2011), we excluded subjects who had experience with an abacus using questionnaires.

4.6   Conclusion

Several limitations of the present study deserve comment. First, we only focused on the neural basis of differences between simple addition and subtraction processes. Therefore, we failed to provide direct evidence for the orthogonal effects of difficulty. Secondly, to ensure computability under the computational loads of network discovery procedures on data from 20 subjects, regions showing deactivation during both addition and subtraction calculations were excluded from DCM analyses. These included the bilateral AG, ITG, the left mPFC, and the right PCC, which responded in line with task-unrelated difficulty effects associated with the default mode network (DMN) (Buckner et al., 2008; McKiernan et al., 2003). Among these regions, the left AG has been repeatedly implicated in mental arithmetic, although its precise functional role has not been well established. Possible functions of the left AG have been linked with task-specific processes, such as arithmetic fact retrieval (Dehaene et al., 2003; Jost et al., 2011) and automatic mapping between mathematical symbols and their semantic

referents (Ansari, 2008; Grabner et al., 2013). However, no evidence has demonstrated that the left AG plays a distinct role from other components of the DMN or that it facilitated calculation in this study. Further study will be necessary to explore whether operation effects exist between the left AG and other calculation-related regions.

Differential cognitive processing during simple multi-digit mental addition and subtraction were examined by means of univariate and multivariate DCM analyses. By exploring information propagation among neuronal systems, our findings endorse earlier hypotheses about differences between mental addition and subtraction in strategic application, laterality, and engagement of neural circuits. Specifically, mental addition mainly relied on the so-called ventral circuit that includes temporo-parietal and subcortical-limbic areas; whereas subtraction depended on ventral as well as dorsal pathways, including extra fronto-parietal regions. Although a common frontal-subcortical-parietal network was recruited by both operations for processing basic numeric quantity and retrieval of arithmetic facts, addition appears to employ a retrieval-based approach based on the left hemisphere, while subtraction shows tendency to draw on magnitude or quantitative processing in bilateral parietal cortex, especially the right IPS. At the easy level of difficulty, mental subtraction is inherently more complex than mental addition. Auxiliary phonological, visual, and motor processes for representing numbers are also needed to complete the calculation of subtraction problems.

Studies on Emotion Regulation Using fMRI

The ability for humans to regulate emotion is a fundamental prerequisite for maintaining intact social lives, which impacts both emotional and mental well-being (Kohn et al., 2014). Generally, emotion regulation includes processes that amplify, attenuate, or maintain an emotion (Davidson et al., 2000). An inability to effectively down-regulate (attenuate) negative emotions when they arise distinguishes those who are vulnerable to emotional disorders—such as anxiety disorders and major depressive disorder (MDD)—from emotionally healthy individuals, and this is thought to underlie the pathogenesis of mental disorders (Johnstone et al., 2007). Therefore, unraveling the neural mechanisms underlying emotion regulation is key to furthering our understanding of emotional disorders. Theoretically, one important dimension of emotion regulation is the discrepancy between conscious regulation (i.e., guided by explicit intentions and accessible to one's own awareness) and automatic regulation (i.e., guided by implicit intentions or outside one's awareness) (Kohn et al., 2014). Although both are interesting and important, there is a lack of neuroscience-based studies addressing the latter issue (Ochsner et al., 2012). That is, studies have shown that when subjects are faced with a specific task requirement (e.g., "imagine that the crying woman in the picture is an actress who is performing"), they use top-down cognitive regulation of their emotion that recruits the cognitive system (e.g., attention or memory). The instruction provided along with the image actively elicits emotion regulation and

changes the way the subject appraises the meaning of an emotional stimulus. This task is followed by what we term a "modulated recovery period" from the emotional response since the instruction necessitate that the subjects change their emotion when confronted with the emotional stimulus. If no such instruction is provided, the subsequent recovery is instead regarded as a natural recovery period. There is still a lack of studies regarding whether cognitive regulation is required during natural recovery. Therefore, we implemented an fMRI experiment on the self-regulation of aversive emotion to investigate the emotion regulation processes underlying the natural recovery period. Moreover, we have proposed a model to explain the dynamic neural activity involved in self-regulating aversive emotion.

5.1 Introduction

Numerous researches on emotional response and its modulation have been yielded along with the widespread use of the fMRI (Davidson et al., 2000; Dolan, 2002; Wager et al., 2003). Compared with positive emotions, emotional experiences with negative valence induced by aversive stimuli are more instinctive, such as fear and disgust. Previous studies proposed specific circuits for fear and disgust respectively. In general, fear arouses a network composed of some prefronto-limbic areas including amygdala, insula, orbitofrontal cortex (OFC), and anterior cingulate cortex (ACC) (Sehlmeyer et al., 2009). On the other hand, the disgust-related processing is implicated to be associated with basal ganglia (Jabbi et al., 2008). However, the involvement of basal ganglia can't be completely excluded from the fear-related network when threat is perceived. Evidence revealed that the caudate nucleus and putamen that are the primary components of basal ganglia were activated during subjects observed the fearful body

expressions (de Gelder et al., 2004). Other neuroimaging studies specifically reported frontal activity together with subcortical activations during processing of threat-related facial expressions (Liddell et al., 2005; Muhlberger et al., 2011). In addition, concurrence of both fear and disgust appeared in some circumstances. Investigations on blood-injection-injury (BII) phobia, spider phobia, and contamination-related obsessive-compulsive disorder (OCD) suggested all these disorders were characterized by both fear and disgust (Cavusoglu and Dirik, 2011; Cisler et al., 2009). Given the debatable independence of fear-specific circuit and the tangled relationship between fear and disgust, we didn't put focus on how to establish the respective network for fear and disgust, but concerned on the experience and self-modulation in treating the aversion induced by both fear and disgust.

Much of the progress has come from studies of aversive emotions, especially emotion conditioning based on the classic Pavlovian paradigm, in which the formation and learning procedure of aversive emotions are particularly highlighted while the aftermaths are always overlooked (Fox, 2006; Sehlmeyer et al., 2009). Relative to the stress response or emotional contagion, researches on the recovery from emotional discomfort is insufficient. It is more valuable to work out the recovery mechanism to those people who are suffering from traumas. For such a research, the longitudinal design is more preferable. Fox et al. (2006) implemented an experiment by tracing the subsequent brain activity at the 90-second resting period following fearful movie clips. Their findings revealed that short emotional events may have prolonged effects on spontaneous brain states at rest. We applied a similar pattern stressing the subsequent discomfort induced by aversive pictures. But the resting period was extended to 4 minutes since we supposed the recovery to be a slower and more gradual procedure.

It has come to light that people are inclined to monitor their mood state and

self-regulate their emotion to comfortable levels (Thayer et al., 1994). Attention deployment and cognitive change are two effective strategies to modulate emotions (Kanske et al., 2011). The present study attempted to investigate the overall process of brain-state shift and emotional self-regulation during the dynamic recovery of subjects, from they began to perceive aversive stimuli until finished the following rest, and also to verify the involvement of strategies during the recovery when considering its role in mediating the emotional regulation.

5.2   Top-Down Construction of Sets of Experiments

Different emotions exert distinctive powerful forces on human behaviors. BI methodology advocates a top-down consideration on the construction of intact brain data sets. A holistic investigation on the emotions requires the identifications and contrasts of fundamental emotions according to a set of definite criteria. Various proposals of categorization of emotions have been raised, such as the one proposed by Robinson, D. L. that distinguishes emotions based on subjective quality (e.g., pleasure or pain), object of emotional response (real or imagined), and induced behavior (Robinson, 2008). The present study only concentrated on the emotion of aversion. The others will be researched in our future works (see Figure 5.1).

Fig. 5.1: Systematic investigations on various types of emotions. A holistic investigation on the emotions facilitates the top-down construction of experiment sets.

5.3 Self-Recovery from Aversive Emotion

Regarding to aversive stimuli, previous studies on emotion response and formation are plentiful, whereas concentrations on the emotional recovery are comparatively insufficient. The present study focused on the discomfort induced by looking at aversive pictures, and the emotional self-regulation during the following recovery period. A functional magnetic resonance imaging (fMRI) experiment with prolonged paradigm was recruited to investigate how brain-state shifted across three stages: picture viewing, earlier resting period, and latter resting period. Comparing with neutral pictures, aversive pictures activated the caudate nucleus centric subcortical areas, which also kept firing during the resting period. Meanwhile an activation pattern gradually appeared in fronto-parietal regions that were found negatively correlated to subcortical areas. Our findings suggest that the emotional recovery from discomfort is also a procedure accompanied by the strategy shift from passively suppressing emotional response to actively controlling the attention.

5.3.1 Materials and Methods

Participants

We recruited twenty right-handed healthy postgraduates (10 females) with the mean age of 25 ± 1.3 years and normal or corrected-to-normal vision, to participate in the experiment. None of them reported any history of neurological or psychiatric diseases. All the subjects signed the informed consent and this study was approved by the Ethics committee of Xuanwu Hospital, Capital Medical University.

Stimuli and Procedure

Fifteen aversive pictures and fifteen neutral pictures were selected from the International Affective Picture System (IAPS) which is based on normative ratings in valence and arousal (Lang et al., 1998). In order to prevent failures of emotional arousal caused by subject's sensitivity differences, typical pictures (with salient ratings in both valence and arousal) with same type of valence but diverse contents were included, so that every subject would be affected by at least part of the pictures. The contents of pictures involving snakes, spiders, attacks, bloody wounds, and dead bodies were adopted for the aversive stimuli, with the mean valence of 2.61 ± 1.60 and the mean arousal of 6.30 ± 2.14. In contrast, pictures of household items in simple contexts (e.g., a cup on a table) were used as the neutral stimuli, with the mean valence of 5.01 ± 1.13 and the mean arousal of 3.05 ± 1.94. Duration for displaying each picture was 4 seconds which had been testified to be optimal by our preparatory experiment.

A one-group, "pre-post" test-designed fMRI experiment was used (see Figure 5.2). We presented the neutral pictures only in the pre-test session and aversive pictures only in the post-test session. In each session, fifteen emotional pictures were successively displayed for 1 minute, at a rate of 4 seconds per picture. Subjects were required to view all the pictures carefully. A four-minute resting period subsequently followed the picture viewing stage (PVS), in which subjects were asked to keep their eyes open and relax without thinking. In order to compare different phases, we divided the resting period into two parts factitiously: the first minute named early resting stage (ERS) and the last three minutes named later resting stage (LRS). The interval between the pre- and post-tests was 15 minutes.

MR Data Acquisition

A 3.0 T MRI system (Siemens Trio Tim; Siemens Medical System, Erlanger, Germany) and a 12-channel phased array head coil were employed for the scanning. Foam padding and headphone were used to limit head motion and reduce scanning noise. 192 slices of structural images with a thickness of 1 mm were acquired by using a T1 weighted 3D MPRAGE sequence (TR = 1600 ms, TE = 3.28 ms, TI = 800 ms, FOV = 256 × 256 mm2, flip angle = 9°, voxel size = 1 × 1 × 1 mm3). Functional images were collected through a T2 gradient-echo EPI sequence (TR = 2000 ms, TE = 31 ms, flip angle = 90°, FOV = 240 × 240 mm2, matrix size = 64 × 64). Thirty axial slices with a thickness of 4 mm and an interslice gap of 0.8 mm were acquired.

Fig. 5.2: Experimental paradigm. Subjects should view 15 neutral pictures in the pre-test session and 15 aversive pictures in the post-test session separately. Each session started with a 1-minute PVS, followed by a 1-minute ERS and a 3-minute LRS subsequently. The interval of the two sessions was 15 minutes. Abbreviations: PVS: picture viewing stage, ERS: early resting stage, LRS: later resting stage.

Data Preprocessing

The preprocessing of fMRI data was implemented with SPM8 software (Wellcome Trust Centre for Neuroimaging, London, UK, http://www.fil.ion.ucl. ac.uk). The first two images have been discarded to allow the magnetization to approach dynamic equilibrium. The data format was converted to make the fMRI data available for the

SPM software, then a series of stages followed: realignment that aimed at identifying and correcting redundant body motions, coregistering that merged the high resolution structural image with the mean image of the EPI series, normalization that adjusted the structural image to the MNI template and applied normalization parameters to EPI images, smoothing that had fMRI data smoothed with an 8 mm FWHM isotropic Gaussian kernel. After normalization, all volumes were resampled into 3×3×3 mm3 voxels. Head movement was less than 2 mm in all cases.

fMRI Analysis

Data from the two sessions were statistically analyzed by using SPM8. In one session, images of PVS, ERS, and LRS, and the contrasts among them were created individually based on the general linear model. In the group-level, paired t-tests were implemented for each stage to examine the different activated patterns between the pre-test and post-test. Moreover, one-sample t-tests were performed for the contrast images. For each session, the contrasts of ERS > PVS and LRS > PVS revealed the pattern of increased activation in the rest period compared with the picture viewing; the pattern of decreased activation was shown by the reverse contrasts. Activations reported survived an uncorrected voxel-level intensity threshold of $p < 0.001$ with minimum cluster size of $k > 30$ voxels. Regions of activation originally obtained in MNI coordinates were converted into Talairach coordinates with the GingerALE and labeled with Talairach Daemon (BrainMap Project, Research Imaging Center of the University of Texas Health Science Center, San Antonio, USA, http://brainmap.org).

Functional connectivity analysis was also applied to elicit the relationship between activation patterns. The ROIs (radius=6 mm) were defined based on the exploratory results. The mean time-course across voxels within an ROI was extracted after the linear

trend was removed, with the help of Resting-State fMRI Data Analysis Toolkit (Song et al., 2011). The Pearson correlation coefficients of the time courses between pairs of ROIs were used to determine the connectivity, with a threshold of the t-tests based on a Fisher's r-to-z transformation. Finally, a seed-oriented connectivity analysis was per-formed voxel-by-voxel all over the brain.

5.3.2 Results

Paired t-Tests between Two Sessions

It was shown that the aversive pictures in the post-test induced stronger and more extensive activation, while the neutral pictures in pre-test activated nowhere but the visual cortex. Images were contrasted in couples between the two sessions for each stage including the picture viewing, early resting period, and latter resting period. Increased activation was identified only in the contrast of Post-test > Pre-test, which may be associated with the discomfort caused by the aversive stimuli (see Table 5.1). In the PVS, significant brain activation was observed in visual cortex, posterior cingulate cortex, striatal-thalamic areas, motor cortex, and frontal cortex including the opercular and orbital parts. Activated regions reduced obviously in the ERS, involving the left lingual gyrus, left caudate nucleus, right superior temporal gyrus, and right posterior cingulate on. In the LRS, only activations of left lingual gyrus, left caudate nucleus, and the rostral portions of right middle frontal gyrus were detected (see Figure 5.3).

Shift of Brain-State in the Post-Test

The emotional arousal in each stage brought by aversive pictures was revealed by the paired t-tests. However, the apparent differences across the three stages could not be

identified unless the three stages were contrasted mutually. Thus, the contrasts of ERS vs. PVS and LRS vs. PVS in the post-test session were performed to show the processing of self-regulation and the shift of brain-state when subjects responded to the emotional discomfort (see Table 5.2). The contrast of ERS > PVS brought about the increased activation in fronto-parietal areas including angular gyrus and middle frontal gyrus, and the decreased activation in visual-spatial processing-related regions and areas corresponding to emotional salience, such as insula and hippocampus. The contrast of LRS > PVS inherited a homologous pattern, but with stronger increased activation in the fronto-parietal circuit and milder decreased activation in subcortical-limbic regions (see Figure 5.4).
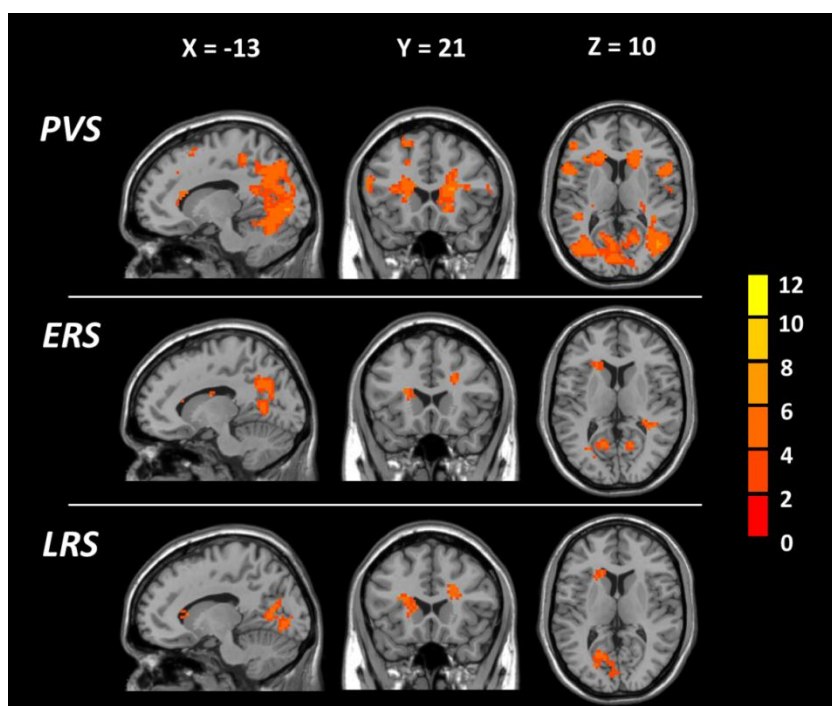
Fig. 5.3: Contrasts of different conditions. Images were compared in couples between the two sessions for each stage with the paired t-tests. Increased activation was identified only in the contrast of Post-test > Pre-test with the threshold of p < 0.001 (uncorrected) and k > 30, revealed in MNI coordinates. The Color bar indicates the t-score. Abbreviations: PVS: picture viewing stage, ERS: early resting stage, LRS: later resting stage.

Table 5.1: Activated regions revealed by the paired t-tests. Loci of maxima are in Talairach coordinates in millimeters.

Stage	Region	BA	Cluster	Talairach			T-score
(Post-test > Pre-test)				x	y	z	
PVS	L. MOG	19	805	-3	-67	-2	7.43
	L..IFG/PreCG	44/6	94	-3	-5	31	6.53
	L. MFG	46	10	-4	32	24	5.60
	L. PCun	31	28	-7	-69	15	5.54
	L. SOG	7	84	-1	-61	21	6.50
	L. Insula/CN		68	-2	19	17	6.62
	L. Thalamus		13	-2	-22	3	5.12
	L. STG	41	11	-4	-40	12	5.87
	R. FFG	37	34	32	-43	-15	6.62
	R. CN		72	18	24	21	7.63
	R. IFG	44	35	46	7	17	6.41
	R. OFC	47	30	46	31	1	4.61
	R. PoCG	4	42	46	-19	28	5.60
	R. PreCG	6	47	38	-5	27	6.62
	R. CG	31	29	12	-40	39	5.87
	L.R. SMA	6	27	-2	-11	64	5.33
	R. Thalamus		12	7	-10	18	5.75
	R. PCun	7	19	15	-57	38	4.88
ERS	L. LinG	19	416	-2	-73	-2	5.54
	L. CN		168	-2	19	17	5.01
	R. STG		46	27	-38	13	6.16
	R. PCC	30 / 3	33	13	-62	5	4.42
LRS	L.LinG	17	470	-1	-71	12	4.9
	L. CN		108	-1	22	7	4.93
	R. MFG	10	30	19	42	9	4.43

Table 5.2: Regions significantly activated following ERS vs. PVS and LRS vs. PVS. Loci of maxima are in Talairach coordinates in millimeters. All regions survived the statistical threshold of p < 0.001 (uncorrected), cluster size k > 30 voxels.

Contrast	Region	BA	Cluster	Talairach			T-score
				x	y	z	
ERS > PVS	L. AG	39/40	196	-46	-70	30	6.35
	R. AG	40	113	54	-56	30	5.95
	R. PCun	31	33	1	-70	31	4.38
	R. MFG	9	15	32	16	42	4.80
LRS > PVS	L. AG	39/40	65	-49	-56	31	4.82
	L. MFG	9	10	-32	22	39	4.67
	R. AG	39	21	54	-59	30	4.77
	R. SMG	40	33	43	-48	31	5.20
	R. MFG	9	38	29	19	40	4.76
ERS < PVS	L. MOG	18	967	-13	-96	7	7.35
	L. SPL	7	76	-27	-52	48	4.73
	R. MOG	19	602	24	-84	3	8.36
	R. SPL	7	215	23	-54	41	4.69
	R. Hipp	27	244	5	-36	-6	6.67
	R. Insula	13	153	40	-2	22	6.30
	R. Putamen		32	27	-8	-3	5.00
	R. PoCG	2	39	60	-23	36	4.50
LRS < PVS	L. MOG	18	1005	-15	-96	7	8.72
	R. MOG	18	643	24	-87	3	8.12
	R. PCun	7	121	29	-50	50	4.74
	R. PoCG	2	35	54	-30	47	4.49

Relationship between Caudate and Fronto-Parietal Network

The activation in caudate nucleus (CN) and posterior cingulate cortex (PCC) can be observed throughout the whole course in the post-test (see Figure 5.3). However, the activation in PCC dropped off as time passed, while the condition of CN seemed to be sustained, especially the one on the left. On the other hand, from the early rest to the latter rest, the activation of the fronto-parietal network (FPN) gradually emerged (see Figure 5.4).
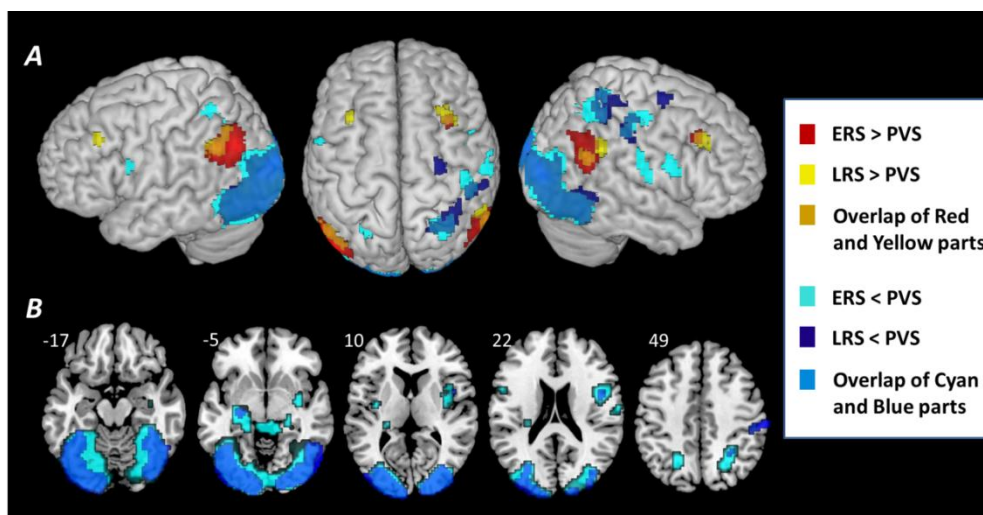
Fig. 5.4: Regions of activation were revealed by contrasts of ERS vs. PVS and LRS vs. PVS. (A) Both increasingly and decreasingly activated regions were rendered on the surface of brain. As increasingly activated regions, the fronto-parietal network (FPN) gradually emerged; (B) the decreased activation was presented in the axial view in MNI coordinates.

In order to understand the roles CN and FPN played during the recovery from emotional discomfort, and make out the interrelation between them, the functional connectivity analysis was performed. Firstly, five ROIs corresponding to left CN, bilateral middle frontal gyrus (MFG), and bilateral angular gyrus (AG) were selected. All the coordinates for the five ROIs were taken from the activated regions in the latter rest period in consideration of the instability of the other two stages. The ROIs were oriented at (-18, 22, 7), (-32, 22, 39), (29, 19, 40), (-49, -56, 31), and (54, -59, 30) respectively, in Talairach coordinates (see Table 5.1 and 5.2). The Pearson correlation coefficients of the time courses between any pair of the ROIs were calculated, followed by a t-test based on the Fisher's r-to-z transformation (see Figure 5.5). It turned out a significant negative correlation between left CN and right AG with the r value of -0.44 at two tailed 0.05 level. Connections between the left CN and other nodes could not be determined. In contrast, the other four nodes except CN demonstrated high correlation

to each other, which may imply the existence of segregation between CN and other fronto-parietal nodes during the emotion recovery. At last, the voxel-based connectivity analyses were conducted, using the left CN (-18, 22, 7) and right AG (54, -59, 30) as the center respectively. A dissociable pattern with two separate networks was generated. The CN centric network primarily involved the subcortical-limbic system, extending posteriorly to visual cortex, and dorsally to motor cortex. The AG centric network seemed to be associated with the default mode network (DMN), but mixed with some regions of emotional modulation and cognitive control, such as OFG and MFG.
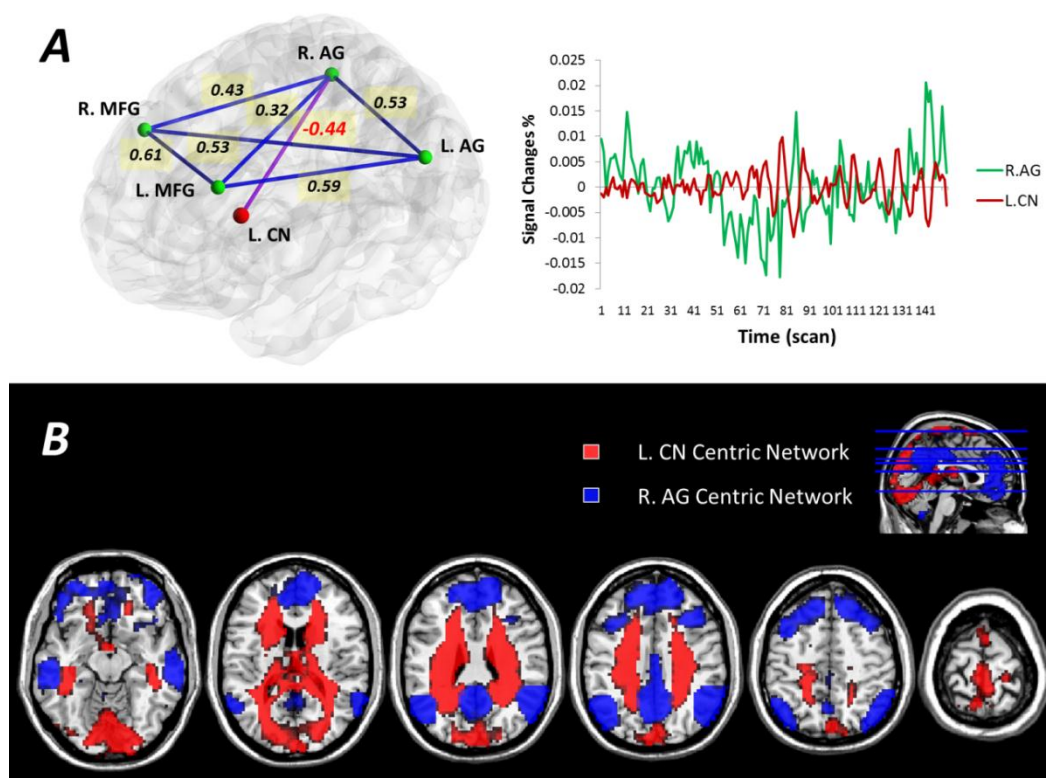
Fig. 5.5: Results of functional connectivity analyses. (A) A significant negative correlation was found between left CN and right AG with the r value of -0.44 at two tailed 0.05 level. The negative correlation can be seen from the blood oxygen level dependent (BOLD) signals extracted from the two ROIs. (B) Two networks were disassociated by voxel-based connectivity analysis. The left CN centric network primarily involved the subcortical-limbic system, together with the visual cortex, and motor cortex; the right AG centric network correlated with the default mode network (DMN), and extending to OFG and MFG.

5.3.3 Discussion

The present study revealed an overall perspective from three aspects: different patterns of brain activation induced by aversive stimuli, brain-state shift over the whole course of emotional self-regulation, and the neural circuits involved in these processing. From perceiving the fearful and disgusting pictures to reducing the emotional discomfort by self-modulation, an intrinsic mode on how to deal with the aversive emotions by switching strategies spontaneously emerged.

Pathways for Transferring the Aversive Information and Discomfort

The discomfort in the experiment was triggered by a complex emotion blending fear and disgust together, which caused activation mainly in caudate centric subcortical areas, but slightly in amygdala. The generation of the discomfort followed the transference of aversive stimuli through the cortico-basal ganglia-thalamo-cortical loop. In general, the basal ganglia was described as a set of input structures that receive direct input from the cerebral cortex, and output structures that project back to the cerebral cortex via the thalamus (Alexander et al., 1986). In this case, aversive stimuli were passed to the sub-cortical areas consisting of basal ganglia and thalamus along the visual ventral stream, which can be evidenced by the connections between visual cortex and subcortical areas in the CN centric network (see Figure 5.5). However, the subcortical areas functioned not only as a relay station, but also a significant node for processing the emotional information. In previous studies, the subcortical pathway was proposed to provide a quick analysis of the affective properties of stimuli that serves as an initial template for subsequent processing (LeDoux, 1998). Moreover, evidence also exists linking the caudate nucleus with aversive learning. Especially lesions to this region have led to failure in conditioned emotional response, conditioned freezing and passive and

active avoidance (White and Salinas, 2003). Thus, it is implied that the CN centric subcortical areas processed the aversive stimuli, and then delivered signals back to cerebral cortex accompanied with discomfort.

The Function of Caudate in Processing Discomfort

As a crucial element of the brain reward system that plays a critical role in the response to pleasure and pain, CN centric basal ganglia is directly activated in anticipation of aversive stimuli (Jensen et al., 2003). In this study, the role of right CN in emotional response can be inferred from the inhibitory activation when picture viewing finished (see Figure 5.3). Most activation in the frontal and temporal cortices including the right CN decayed rapidly from the resting periods began, which illustrated the dependence of such regions on the emotional stimuli. Nevertheless, the consistent activation in left CN presented its participation in the aftertreatment to the aversive emotion, indicating the function of some parts of caudate engaging in the modulation during emotional recovery. This processing may be connected to motor functions. In addition to the emotional functions, the primary function of basal ganglia is proposed to control and regulate activities of the motor and premotor cortical areas to promote the voluntary movements and manual response inhibition (Stocco et al., 2010). The striatum, the main input station of the basal ganglia, is considered as an important region for stopping. It is suggested that the striatum is involved in proactive inhibitory control over the primary motor cortex (M1) by suppression (Stocco et al., 2010). A similar procedure may have been applied to emotional self-regulation. Associating the connection to the regulation of aversive emotion, it is more likely that the CN centric basal ganglia modulate emotion by suppressing the emotional response to aversive stimuli.

The Switch of Strategies on Emotional Self-Regulation

Different strategies can be applied to regulate emotional responses (Kanske et al., 2011). Over the whole course of post-test session, two dissociable networks were displayed supporting two different strategies on emotional self-regulation. The left CN centric network made up of subcortical areas, visual cortex, and motor cortex, referred to a passive "strategy" of suppression; the right AG centric network primarily based on the DMN network mixed with bilateral MFG and OFG, referred to a strategy of active control. These right AG related regions were highly consistent with the executive-control net-work (ECN) that has been verified to be connected to working memory and control processes (Seeley et al., 2007). During the recovery procedure, the connection between MFG and posterior parietal cortex (PPC) tended to be closer as time went on, with increasingly common activation in the relevant areas. As shown in Figure 5.4, the pattern of common activation can be revealed more conspicuously in the latter resting state than in earlier resting state through the longitudinal contrasts among stages. The involvement of DMN and ECN can be interpreted to the deployment of attention in the latter resting period, moving from concentration on aversive emotions to self-referential processes, such as mind wandering. The BOLD signal of the right AG rising after initiatory dropping suggested the effect of attention deployment was getting stronger in the latter resting period, and the discomfort caused by aversive stimuli was getting attenuated corresponding to the negative correlation between right AG and left CN. It is implied that subjects gradually shifted their concerns away from the turning point. Therefore, the emotional recovery from discomfort is also a procedure accompanied by the strategy shift from passively inhibiting emotional response to actively control-ling the attention, although the both strategies were spontaneously utilized.

5.4 A Dynamic Causal Model of Emotion Self-Regulation in Healthy Subjects

In the previous fMRI study, twenty healthy volunteers were recruited to investigate the discomfort induced by viewing aversive pictures (with fearful and disgusting contents), and to prospect the emotional self-regulation during the following natural recovery period. Significant activation was continuously observed in the striatal region throughout the whole course of experiment (even when the display of aversive pictures stopped for a long while), showing the role of this subcortical region in not only generation of emotions (Wager et al., 2003), but also a bottom-up regulation on emotion by suppression. Due to the limited explanatory power of functional connectivity analysis utilized in the previous study, its results were insufficient to thoroughly interpret how the two disassociated systems interplay at a neuronal level. Therefore, further research was conducted. In this section, data derived from the same group of twenty volunteers that correspond to the period of picture viewing were reanalyzed with dynamic causal modeling (DCM) (Friston et al., 2003).

5.4.1 Materials and Methods

Since this part of study is extended from the investigation mentioned in the last section, the information about participants, experimental design, MR data acquisition, and preprocessing steps here is same as that described in Section 5.3.1.

fMRI Analysis

We divided the 1-minute period of picture viewing into three phases for both the neutral and aversive conditions, consisting of early phase (1-10 s), middle phase (11-30 s),

and late phase (31-60 s). Because we hypothesized that the emotional responses of subjects at the very onset of displaying aversive pictures differ from their responses after viewing similar pictures continuously for about one minute. Paired t-tests were performed for each phase between the fMRI data acquired from the neutral condition and aversive condition. Results would disclose the brain activation induced by aversive stimuli compared to neutral stimuli in a form of triple jump across the three phases.

Specification of DCMs

In the past decade, an increasing number of neuroimaging studies have focused on neural correlates of emotion regulation, most of the previous studies have put explicit focus on cortical-subcortical interactions to elucidate the regulatory processes underlying successful emotion regulation. Four brain regions are consistently regarded as the major nodes within the network for emotion regulation: the amygdala / ventral striatum (VS), ventrolateral prefrontal cortex (VLPFC), dorsal part of anterior cingulate cortex (dACC), and dorsolateral prefrontal cortex (DLPFC) (Kohn et al., 2014; Ochsner et al., 2012). The MNI coordinates of these four regions with the peak t values resulted from aforementioned comparisons were used as the nodes for the next DCM analysis. Because the precise function of these regions and their interactions are still being debated (e.g., whether the VLPFC is involved in the generation of emotion or whether the DLPFC modulates the VS in a direct way), fifty models were chosen to cover each of the hypotheses (see Figure 5.6). In this study, the nonlinear option was not applied, thus, the term "modulation effects" denotes bilinear modulation effects. Moreover, neither "center input" nor "stochastic" options were chosen.

Bayesian Model Comparison

Among the fifty proposed models, the optimal model that represented the best fit to the data was identified using Bayesian Model Selection (BMS) (Penny et al., 2004). Random effects (RFX) inference was performed for the group-level comparison, and the "Protected Exceedance Probabilities (PXPs)" were applied to determine the optimal model (Rigoux et al., 2014).

5.4.2 Results

Similar to the our previous results, the DCM analysis demonstrates that there were shifts in how the brain controls emotion when viewing the pictures (see Figure 5.7), which corresponded to three states: the initial response to the aversive pictures (perception and encoding of stimuli), which activated the visual and encoding regions; response suppression (inhibition), which induced significant activation in VS and supplementary motor area (SMA); and response modulation, which led to significant activation in the DLPFC ($p < 0.05$, FDR corrected, for each state when compared with neutral images). The coordinates of the major regions activated in the three phases are listed in Table 5.3.

Next, the dynamic causal connections (or directional interactions) were modeled for the four regions that were activated during the three states: VLPFC, dACC, VS, and DLPFC. The result of the BMS analysis indicated that No. 33 model fitted the observed data best with the greatest posterior probabilities (Figure 5.8). As a result, bidirectional endogenous connections were identified between the pairs of VS and VLPFC, VS and dACC, VS and DLPFC, VLPFC and DLPFC, and dACC and DLPFC (Figure 5.9A).
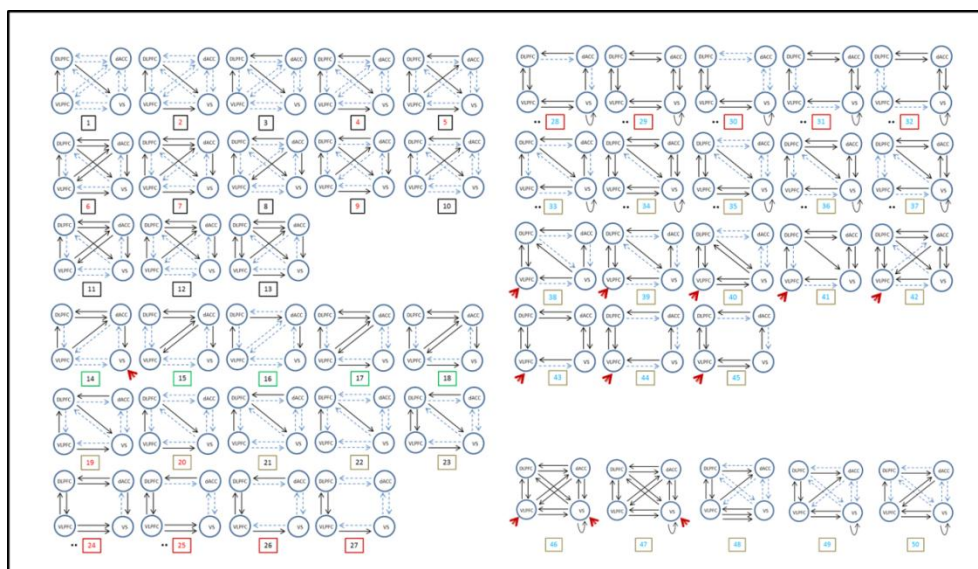
Fig. 5.6: Proposed 50 models of emotion regulation for DCM analysis. Each model comprises four nodes, including the amygdala / ventral striatum (VS), ventrolateral prefrontal cortex (VLPFC), dorsal part of anterior cingulate cortex (dACC), and dorsolateral prefrontal cortex (DLPFC).
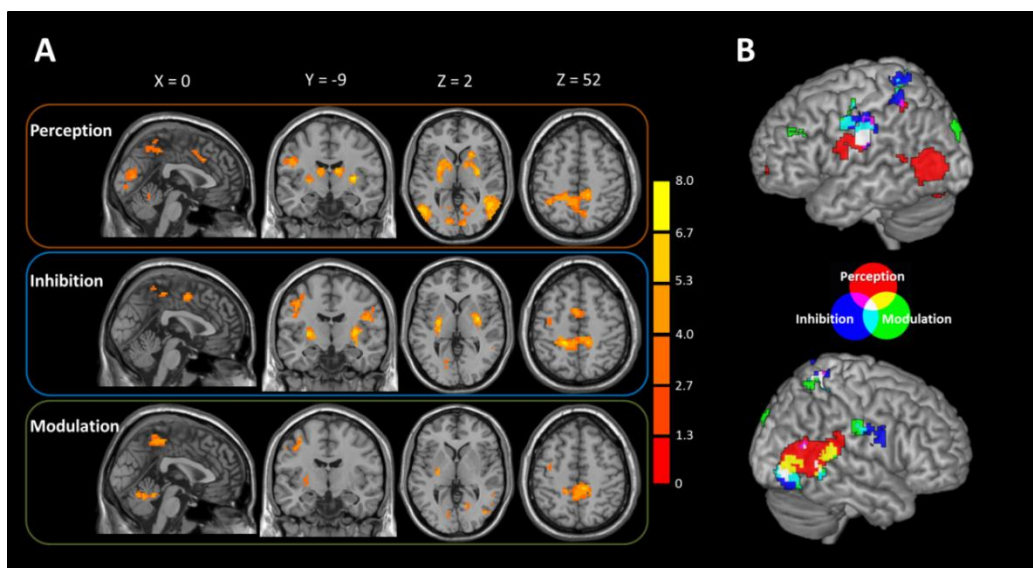
Fig. 5.7: fMRI images of subjects viewing aversive pictures compared with neutral pictures. Aversive stimuli induced significant brain activation that differed across regions depending upon three states: perception, inhibition, and modulation. (A) Significant activation at (0, -9, 2/52) displayed in Montreal Neurological Institute (MNI) coordinates is shown in sagittal, coronal, and axial planes. Activation in each region reached statistical significance of $p < 0.05$ (FDR corrected), cluster size $k > 10$ voxels. (B) The brain regions where significant activation occurred during the three states are depicted on the surface of brain in different colors.

Table 5.3: Regions with significantly increased activation elicited by aversive condition compared with neutral condition. Abbreviation: VS, ventral striatum; VLPFC, ventrolateral prefrontal cortex; dACC, dorsal part of anterior cingulate cortex; DLPFC, dorsolateral prefrontal cortex; L, left; R, right; BA, Brodmann area.

Phase	Region	BA	MNI Coordinates		
			x	y	z
Early	L. VS		-30	-15	0
Middle	L. VLPFC	10	-24	54	-6
	R. dACC	32	6	15	33
Late	L.DLPFC	9	-27	30	33
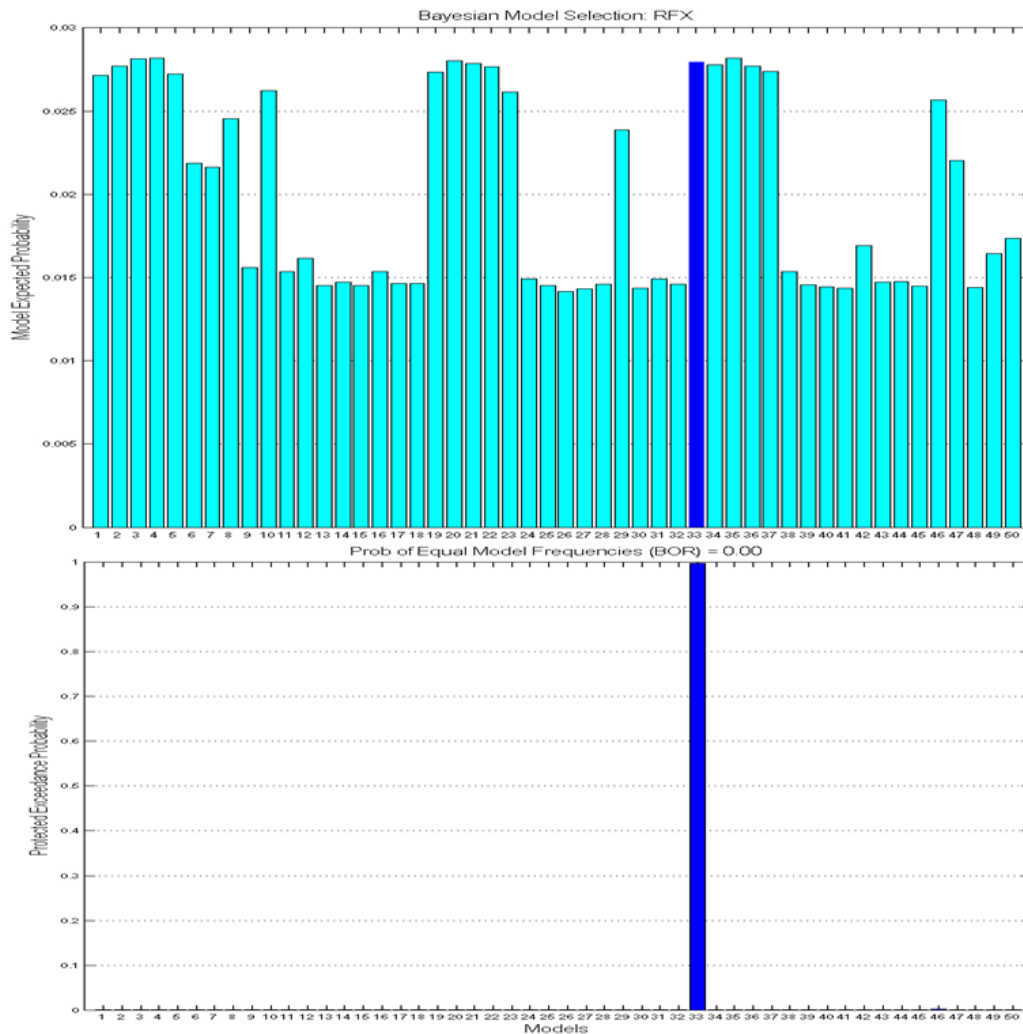
Fig. 5.8: The result of BMS analysis on the proposed 50 models. The No. 33 model fitted the observed data best with the greatest posterior probabilities. The "Protected Exceedance Probabilities (PXPs)" were applied to determine the optimal model.

5.4.3 Discussion

The overarching idea is that the prefrontal and cingulate systems support the control processes that modulate activity in subcortical systems, which generate emotional responses (Ochsner et al., 2012). Although the amygdala is more commonly reported to be activated during emotion generation than the VS, our study did not find significant activation in this region. However, our data is in agreement with the abovementioned study in which the VS was associated with both emotion generation and bottom-up regulation via suppression. Moreover, emotion-inducing stimuli only accessed to the VS and not the VLPFC, which refutes the possibility that the VLPFC is engaged when generating emotions (Kohn et al., 2014). The stimuli lead to a self-connection within the VS (Figure 5.9A), which manifests an inhibition caused by preventing uncontrolled outbursts of neural activity. However, the aversive emotion induced by viewing pictures in our study was intense enough to override this inhibition and enabled the activation of the DLPFC via two indirect paths: the dACC and the VLPFC. The DLPFC exerted modulatory effects on the VS directly, which down-regulated the subjects' emotional responses. During indirect transmission of emotional signals from VS to DLPFC, the VLPFC and dACC are involved in evaluating the positive or negative valence of afferent signals and monitoring conflicts between the responses to the overriding emotion and initial inhibition, respectively (Ochsner and Gross, 2005; Ochsner et al., 2012). The DLPFC has been reported to be related to higher order (or "cold") regulatory processes, which are reliant on only attention and memory, and are free of affective processing (Ochsner and Gross, 2005). Note that these processes are quite possibly utilized spontaneously during the emotional self-regulation.
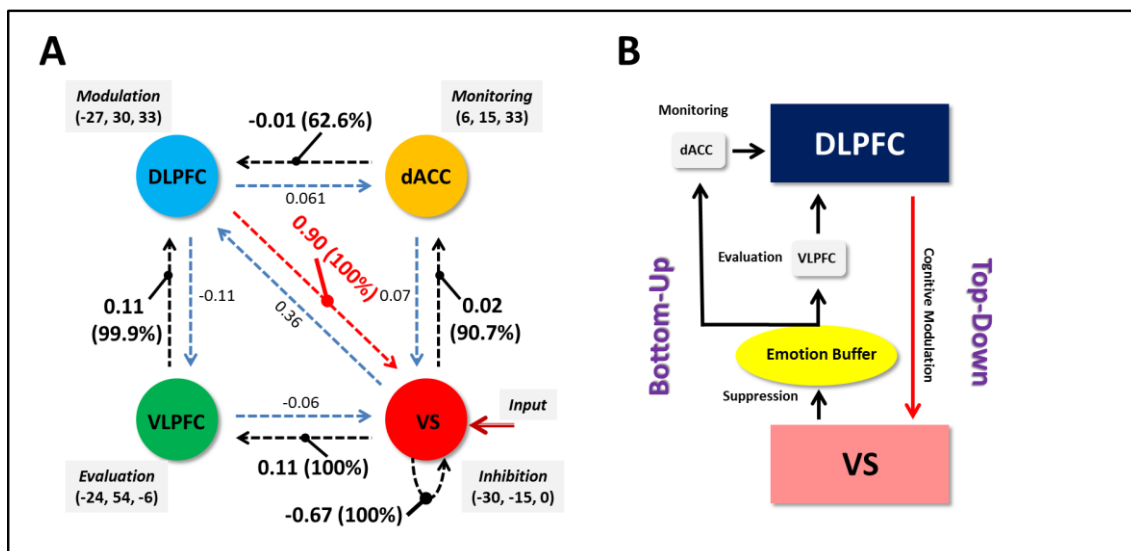
Fig. 5.9: Dynamic models for self-regulating aversive emotions. (A) The optimal dynamic causal model depicts the connections between the VS, dACC, DLPFC, and VLPFC. Bidirectional endogenous connections (the fixed connections) were identified between each pair of nodes, except between the dACC and VLPFC. Cognitive functions and Montreal Neurological Institute (MNI) coordinates are shown for each region. Connection strength indicating frequency of exertion and posterior probability (%) representing the conditional probability given the observed data are also shown for each modulatory effect. (B) A dual regulatory model is proposed for the regulation of emotion. Bottom-up regulation involves an indirect pathway that is initiated by the VS to the DLPFC via both the VLPFC and dACC. Top-down regulation involves modulation imposed by the DLPFC on the VS directly.

Self-Regulation Models for Aversive Emotion

Based on the shifts in brain activity across perception, inhibition, and modulation to control emotion and the optimal dynamic causal model described above, we have proposed that a frontostriatal circuit underlies a dual regulation model for emotional self-recovery (Figure 5.9B), in which both bottom-up and top-down regulation are involved. Bottom-up regulation initially attenuates emotions with negative valence (such as that induced by aversive stimuli) via the VS serving as an "emotion buffer" that enables the brain to endure the emotions by exerting a certain level of inhibition, until the emotions are defused over time. For intense emotions that exceed the magnitude that

the VS can bear, the VS will recruit help from the DLPFC by transmitting signals about the intense emotions along indirect pathways via the VLPFC and dACC. This enables a top-down cognitive regulation by the DLPFC that directly modulates the VS (Ochsner et al., 2012).

5.5 Conclusion

Two dissociable networks were revealed during the dynamic recovery from the discomfort induced by aversive pictures. The left CN centric subcortical network was found to be associated with the processing on aversive stimuli, and the right AG centric fronto-parietal network was related to attentional control. The spontaneous switch of the two networks underlaid the brain-state shift over the whole course of recovery, and enabled the transition of strategies from suppression to attention deployment, which facilitated the emotional self-regulation.

Our data demonstrates that the brain recruits cognitive regulation during emotional self-recovery to decrease emotional-related discomfort after receiving aversive stimuli. Furthermore, our findings suggest that both VS-centric bottom-up and DLPFC-centric top-down regulation are recruited for self-regulating emotions with negative valence. The DLPFC exerts a modulatory effect on the VS only when the VS fails to suppress the induced emotions by self-inhibition. The underlying neuronal responses of this dual regulatory model may be attributed to the interaction between glutamatergic excitation and GABAergic inhibition. We plan to further investigate the dynamic causal connectivity of brain regions in patients with MDD, and investigate whether their emotional abnormalities are related to impaired top-down regulation, impaired bottom-up regulation, or both.

Chapter 6

Interactions among
Cognition, Emotion, and Depression

Cognition and emotion are two major aspects of human mental life that are widely regarded as distinct but interacting. (Gray et al., 2002). Traditional notion of functional specialization partitioned the brain into many regions conceptualized as either 'affective' or 'cognitive' (Pessoa, 2008). But sometimes, emotion is likely to override cognition to influence our behavior choices. Intuitive responses, if unchecked, may turn out to be suboptimal and even destructive (Luo and Yu, 2015). Cognition can in turn exert powerful modulation on emotion in many circumstances (Eisenberg et al., 2000; Webb et al., 2012). A high possibility is that complex cognitive-emotional behaviors have their basis in dynamic coalitions of networks of brain areas. It is essential to figure out the neural underpinnings of the cognition-emotion interactions, since balanced mutual effects between the two systems keep us living in a steady state. On the other side, for the patients who are depressed, the mental disease hinders not only their ability to experience emotions appropriately, but also their ways of thinking. Researches on the patients help us ponder what factors could disenable the right functioning of human in both the cognition and emotion.

This chapter concerns on the interplays of diverse systems. We pay more attention on the depressed patients, to elucidate the relationship between cognition and emotion from another angle.

6.1 Introduction

Neuroimaging data are widely used to provide evidence for a specialization or fractionation of psychological function (based on double-dissociation logic). However, research in the past decades has shown the cognition-emotion interactions and that, if we are to understand how complex behaviors are carried out in the brain, an understanding of the two is indispensable (Pessoa, 2008). One of the most influential and widely accepted concepts on how emotions are generated and regulated is often termed appraisal theory, which proposes that our emotional response is mediated by a physiological reaction triggered by internal or external stimuli and lastly shaped by appraisal (Gross, 1998). Emotional experience may thus be separated into different components, which can be modulated by the process of "emotion regulation". Importantly, dysregulation of this process has been argued to lie at the heart of various psychiatric diseases.

Although emotion and cognition may be mostly separable, the presence of such a highly specific pattern means that the emotional and cognitive influences are also inseparable. If the integrated signal has a functional role, emotion and cognition can conjointly contribute to the control of thought, affect, and behavior. Formally, we define integration in terms of a specific experimental design and a logically sufficient pattern of results. Given such a design, emotion-cognition integration is implied by the existence of a brain region having a crossover interaction between the emotional and cognitive factors (Gray et al., 2002). However, if the brain regions corresponding to joint functions related to both emotion and cognition, then the abnormal functioning may occur to the both sophisticated systems. Regarding the testification of this hypothesis, studies on patients with mental disorder would provide the direct evidence.

Major depressive disorder (MDD) is characterized by emotional and cognitive impairments, including alterations in emotion processing, cognitive control, affective cognition, and reward processing (Diener et al., 2012; Hamilton et al., 2012; Kerestes et al., 2014; Miller et al., 2015b). Neuroimaging methods such as positron emission tomography (PET) and functional magnetic resonance imaging (fMRI) have provided profound insights about the neural mechanisms in MDD, highlighting aberrant function and interaction of cortical, subcortical, (para)limbic, and midbrain regions mediating cognition, emotion, as well as metabolism (Lener and Iosifescu, 2015; Phillips et al., 2015; Wise et al., 2014). However, due to remarkable heterogeneity in the localization and direction of altered activity in key regions revealed by neuroimaging approaches (Diener et al., 2012), debates regarding neural correlates underlying the pathology and cardinal symptoms of MDD still exist.

Brain abnormalities in MDD reported in previous studies were primarily localized in brain regions involved in emotional processing, such as prefrontal cortex, limbic system, and basal ganglia (Ressler and Mayberg, 2007). Besides functional deficits, brain structural changes were also revealed in MDD. Voxel-based morphometry (VBM) (Ashburner and Friston, 2000) is a user-independent, fully automated method for detecting potentially unsuspected brain structure abnormalities, and has been widely used for finding differences in patients with neuropsychiatric disorders such as obsessive-compulsive disorder (OCD), and bipolar disorder (Adler et al., 2007; Hou et al., 2013). With the help of VBM, many MRI studies focusing on structural abnormalities in MDD have found evidence of volume reductions in the anterior cingulate cortex (ACC), orbitofrontal cortex, hippocampus, amygdala, as well as caudate and putamen (Hamilton et al., 2008; Koolschijn et al., 2009). Furthermore, it has been found that the gray matter volume (GMV) in MDD patients was positively

correlated with their executive performance and the effect of treatment with cognitive behavioral therapy (Fujino et al., 2015). Therefore, a growing consensus is being achieved on the importance of structure changes as biomarkers related to MDD. However, evidence on how the abnormal GMV affects brain functions and symptomatic progression is still insufficient. In addition, increasing evidence exhibits that the disturbances in MDD are unlikely to be the results of a single region with abnormal function and / or structure, MDD could be considered as a disorder with distributed brain networks (Damasio, 1997).

As a hallmark symptom of MDD, the ahedonia was defined in DSM-IV-TR (American Psychiatric Association, 1994) as diminished interest or pleasure in response to stimuli that were previously perceived as rewarding during a pre-morbid state. Because the capacity to feel pleasure is a critical step during the normal processing of rewards, anhedonia has been greatly implicated in the reward deficits of MDD patients (Der-Avakian and Markou, 2012). Reduced reward responsiveness was found in MDD patients when they engaged in reward-related functional tasks (Pizzagalli et al., 2008; Vrieze et al., 2013), such as the Monetary Incentive Delay task (MID) which is well-known to elicit strong activations in the reward circuit related to the anticipation and outcome of rewards (Knutson et al., 2001). Anatomically, the ventral striatum including the ventral tegmental area (VTA) and the nucleus accumbens (NAcc) are at the core of the reward circuit. Further key structures include the caudate nucleus, putamen, insula, amygdala, hippocampus, thalamus, both anterior and posterior portions of cingulate cortex, and orbitofrontal cortex (OFC) (Liu et al., 2011). Increased activations in these areas are normally associated with the reward anticipation, reward receipt, as well as responses to stimuli with positive emotional valence in healthy individuals (Kumar et al., 2014; Schultz et al., 1998; Silverman et al., 2015b). However, reward processing does not

represent a unitary construct nor does it rely on a singular biological circuit (Whitton et al., 2015). Other distinct cognitions can also contribute to reward processing, such as attention (Bourke et al., 2010; Miskowiak and Carvalho, 2014). Emerging evidence suggests the relationship between the biased attentional processing and altered recognition of reward or positive stimuli in MDD patients. For example, depressed patients exhibited reduced attention to positive facial emotion expressions compared with increased vigilance towards negative expressions (Asthana et al., 1998; Henderson et al., 2014). Patients with depression also showed decreased perceptual sensitivity to positive words and pictures (Atchley et al., 2012). Generally, the relative salience of stimuli determines which inputs are more likely to capture attention when the brain is constantly bombarded by stimuli. A growing body of literature has identified misappropriated stimulus-driven salience detection and altered attentional processes in psychiatric patients, such as autism, schizophrenia, and social anxiety disorder (Palaniyappan and Liddle, 2012; Pannekoek et al., 2013; Uddin, 2015). An insula-anterior cingulate cortex (ACC) salience network has been proposed to be responsible for the salience processing, and also serve as a hub that enables switching of brain states from the default mode to a task-related activity mode (Menon and Uddin, 2010; Seeley et al., 2007). For that reason, the salience network functioning has been conceived as key to the morbid rumination which is a core vulnerability in MDD, because the aberrant toggle system is likely to result in imbalance between default mode and executive networks (Belleau et al., 2015). Recently the potential role of altered salience processing in abnormal response to rewards has also been highlighted due to the evidence showing disrupted interactions between insula-ACC regions and reward-related areas in psychotic patients (Gradin et al., 2013). This is of interest, because for long concerns of researchers have been put on the brain regions related to emotional responses per se. But it appears that blunted processing of incentive

salience may become another possible reason for the ahedonia observed in MDD patients. However, further investigations need to be implemented to transparentize intrinsic neural mechanisms regarding how impaired salience system influences the reward processing.

In the past few years, resting-state fMRI (rs-fMRI) has been pervasively employed to investigate the spontaneous neural fluctuations of human brain. Particularly, rs-fMRI functional connectivity based on temporal dependency of neural activation of anatomically separated brain regions enables the exploration on the overall organization of functional communication in the brain networks (van den Heuvel and Hulshoff Pol, 2010). The rs-fMRI provides a promising approach to discover useful imaging endophenotypes associated with MDD. Studies with resting-state functional connectivity showed increased connectivity and nodal centralities within the default mode network (DMN) which indicated hyperactivity for self-referential and disruption to emotional modulation in MDD patients (Zhang et al., 2011). On the other hand, decreased activation found within fronto-parietal network during cognitive control-related tasks after MDD patients were shown negative self-referential statements implicated their inability to shift attention away from self-related stimuli (Wagner et al., 2015). Therefore, the rs-fMRI functional connectivity has also been applied as a powerful method to reveal the abnormalities in intrinsic connectivity between salience network and other cognitive or affective systems of patients with psychiatric disorders (Dutta et al., 2014; Pannekoek et al., 2013; Uddin et al., 2014). Prior studies documented disrupted connections from hippocampus and amygdala to the dorsomedial-prefrontal cortex and salience-related fronto-insular operculum (Tahmasian et al., 2013) Furthermore, altered rs-fMRI functional connectivity between the pregenual anterior cingulate cortex and the right anterior insula was found exclusively in the subgroup of severely depressed patients compared to healthy subjects and mildly

depressed patients (Horn et al., 2010). Given that more and more studies have shown the strong association between spontaneous blood-oxygen-level dependent (BOLD) fluctuations and simultaneous measured fluctuations in neuronal spiking (Shmuel and Leopold, 2008; Shmuel et al., 2002), an integration of task-state and resting-state fMRI is more likely to facilitate our understanding on the relationship between salience processing and neural basis of MDD symptoms.

Taken together, we examine the responses to affective images and attentional control of healthy and MDD cohorts by using a distraction task paradigm (Kanske et al., 2011; Van Dillen et al., 2009). Furhtermore, we attempted to find out differences between MDD and healthy groups in the structural alterations in the volume of gray matter, brain activation elicited by functional task, spontaneous BOLD oscillations based on rs-fMRI, as well as fractional anisotropy of white matter. We hypothesized that, 1) interacting effects between emotion and cognition could be found by the distraction paradigm combining emotional response and mental calculation; 2) we would find differences in salience processing between MDD patients and healthy subjects when they were asked to shift attention from viewing images with different valences to solving arithmetic problems acting as distractors; 3) moreover, common regions showing abnormalities in both task-state and resting-state would provide reference to predict depressive symptoms.

6.2 Systematic Investigation Based on Multi-Modal Data

Multi-modal approaches can cross-validate findings from different sources and identify associations and patterns. BI methodology stresses the significance of collecting as many as possible data even in a single experiment. The morphological, resting-state, task-state, and diffusion data enabled a holistic study on the structural and functional abnormalities in MDD patients (see Figure 6.1).
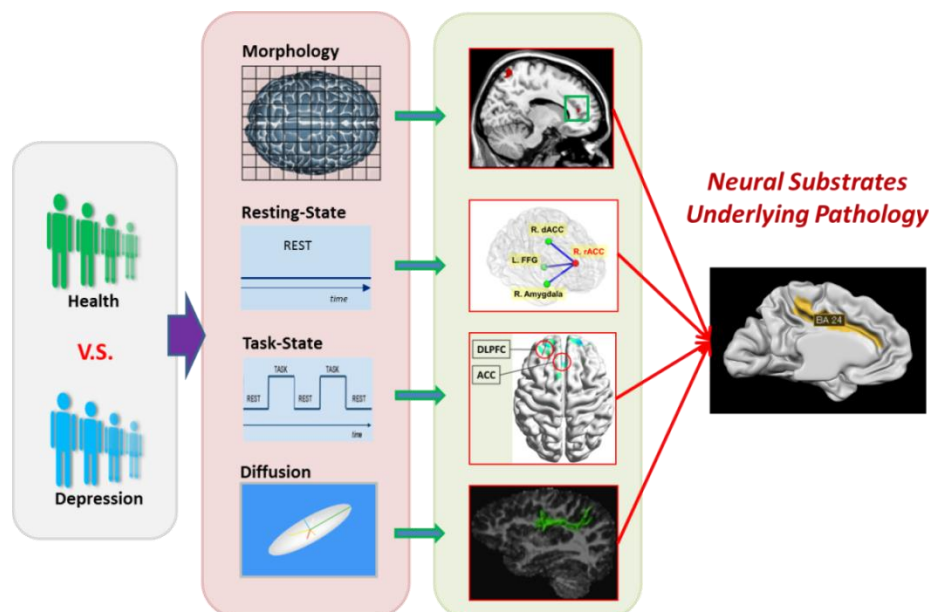
Fig. 6.1: Systematic investigation based on multi-modal data. Systematic investigation on MDD patients enabled by multi-modal data furthers the understanding on the neural substrates underlying the pathology of MDD.

6.3 Interactions between Mental Arithmetic and Emotional Response

Cognitively influencing emotional experience is highly relevant for adaptive social behavior and mental and physical health (Eftekhari et al., 2009). Different strategies can be applied to regulate emotional responses ranging from attentional control to cognitive change (Ochsner and Gross, 2005).

Distraction, in contrast, relies on attentional control to focus on a concurrent task, thereby reducing emotional responding. A number of studies showed its efficiency in attenuating subjective emotional experience and amygdala activity (Blair et al., 2007; Pessoa et al., 2002). A recent study by Van Dillen et al. (2009) clearly demonstrated that amygdala down-regulation is related to the difficulty of the concurrent task. More difficult tasks also engage areas in the DLPFC and superior parietal cortex that typically respond

to task demands (de Fockert et al., 2001). The study provides some indication that activity in these control areas covaries with amygdala activation, but clear evidence for the connectivity of the amygdala during distraction is still lacking.

The present study utilized mental addition and subtraction problems as the distractors, respectively, for down-regulating the emotions in healthy subjects induced separately by positive, neutral, and negative images. We hypothesized that the two operations would exert distinct influences on the elicited emotions, because it has been evidenced in Chapter 4 that the subtraction process corresponds to higher task demands than addition calculation. In addition, the aforehand states of emotion aroused by affective pictures were selectively expected to impose effects on mental calculation as well.

6.3.1 Materials and Methods

Participants

Data from 24 healthy college graduates (10 females) with ages of 23-28 years were included in the final analysis. All of the participants were right-handed, educated with identical techniques, had normal or corrected-to-normal vision, and reported no history of neurological or psychiatric disorders. Prior to their participation in the study, written informed consent was obtained from each participant after the nature and possible consequences of the studies were explained. This study was approved by the Ethics committee of Xuanwu Hospital, Capital Medical University, Beijing.

Stimuli and Procedure

The task design modifies and combines previous paradigms of distraction task to study attention control of MDD patients (Kanske et al., 2011; Van Dillen et al., 2009). Three

task conditions were included and presented in a block-designed pattern. Subjects were shown pictures and then required to solve mental arithmetic problems presented as overlays on the pictures. Three types of pictures corresponding to each task condition were applied, with positive (e.g., joyful, exciting), neutral, and negative (e.g., aversive) valences, respectively. As distractors, 2-digit simple mental addition and subtraction problems without carrying and borrowing were employed.

Each trial consisted of an emotion induction phase and a distraction phase. During the induction phase (2000 ms), a picture with a specific valence was displayed. Subjects passively viewed the picture to elicit an initial emotional response. During the distraction phase (4000 ms), subjects needed to shift attention from the picture to an arithmetic problem, and then decide whether the displayed solution was correct or incorrect by pressing two response keys using the left and right thumbs. The accuracy and reaction time of each response were recorded. Incorrect displayed solutions deviated by $\pm$ 1 or $\pm$ 10 from the correct solutions in 50% of all the trials. The frequency of occurrence of each number was balanced and the proportion of each arithmetic operation was 50% for all conditions. Neither "tie" problems (e.g., 32 + 32, 67 - 67) nor repeated problems were recruited. Twelve successive trials with same task condition constituted a task block. Blocks of three conditions were mixed and counterbalanced, and every two task blocks were separated by a rest block. Data were acquired in three functional runs with a total of 36 trials for each type of task.

Affective pictures were selected from the International Affective Picture System (IAPS) which is based on normative ratings in valence and arousal (Lang et al., 1998). The contents of positive pictures included beautiful scenery, delicious food, scenes of sports, romance, and money, with mean valence of 7.49 $\pm$ 1.54 and mean arousal of 5.36 $\pm$ 2.25. Aversive pictures, such as snakes, spiders, attacks, bloody wounds, and dead bodies were

adopted for the negative stimuli, with mean valence of 2.61 ± 1.60 and mean arousal of 6.30 ± 2.14. Pictures of household items in simple contexts (e.g., a cup on a table) were used as the neutral stimuli, with mean valence of 5.01 ± 1.13 and mean arousal of 3.05 ± 1.94.

MR Data Acquisition

The fMRI data were acquired with a 3.0 Tesla MRI scanner (Siemens Trio Tim; Siemens Medical System, Erlanger, Germany) using a 12-channel phased array head coil. Foam padding and headphones were used to limit head motion and reduce scanning noise. One hundred ninety two slices of anatomical images with a thickness of 1 mm were obtained using a T1 weighted 3D magnetization prepared rapid gradient echo (MPRAGE) sequence (TR = 1600 ms, TE = 3.28 ms, TI = 800 ms, FOV = 256 mm, flip angle = 9°, voxel size = $1 \times 1 \times 1$ mm^3). Functional images for both task state and resting-state were collected through an echo-planar imaging (EPI) sequence (TR = 2000 ms, TE = 31 ms, flip angle = 90°, FOV = 240×240 mm2, matrix size = 64×64). Thirty axial slices with a thickness of 4 mm and an interslice gap of 0.8 mm were acquired.

Data Preprocessing

The preprocessing of fMRI data was performed with SPM12 software (Wellcome Trust Centre for Neuroimaging, London, UK, http://www.fil.ion.ucl.ac.uk) and REST Toolkit (Song et al., 2011) implemented on a MATLAB platform (MathWorks, Natick, MA). The first two images of task-state and ten images of resting-state data were discarded to allow the magnetization to approach dynamic equilibrium. Functional images were corrected for slice-timing differences and realigned to the median image to correct rigid body motion. Patients with head movement exceeding 3 mm or 3 degrees and healthy subjects exceeding 2 mm or 2 degrees were rejected. The high resolution anatomical image was

co-registered with the mean image of the EPI series and then spatially normalized to the MNI template. After applying the normalization parameters to the EPI images, all volumes were resampled into $3 \times 3 \times 3$ mm^3. Then the normalized task-state images were smoothed with an 8-mm FWHM isotropic Gaussian kernel.

Functional MRI Analysis

Task-state data were statistically analyzed using SPM12. After specifying the design matrix, each participant's hemodynamic responses induced by the trials were modeled with a box-car function convolved with a hemodynamic function. The parameters for addition and subtraction calculations, as well as the effects of the positive task (PT), neutral task (NEUT), and negative task (NT) which displayed pictures with respective valences were estimated. Contrast images were constructed individually based on the general linear model (GLM). Due to the involvement of two factors in the present study, the group-level analysis was implemented based on a 2 by 3 factorial design with factors of "Operation" (2 levels) and "Emotion" (3 levels). Interactions between the two experimental factors are also examined. Simple effect analyses will be performed if interaction could be confirmed.

6.3.2 Results

As shown in Figure 6.2, the main effects were identified for both calculation and emotion factors ($p < 0.05$, FDR corrected, with a minimum cluster size of $k > 30$). The main effect of calculation revealed by contrast of "Subtraction > Addition" showed significantly increased activation in the bilateral IPS, bilateral DLPFC, bilateral IFG, and SMA, which are highly accordance with the regions we reported in Chapter 4. The main

effect of emotion elicited by contrast of "Negative > Neutral" exhibited greater activation in the regions of the bilateral amygdala, bilateral parahippocampal gyri, ventromedial prefrontal cortex (VMPFC), dorsomedial prefrontal cortex (DMPFC), and visual cortex.

Simple effect analyses were also performed due to the identification of interactions between the two factors ($p < 0.05$, FDR corrected, with a minimum cluster size of $k > 30$). Firstly, brain activation induced by different emotions was compared at a single level of calculation factor (see Figure 6.3). At the level of addition calculation, the arithmetic process under positive emotional state induced the increased activation in the angular gyrus (AG), while the calculation under negative emotional state led to increased activation in the AG, inferior temporal gyrus (ITG), fusiform gyrus (FFG), DLPFC, and VLPFC. Notable differences could be revealed by contrast of "Negative > Positive", which showed significantly greater activation in the dorsal attention network (DAN), including the bilateral posterior parietal cortex, bilateral SMA/pre-SMA, and bilateral DLPFC. At the single level of subtraction calculation, patterns of activation were similar to those over served for addition processing. Negative stimuli caused greater activation in the (DAN).

Main Effect of Calculation
Subtraction > Addition

Main Effect of Emotion
Negative > Neutral
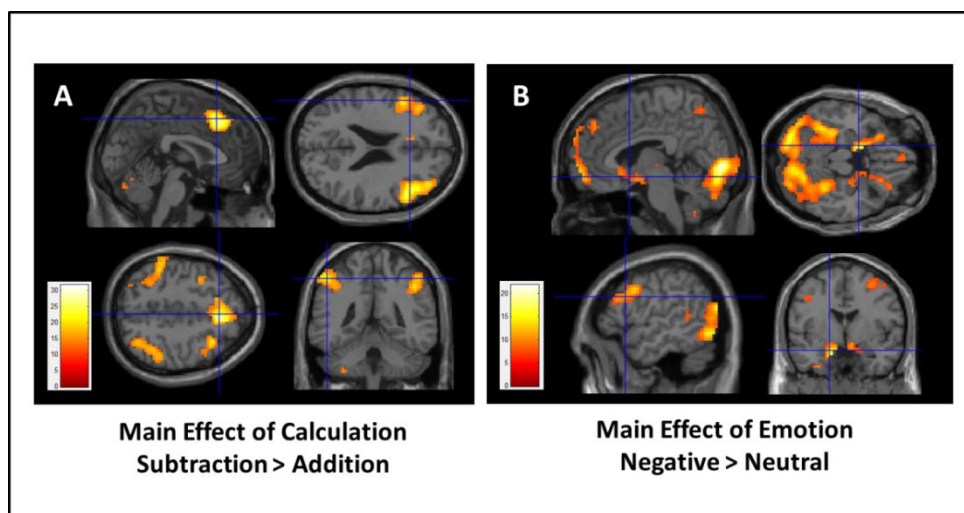
Fig. 6.2: Main effects of calculation and emotion revealed by factorial analysis. All regions survived the statistical threshold of $p < 0.05$ (FDR corrected), cluster size $k > 30$.
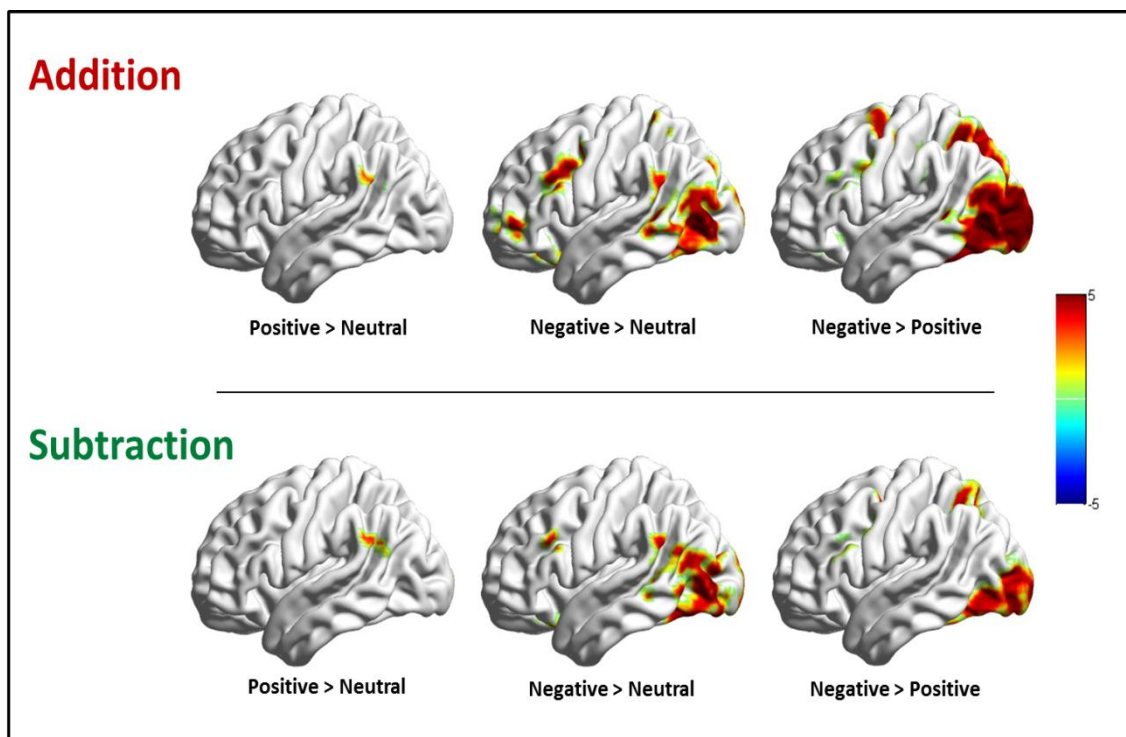
Fig. 6.3: Results showing how emotion affects cognition. Simple effect analyses were performed at single levels of calculation factor. Negative stimuli caused greater activation in the dorsal attention network than positive stimuli for both addition and subtraction processes.

Secondly, the percent changes of blood-oxygen-level dependent (BOLD) signals were computed for each calculation, under positive, neutral, and negative emotional state, respectively (see Figure 6.4). The left amygdala and bilateral parahippocampal gyri were selected as ROIs to confirm the regulatory effect of each operation exerting on different emotion states. Generally, both addition and subtraction realized the down-regulation effects on the three ROIs over the three emotional states. However, addition calculation presented better intervention effects on different emotion states, indicating that addition is more appropriate to serve as distractors than subtraction. Particularly, under the negative emotional state, the modulatory effects imposed by subtraction were very little.
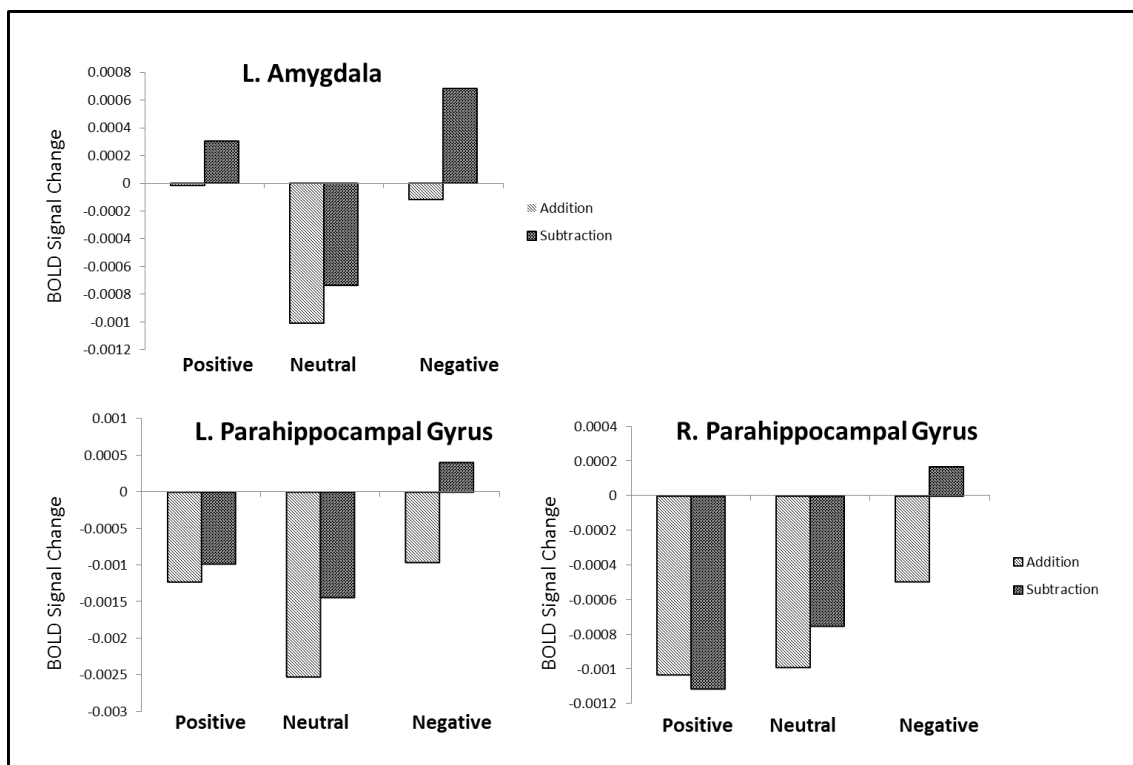
Fig. 6.4: Results showing how cognition affects emotion. Percent changes of BOLD signals were computed for each calculation under different emotional states. Subtraction is not as effective as addition to play the role of distractor for modulating emotions.

6.3.3 Discussion

Previous studies have suggested that different types of emotional stimuli selectively interact with verbal or spatial working memory (Gray et al., 2002). Gray, J. R. and colleagues used 3-back working memory task to explore the interplays by integrating emotion and working memory tasks together. Their results indicated that the pleasant stimuli facilitated the verbal working memory but blunted the spatial working memory; for the unpleasant stimuli, the opposite is true. This highly specific result indicates that emotion and higher cognition can be truly integrated.

In the present study, our data are not adequate to verify Gray, J. R.'s theory. But it is certain that interacting effects exist between calculation and emotion factors. Although interfered by distractors, emotions aroused by both the positive and negative stimuli are

able to persist and impose influences on the following calculation. For both the two operation, the negative emotion brings much more interferences to calculations, resulting in apparently greater activation in the DAN which implies more effort needed for staying focused.

Although both addition and subtraction can be used as distractors to modulate emotions, effects brought about by subtraction are not enormous, especially for negative emotion. As we discussed in Chapter 5, the top-down regulation is engaged in the emotional self-recovery, even when the behavior is out of awareness. Executive control function is necessary to enable the direct regulation from the DLPFC to the subcortical areas. However, because of the high task demand, the DLPFC is occupied by the subtraction calculation. As a result, subtraction is not as effective as addition to play the role of distractor.

Our findings demonstrate that cognition and emotion influence each other, since some cognitive resources and brain regions are shared by the both brain functions. It is possible that some concurrences of emotional and cognitive activities conflict with each other due to the competition for cognitive resources.

6.4   Morphologic and Functional Connectivity Alterations in Patients with MDD

In order to obtain a panorama of structural and functional brain abnormalities as well as the association between the anatomic and functional alterations and clinical symptoms in patients with major depressive disorder (MDD), integrated magnetic resonance imaging (MRI) measures were implemented on 21 MDD patients and 21 healthy controls, to facilitate the multimodality of voxel-based morphometry (VBM)

analysis, resting-state functional connectivity analysis, and symptom rating. MDD patients showed significantly decreased gray matter volume (GMV) in the rostral part of anterior cingulate cortex (rACC), precuneus, and superior parietal lobule in the right hemisphere. By using the above morphologic deficits areas as seed regions, functional connectivity analysis revealed reduced coupling in the limbic-cortical and fronto-parietal networks, respectively. Subsequent correlation analyses revealed that GMV in the rACC negatively correlated with the depressive symptom severity and anxiety level. Our findings provide evidence supporting both morphologic and functional deficits in the limbic-cortical and frontal-parietal areas in MDD patients which could account for their dysfunctions on emotional regulation and cognition. Moreover, the neural changes found in rACC could be possible state markers for evaluating effects of anti-depressive treatment and anxiety level.

6.4.1 Materials and Methods

Participants

Twenty-one right-handed MDD patients (9 males and 12 females) were recruited among outpatients from Beijing Anding Hospital, China, and 21 healthy controls matched for gender, age, and years of education with MDD patients were recruited from community. Diagnostic assessments for all participants were performed by clinically trained and experienced raters (T. Tian and B. Fu) using the Mini International Neuropsychiatric Interview 6.0 (MINI 6.0) (Sheehan et al., 2010) based on DSM-IV. Clinical symptom severity of depression and anxiety level were evaluated for patients using Hamilton Depression Rating Scale 17 items (HDRS-17) and Trait Anxiety Inventory (T-AI), respectively (see Table 6.1). The exclusion criteria were: (1)

depressive patients with any mania episode or history of any comorbid major psychiatric illness on Axis I or Axis II; (2) concurrent serious medical illness or primary neurological illness; (3) history of head injury resulting in loss of consciousness; (4) abuse of or dependence on alcohol or other substances; (5) and contraindication for MRI. All subjects signed the informed consent and this study was approved by the Ethics committee of Beijing Anding Hospital, Capital Medical University.

MR Data Acquisition

A 3.0 T MRI system (Siemens Trio Tim; Siemens Medical System, Erlanger, Germany) and a 12-channel phased array head coil were employed for the scanning. Foam padding and headphone were used to limit head motion and reduce scanning noise. 192 slices of structural images with a thickness of 1 mm were acquired by using a T1 weighted 3D MPRAGE sequence (TR = 1600 ms, TE = 3.28 ms, TI = 800 ms, FOV = 256×256 mm2, flip angle = $9°$, voxel size = $1 \times 1 \times 1$ mm^3). Functional images were collected through a T2 gradient-echo EPI sequence (TR = 2000 ms, TE = 31 ms, flip angle = $90°$, FOV = 240×240 mm2, matrix size = 64×64). Thirty axial slices with a thickness of 4 mm and an interslice gap of 0.8 mm were acquired.

Voxel-Based Morphometric Analysis MR Data Acquisition

The voxel-based morphometric analysis was performed using SPM8 software (Statistical Parametric Mapping; http://www.fil.ion.ucl.ac.uk/spm/) and the VBM 8 toolbox (http://dbm.neuro.uni-jena.de/vbm/). All T1 structural images were bias-corrected and segmented into gray matter (GM), white matter (WM), and cerebrospinal fluid (CSF) using the Maximum A Posterior spatial probability segmentation approach. The deformations that best aligned the images together were estimated by iteratively registering the imported images with their average through the

Diffeomorphic Anatomical Registration Through Exponential Lie Algebra (DARTEL) algorithm (Ashburner, 2007). Then the images were normalized to the standard Montreal Neurological Institute (MNI) brain template using the parameters obtained in the DARTEL's template normalization to MNI template. The voxel values of segmented and normalized gray matter images were modulated by the Jacobian determinants obtained from non-linear normalization steps. Finally, all wrapped modulated gray matter images were smoothed with an 8 mm Gaussian kernel.

Comparisons of GM volume between the MDD and control groups were performed using two-sample t tests. Age, gender, years of education, and total intracranial volume were modeled as covariates of no interest. The statistical significance of group differences in each region was set at uncorrected $p < 0.001$ with a minimum cluster size of $k > 50$. The average values of gray matter volume for all the voxels in abnormal areas revealed by VBM were extracted and correlated with the HDRS-17 and T-AI scores using Pearson correlation analysis, to identify the association between gray matter abnormalities and clinical characteristics.

Table 6.1: Demographic and clinical characteristics of participants. Abbreviation: HDRS-17, Hamilton Depression Rating Scale 17 items; T-AI, Trait Anxiety Inventory.

Characteristics	MDD Patients (n = 21)	Controls (n = 21)	p -Value
Gender (male: female)	9 : 12	9 : 12	1
Mean age (years)	33.8 ±9.1	29.9 ±7.7	0.15
Education level	13.1 ±3.1	11.9 ±2.4	0.18
HDRS-17 Total Score	19.2 ±6.3	-	-
T-AI Total Score	52.9 ±10.6	-	-

Functional Connectivity Analysis

The preprocessing of resting-state fMRI data was implemented with SPM8. The first 10 volumes have been discarded to allow the magnetization to approach dynamic equilibrium. Slice timing was applied to the rest of EPI images, then a series of stages followed: realignment that aimed at identifying and correcting redundant body mo-tions, co-registration that merged the high resolution structural image with the mean image of the EPI series, normalization that adjusted the structural image to the MNI template and applied normalization parameters to EPI images, smoothing that had fMRI data smoothed with an 8 mm FWHM isotropic Gaussian kernel. After normalization, all volumes were resampled into $3 \times 3 \times 3$ mm^3 voxels. Head movement was less than 2 mm and 2 degree in all cases.

Functional connectivity was analyzed using a seed-oriented correlation approach with the REST software package (http://www.restfmri.net). Regions with gray matter abnormalities that resulted from voxel-based morphometric analysis were utilized as the seeds. Several possible spurious sources of variances, including the estimated head motion parameters and average signals from the cerebrospinal fluid and white matter, were removed from the data through linear regression. Time courses were extracted from each voxel after linear detrend and bandpass filtering (0.01 - 0.08 Hz). Based on the corrected time courses, we computed the Pearson correlation coefficients between one seed and the rest parts of the brain voxel-by-voxel. Differences in functional connectivity between the MDD patients and healthy control group were compared by using two-sample t-tests. Age, gender, years of education, and total gray matter volume were entered as covariates of no interest. The significance level of group differences was set at a $p < 0.05$ with the AlphaSim correction (combined height threshold of a $p < 0.001$ and a minimum cluster size of 22 voxels).

6.4.2 Results

Morphometric Analysis

Compared with healthy control group, MDD patients showed reduced gray matter volume (GMV) in the rostral part of anterior cingulate cortex (rACC), precuneus, and superior parietal lobule (SPL) in the right hemisphere (see Table 6.2 and Figure 6.5). No significantly increased GMV was found in MDD patients relative to healthy controls.

Table 6.2: Regions of gray matter reduction in MDD patients compared to healthy controls. Abbreviation: rACC: rostral part of anterior cingulate cortex, SPL: superior parietal lobule, R: right, BA: Brodmann Area.

Region	BA	Cluster	Talairach x	y	z	T-score
R. rACC	32	56	11	41	9	6.61
R. Precuneus	7	146	1	-73	41	4.49
R. SPL	7	76	35	-56	55	3.84

Resting-State Functional Connectivity Analysis

Seed-oriented functional connectivity analyses were performed based on seeds corre-sponding to R. rACC (11, 41, 9), R. Precuneus (1, -73, 41), and R. SPL (35, -56, 55) that showed abnormalities in MDD patients in the above VBM analysis. As results of two-sample t-tests, MDD patients exhibited a general pattern with decreased connec-tivity between seeds and several emotion or cognition-related brain regions. When the seed was located in the R. rACC, patients showed decreased connectivity mainly in the right amygdala, dorsal anterior cingulate cortex (dACC), as well as the left fusi-form gyrus. When the seed was located in the R. SPL, patients showed

decreased connectivity in the left insula, dACC, and bilateral dorsolateral prefrontal cortex (DLPFC) (see Table 6.3 and Figure 6.6). No significant group difference was found when the seed was located in the right precuneus.
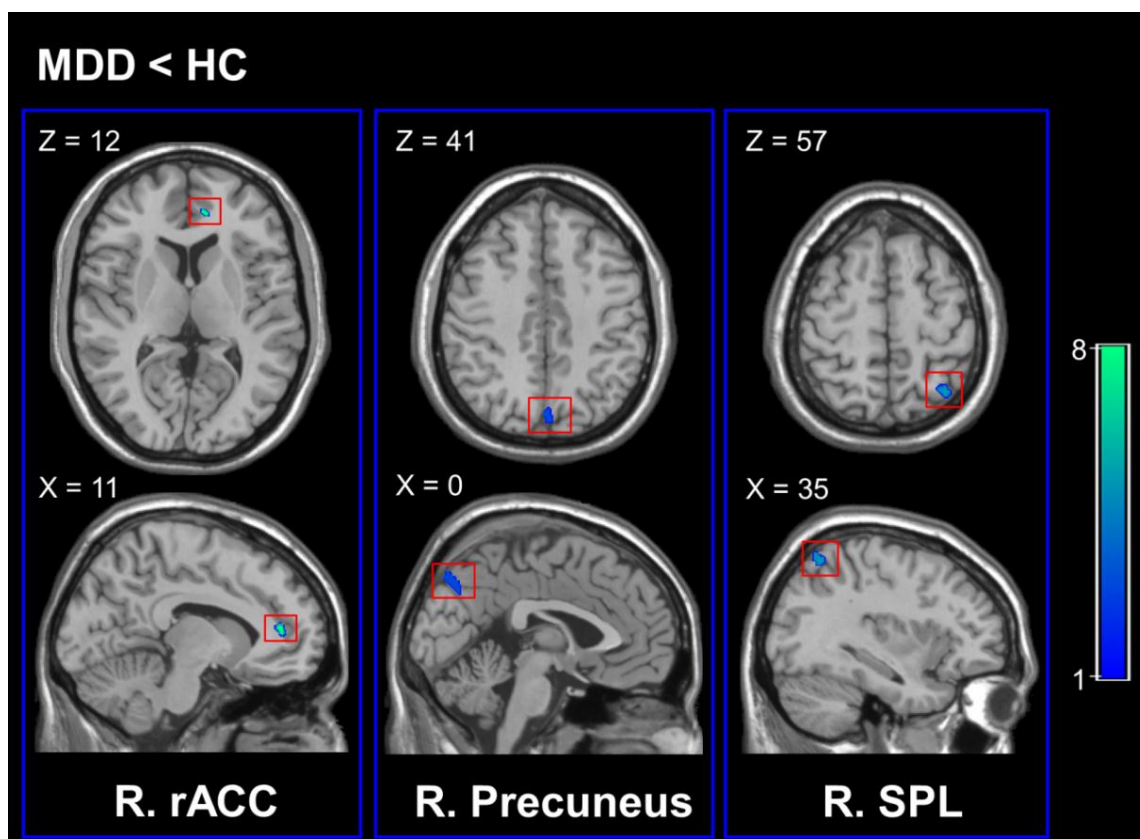
Fig. 6.5: Gray matter differences between MDD patients and healthy controls (HC). Cold color denotes the brain regions having significantly decreased gray matter volume in MDD patients compared with healthy controls.

Table 6.3: Brain regions with significantly altered functional connectivity in MDD patients. Abbreviation: rACC, rostral anterior cingulate cortex; SPL, superior parietal lobule; FFG, fusiform gyrus; Amy, amygdala; dACC, dorsal anterior cingulate gyrus; DLPFC, dorsolateral prefrontal cortex.

Seed	Connected Region	BA	Cluster	Talairach Coordinates			T-score
				x	y	z	
R. rACC	L. FFG	37	42	-45	-37	-15	4.32
	R. Amy	34	31	21	4	-10	3.52
	R. dACC	31	37	3	-29	40	3.69
R. SPL	L. Insula	47/13	48	-33	16	-3	4.33
	L. DLPFC	10	53	-39	42	17	4.65
	L. dACC	32	37	-9	17	18	4.13
	R. DLPFC	6	70	21	4	55	4.87
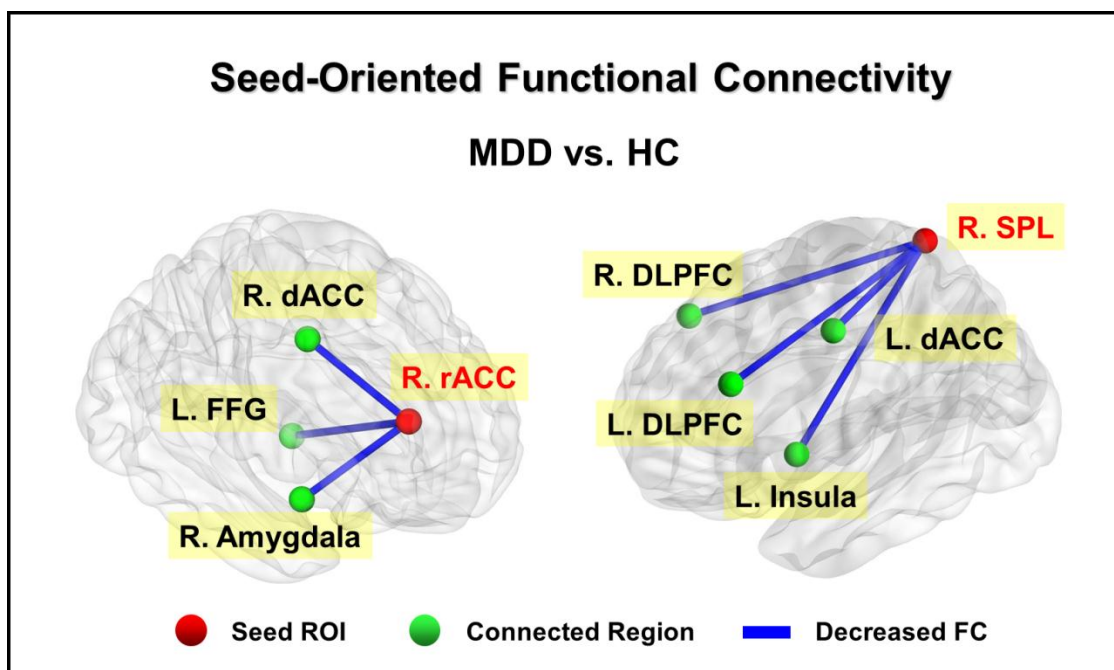
Fig. 6.6: Functional connectivity differences between MDD patients and healthy controls (HC). The blue line denotes the reduced functional connectivity between seeds and connected regions in MDD patients.

Brain-Symptom Associations

The average gray matter volume values of abnormal brain regions in MDD patients were extracted and correlated with the MDD symptom severity and anxiety level. As shown in Figure 6.7, significant negative correlations were only observed between gray matter volume in the rostral part of the anterior cingulate cortex and HDRS-17 total score ($r = -0.51$, $p < 0.05$), as well as T-AI total score ($r = -0.65$, $p < 0.01$). No significant correlations were found between other brain regions and clinical symptoms.
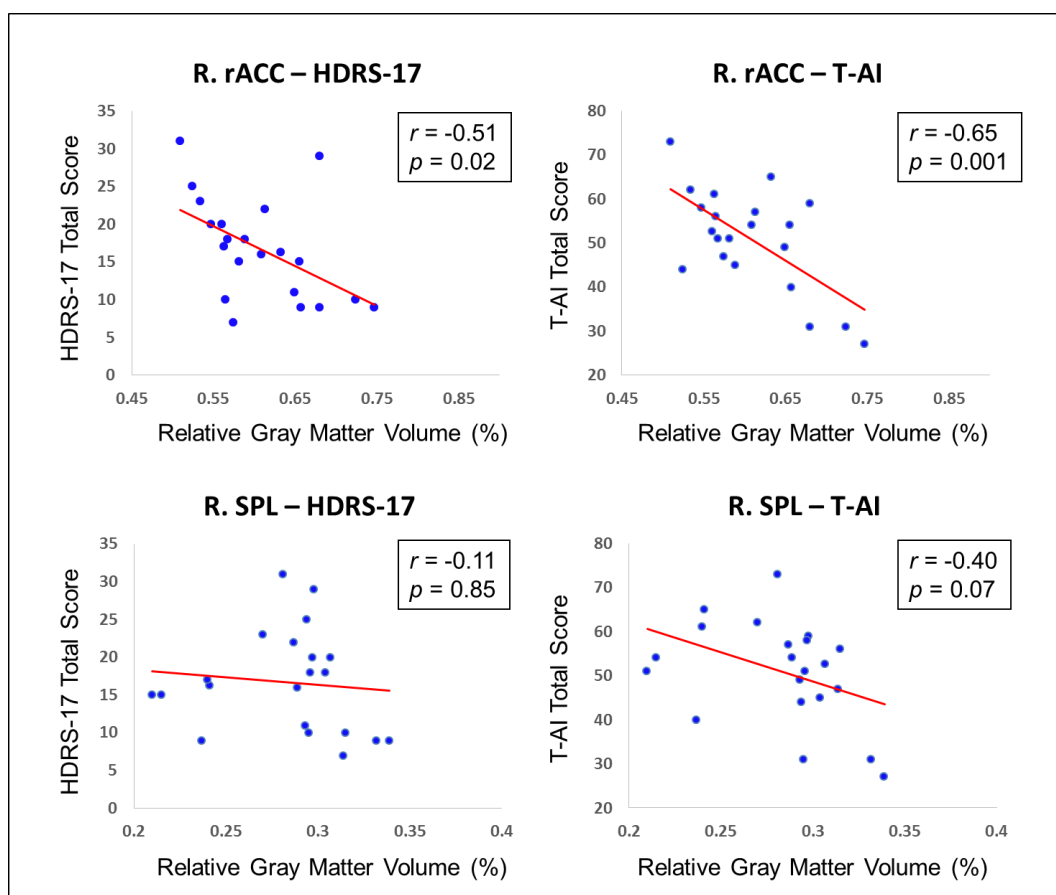
Fig. 6.7: Results of brain-symptom correlation analysis. Negative correlation between brain gray matter volume and total scores of HDRS-17 as well as T-AI.   Significant negative correlations were only observed in R. rACC (upper panel). Although R. SPL showed both structural and functional deficits in patients, correlations between R. SPL and clinical symptoms were not significant (bottom panel).

6.4.3 Discussion

The present study revealed an overall perspective about structural and functional abnormalities in patients with major depressive disorder (MDD) based on three aspects: gray matter volume (GMV) deficits, decreased resting-state functional connectivity between GMV deficits areas and other emotion or cognition-related regions, and the negative correlations between GMV and clinical symptom severity. Through the investigations using multiple structural and functional imaging modalities, we have not only verified the consistency of rostral part of anterior cingulate cortex (rACC) as the morphologic focal region for MDD, but also found out the functional changes and clinical characteristics that were related to the regions with morphologic abnormalities.

rACC and State-Dependent Morphologic Biomarker

Despite an incomplete understanding of the neural circuitry underlying MDD, there is growing consensus that some specific brain areas are significant to depression. Many studies have identified reduced grey matter volume (GMV) in anterior cingulate cortex (ACC) of MDD patients' brains (Depping et al., 2015). Three independent meta-analyses also revealed a robust relationship between MDD and the grey matter loss in ACC (Graham et al., 2013; Koolschijn et al., 2009; Zhao et al., 2014). Especially, a recent meta-analysis study, using signed differential mapping approach which can reconstruct both positive and negative differences in the same map (signed map), suggested that the most consistent region exhibiting GMV reductions in MDD patients were located in rACC (Bora et al., 2012). Although mass of studies have also focused on hippocampus and amygdala which are strongly related to depression as well, it was implied that, amygdalar reductions were more associated with untreated or comorbid depressive patients (Bora et al., 2012; Hamilton et al., 2008), and hippocampal

reductions can be only found subtly in patients with stress-related recurrent depressive episodes (Warner-Schmidt and Duman, 2006). Our finding of rACC GMV reductions in MDD is consistent with the previous investigations. The decreased volume in this area has been indicated to be associated with an abnormal reduction of cerebral blood flow (CBF), glucose metabolism, and glial cells that were observed by PET studies (Drevets et al., 2008). These findings have demonstrated that the rACC is robust to act as a focal region which showed neurophysiological abnormalities in MDD. Moreover, GM reductions were also found in the posterior parietal cortex in the current study, including the right precuneus and superior parietal lobule (SPL). Although less evidence could be found on the association between affective abnormalities and PPC, it was likely that the PPC deficits were related to the cognitive dysfunctions in MDD.

We also computed the correlation coefficients between regions with GMV deficits and symptom severity. It turned out that only the rACC showed significantly negative correlationship with depressive symptom severity (p = 0.02). The result suggests high sensitivity of GMV in rACC to depressive severity, and the potential association between GMV in rACC and prediction of disease progression. This is in line with the previous study (Drevets et al., 2008), and illustrates that the rACC may be a candidate for the state-dependent biomarker that can evaluate responses to anti-depressive treatments. Furthermore, the rACC appeared more sensitivity to anxiety level (p = 0.001) which presented a feasibility to predict anxiety level in MDD.

Disrupted Limbic-Cortical and Fronto-Parietal Networks in MDD

rACC is considered as a critical node in the limbic-cortical network and known to control emotional regulation by inhibiting the activity of limbic regions such as the hippocampus and the amygdala (Koolschijn et al., 2009). In the present study, the

decreased resting-state functional connectivity between the right   rACC and amygdala demonstrated a disrupted connection between the two regions which could account for the neuropathology underlying the disability to control negative emotions in MDD. MR spectroscopic studies detected an abnormal relationship between GABAergic-mediated neural inhibition as well as glutamatergic-mediated neural excitation in rACC in MDD (Northoff and Sibille, 2014). These observations pointed in the direction of an imbalance in MDD between excitation and inhibition in the rACC and provided further explanations for understanding the decreased functional connectivity observed in the present study. Moreover, reduced coupling of right rACC was also found in the connections to the left fusiform gyrus and the right dorsal anterior cingulate cortex (dACC). These results may reflect perturbations in neural networks related to social functioning and cognitive processing, due to the roles of the relevant regions in facial recognition and cognitive task achievement, respectively.

On the other hand, when the seed was located in the right SPL, MDD patients showed decreased functional connectivity in the left insula, dACC, and bilateral dorsolateral prefrontal cortices, which depicted a decoupling fronto-parietal network. The fronto-cingulo-parietal regions are believed to act as important nodes involved in the "task-positive" network that responds with activation increases to attention-demanding tasks. The deceased activation and impaired cognitive functions discovered in MDD patients might be elicited by the break-down of the fronto-parietal network (Wagner et al., 2015).

6.5   Neural Correlates Underlying Ahedonia in MDD

Ahedonia, reflected in the reduced neural responses to reward, has been constantly identified in patients with major depressive disorder (MDD). However, less is known regarding the underlying mechanism of ahedonia. To find out the answers, we implemented an fMRI experiment and collected both task-state and resting-state data from 19 MDD patients and 19 healthy controls matched for gender, age, and years of education with MDD patients. The distraction paradigm was applied to investigate the attention deployment under different emotional conditions. We find concurrent deficits in arousing activations in both reward processing-related regions and salience network consisting of the dorsal part of anterior cingulate cortex (dACC) and bilateral anterior insula (AI) during positive condition in only MDD group. Subsequent amplitude of low frequency fluctuations (ALFF) analysis based on resting-state data showed abnormalities in the bilateral AI of MDD patients as well. Voxel-wise resting-state functional connectivity analyses revealed disrupted salience system in MDD patients and indicated their difficulties in regulating the balance between central executive network (CEN) and default mode network (DMN) owing to the altered connectivity among the three networks. These results provide the first evidence demonstrating design-independent, generalized abnormalities in the salience network of MDD patients by integrating task-state and resting-state data. Our findings suggest that the altered salience detection for positive stimuli may contribute to the ahedonia. Moreover, the right AI could be a candidate region for evaluating ahedonia severity and effects of anti-depressive treatment.

6.5.1 Materials and Methods

The information about experimental design, MR data acquisition, preprocessing and analysis of task-state data here is same as that described in Section 6.3.1

Participants

Nineteen right-handed MDD patients (8 males and 11 females) were recruited among outpatients from Beijing Anding Hospital, China, and 19 healthy controls (HC) matched for gender, age, and years of education with MDD patients were recruited from community. Diagnostic assessments for all participants were performed by clinically trained and experienced raters (T. Tian and B. Fu) using the Mini International Neuropsychiatric Interview 6.0 (MINI 6.0) (Sheehan et al., 2010) based on DSM-IV. Hamilton Depression Rating Scale 17 Items (HDRS-17) was used to evaluate the clinical symptom severity of depression for only MDD patients. The 9-item Patient Health Questionnaire (PHQ-9) and 16-item Quick Inventory of Depressive Symptomatology (QIDS) were applied to make self-reports about the depressive symptoms for both MDD and HC groups. Anxiety level of all participants was evaluated by using Trait Anxiety Inventory (T-AI). Participant demographics and clinical characteristics are presented in Table 6.4. The exclusion criteria were same as that described in Section 6.4.1.

Functional MRI Analysis

Both resting-state and task-state data were collected in the present study. Task-state data were statistically analyzed as depicted in Section 6.3.1.

Table 6.4: Demographic and clinical characteristics of MDD patients and healthy controls. Abbreviation: HDRS-17, Hamilton Depression Rating Scale 17 items; PHQ-9, Patient Health Questionnaire 9 items; QIDS, Quick Inventory of Depressive Symptomatology; T-AI, Trait Anxiety Inventory.

Characteristics	MDD Patients (n = 19)	Controls (n = 19)	p -Value
Gender (male: female)	8 : 11	8 : 11	1
Mean age (years)	33.8 ± 10.5	33.3 ± 9.9	0.88
Education level (years)	14.1 ± 3.2	13.9 ± 3.6	0.89
HDRS-17 Total Score	15.8 ± 8.0	-	-
PHQ-9	11.3 ± 6.2	3.9 ± 3.1	0.00
QIDS	11.4 ± 5.6	4.3 ± 3.5	0.00
T-AI Total Score	51.2 ±11.6	38.1 ± 8.8	0.00

Mental addition and subtraction were regarded as one task (calculation task) in this part of study. Therefore, the group-level analysis was implemented based on a 2 by 3 factorial design with factors of "Group" (2 levels, between-group) and "Condition" (3 levels, within-group). Main effects of "Group" and "Condition" were analyzed to confirm whether differences in brain activation pattern exist between MDD patients and healthy controls (HC), and among positive task (PT), neutral task (NEUT), and negative task (NT). Interaction was also examined for the two factors. Further inspections for the simple effects could be computed following a significant interaction, by which comparisons between groups under either emotion state would be allowed. Thresholds were set at a voxel-level $p < 0.005$, cluster size > 1242 mm^3, corresponding to a corrected $p < 0.05$ as determined by AlphaSim correction.

Prior to the start of the task experiment, a five-minute resting-state fMRI measurement was implemented for all subjects. Compared with the preprocessing of task-state data, resting-state images were spatially smoothed with a 4-mm FWHM isotropic Gaussian kernel for conventional sake. The linear detrending and band-pass

filtering (0.01-0.08 Hz) were performed on the resting-state time series, followed by regressing out mean time series of global, white matter and cerebrospinal fluid signals, to remove artifacts and reduce physiological noise. Analyses for resting-state data were conducted by using REST Toolkit. A whole-brain amplitude of low frequency fluctuations (ALFF) map of each subject was calculated and transformed to zALFF map via a standardization processing. Two-sample t-test was performed on the zALFF maps between MDD and HC groups. Resulting brain regions with significant differences were overlapped with the aforementioned brain maps that resulted from task-state analyses. Common regions with differences implicating consistence of neural alteration of MDD patients in both task-state and resting-state, especially those regions included in salience network, were considered as seeds for the further analyses. Functional connectivity analysis was performed using a voxel-wise correlation approach based on the resting-state time series. Pearson correlation coefficients between one seed and the rest parts of the brain were computed voxel-by-voxel. Differences in functional connectivity between the MDD and HC groups were compared by two-sample t-tests following a Fisher's r-to-z transformation. Thresholds were set at a voxel-level $p < 0.005$, cluster size > 351 mm^3, corresponding to a corrected $p < 0.05$ as determined by AlphaSim correction.

Mean percentage BOLD signal change acquired during each task condition and averaged zALFF score of each seed were extracted with a 6mm-radius sphere for each subject, and correlated with the symptom scores of depression and anxiety to investigate the interaction between altered brain functions severity of clinical symptoms. SPSS 19.0 software (SPSS, Chicago, IL, USA) was used for the statistical analyses.

Diffusion Image Acquisition and Processing

DTI data were acquired on a 3.0 Tesla MRI scanner (Siemens Trio Tim; Siemens Medical System, Erlanger, Germany) with a 12-channel phased array head coil using a spin-echo, echo-planar sequence including 12 non-collinear, icosahedrally distributed directions, 3 b0 images and 45 axial slices (TR/TE: 6000 / 87 ms, b = 2 : 1000 s/mm^2; FOV = 256 × 256 mm^2). For processing, images were corrected for slice prescription and for residual eddy current distortions and motion artifacts using combined nonlinear 2-dimensional and 3-dimensional rigid body registrations. The diffusion tensor was computed at each voxel using a linear least squares method. The resultant eigenvalues were used to compute the fractional anisotropy (FA, degree of anisotropic diffusion).

FSL's Randomize tool (http://www.fmrib.ox.ac.uk/fsl/randomise/index.html), which combines the general linear model (GLM) with permutation testing, was used for voxel-based analysis of each diffusion metric. Two-sample t-tests were performed to obtain differences in FA value between groups.

6.5.2   Results

Behavioral Results

We carried out two-way repeated-measures analyses of variance on the accuracy (ACC) and reaction time (RT) by specifying the 3 task conditions as within-group factor and the 2 groups as between-group factor. In the MDD group, the average ACC was 86.84 ± 11.51% (mean ± SD) for the positive task (PT), 85.96 ± 15.94% for the neutral task (NEUT), and 85.75 ± 12.46% for the negative task (NT). In the HC group, the average ACC was 92.25 ± 7.49% for the PT, 92.98 ± 6.10% for the NEUT, and 90.94 ± 5.23% for the NT. Only the main effect of group was significant, with the $F_{(1, 108)} = 8.897$, p =

0.004. MDD patients showed significantly lower ACC than the healthy subjects.

In the MDD group, the average RT was 2461.96 ± 463.03 ms for the PT, 2467.21 ± 498.99 ms for the NEUT, and 2500.29 ± 485.92 ms for the NT. In the HC group, the average RT was 2391.31 ± 375.99 ms for the PT, 2405.70 ± 346.38 ms for the NEUT, and 2452.68 ± 384.96 ms for the NT. Neither main effect nor interaction reached significance.

Group Comparison of Task-Induced Activation

The group-level analysis based on factorial design exhibited significant main effects of group and condition, as well as significant interaction between group and condition. Post hoc 2-sample t-tests were implemented to examine brain activation differences of emotional responses and attentional control between MDD and HC groups under different emotional state. In the positive condition, MDD patients showed only decreased brain activation in the left anterior insula (AI), right orbital portion of inferior frontal gyrus around the AI, left precuneus, bilateral angular gyri (AG), bilateral dorsolateral prefrontal cortices (DLPFC), and bilateral thalamus extending to putamen, caudate nuclei, pallidum, and other subcortical areas (see Figure 6.8A). In the neutral condition, decreased brain activations were observed in the right precuneus and left DLPFC in MDD patients compared with healthy subjects. In the negative condition, MDD group showed a similar pattern as in neutral condition with only decreased activation in the right precuneus and left DLPFC. All the regions with significant activation are listed in Table 6.5. No increased activation was found for MDD patients in either condition.
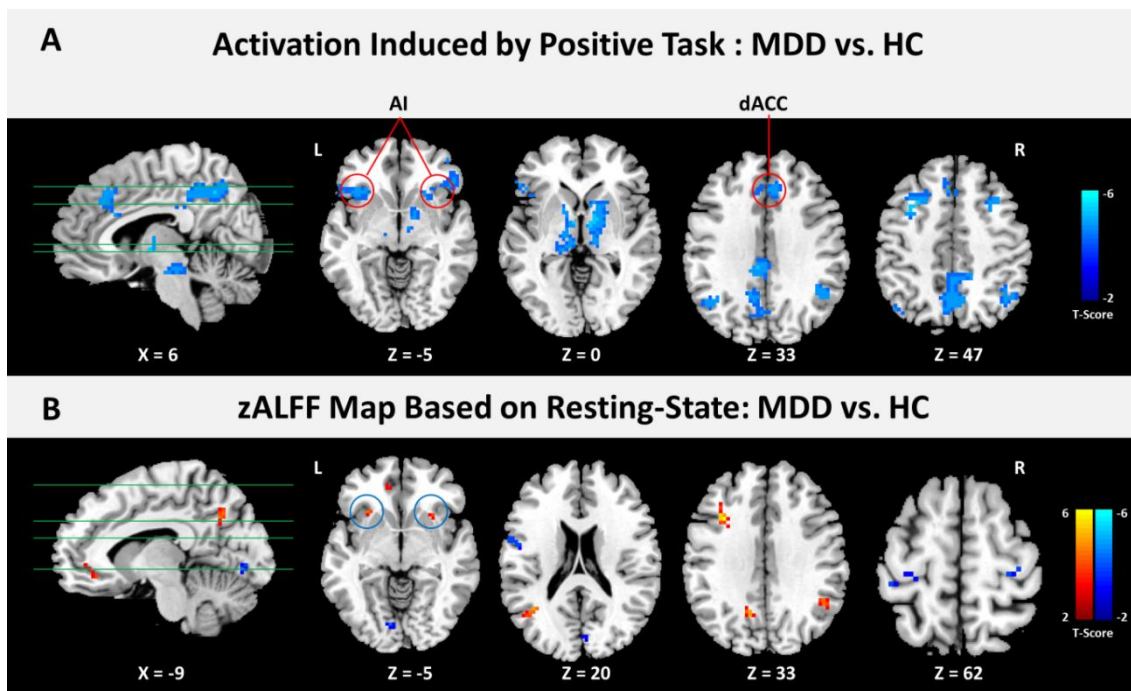
Fig. 6.8: Regions showing significant differences in brain activation and zALFF between MDD and HC groups. (A) Compared with HC group, MDD group showed only decreased activation in frontal-parietal, subcortical, and midbrain areas, especially in the dorsal part of anterior cingulate cortex (dACC) and anterior parts of bilateral insula (AI) which constitute the salience network. (B) Comparison between the two groups demonstrated significant differences in the zALFF values based on resting-state data. The bilateral AI showed significantly increased zALFF values in MDD group. The color bars indicate t-values from each t-test analysis.

Group Comparison of zALFF Values Based on Resting-State Data

A two-sample t-test was applied to reveal differences in zALFF values between MDD and HC groups. As shown in Figure 1B, regions presenting significantly increased zALFF values in MDD group included the left subgenual part of anterior cingulate cortex (sgACC), left DLPFC, left precuneus, right AG, bilateral middle temporal gyri (MTG), and bilateral AI. Compared with HC group, regions with significantly decreased zALFF values in MDD group included the left postcentral gyrus, left lingual gyrus, right cuneus, bilateral precentral gyri, and bilateral parahippocampal gyri/

amygdalae. All the regions presenting significant differences in zALFF values between the two groups are listed in Table 6.6.

Resulting zALFF maps with group differences were overlapped to the brain maps involving activation differences observed in task conditions. The common regions located at the bilateral AI, left precuneus, and right AG (see Figure 6.9 and Table 6.7). In order to conduct the further functional connectivity analyses and compute the correlations between functional values and clinical data, the bilateral AI entered at (-30, 21, -6) and (30, 15, -9) in MNI space were selected as seeds, considering their roles in salience detection and reward processing according to our hypothesis.

Table 6.5: Regions with decreased activation elicited by contrasts of MDD versus HC in positive task, neutral task, and negative task, respectively. Abbreviation: IFGorb, orbital portion of inferior frontal gyrus; DLPFC, dorsolateral prefrontal cortex; AG, angular gyrus; L, left; R, right; BA, Brodmann area.

Condition	Region	BA	Cluster	Peak MNI			T-score
				x	y	z	
Positive Task	L. Insula	47/13	114	-36	24	-12	-4.09
	R.IFGorb	47	67	42	51	-12	-4.34
	L.Thalamus		299	12	-3	0	-4.69
	R.Thalamus		187	-6	-6	0	-4.80
	L. DLPFC	8/6	245	-30	12	45	-4.59
	R. DLPFC	8/6	49	33	15	57	-4.18
	L. Precuneus	7	406	3	-54	42	-4.58
	L. AG	40	57	-45	-63	30	-3.38
	R. AG	40	126	42	-57	51	-3.81
Neutral Task	R. Precuneus	7	150	6	-57	39	-3.83
	L. DLPFC	8/6	52	-33	15	42	-3.54
Negative Task	R. Precuneus	7	60	3	-60	42	-3.97
	L. DLPFC	6	60	-30	6	57	-3.68

Table 6.6: Regions with group differences in zALFF values calculated based on resting-state data. Abbreviation: sgACC, subgenual part of anterior cingulate cortex; MTG, middle temporal gyrus; Parahip, parahippocampal gyrus; Amyg, amygdala; PreCG, precentral gyrus; PostCG, postcentral gyrus; LG, lingual gyrus.

Contrast	Region	BA	Cluster	Peak MNI			T-score
				x	y	z	
MDD > HC	L. Insula	13	25	-27	21	-3	4.89
	R. Insula	13	58	30	12	9	5.19
	L. sgACC	10	16	-9	36	-12	3.69
	L. MTG	39	26	-42	-60	18	5.28
	R. MTG	21	16	66	-54	9	4.03
	L. DLPFC	9	18	-33	15	33	5.46
	L. Precuneus	7	28	-12	-60	36	4.65
	R. AG	40	23	45	-51	30	5.63
MDD < HC	L. Parahip/ Amyg	28	13	-21	-9	-24	-3.66
	R. Parahip/ Amyg	28	16	18	-6	-27	-3.77
	L. PreCG	6	20	-54	0	18	-4.28
	R. PreCG	4	22	39	-24	51	-4.02
	L. PostCG	4	18	-36	-30	69	-4.39
	L. LG	18	15	-9	-81	-6	-3.85
	R. Cuneus	19	18	6	-90	27	-4.12

Table 6.7: Common regions showing group differences in both task state and resting state. The bilateral anterior insulae (AI) were determined as seeds for further analyses.

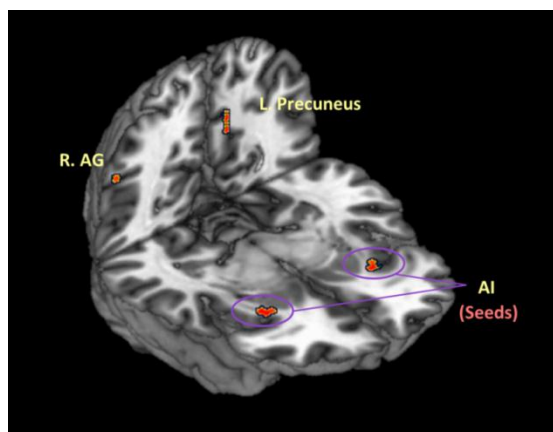| Region	BA	MNI Coordinates		
		x	y	z
L. Insula	13	-30	21	-6
R. Insula	13	30	15	-9
L. Precuneus	7	-12	-60	36
R. AG	40	45	-51	30

Fig. 6.9: Common regions showing significant differences in both task-state and resting-state between MDD and HC groups. The bilateral anterior insulae (AI) were determined as seeds for further analyses.

Group Comparison of Resting-State Functional Connectivity

Voxel-wise functional connectivity (FC) analyses revealed the Pearson correlation coefficients between the seeds and the rest parts of the brain. Two-sample t-tests were used to disclose the group differences in the connectivity (see Figure 6.10 and Table 6.8). After the comparison of the L. AI-centered FC maps, regions revealing significantly increased correlation to the seed contained the left sgACC, left medial prefrontal cortex (mPFC), left LG, right calcarine, and left precuneus. Regions showing significantly decreased correlation included the right insula, right caudate nucleus (CN) ventrally extending to the nucleus accumbens (NAcc), right dACC, left middle cingulate gyrus (MCG), right supplementary motor area (SMA), right superior parietal lobule (SPL), and bilateral DLPFC. On the other hand, comparison of the R. AI-centered FC maps in MDD versus HC showed significantly increased correlation between the seed and the right insula, right middle occipital gyrus (MOG), bilateral LG, and bilateral superior temporal gyrus (STG). Regions showing decreased correlation to the right AI included the right CN, left putamen, left mPFC, left dACC, right MCG, right SMA, bilateral posterior cingulate cortex (PCC), bilateral AG, and bilateral DLPFC.
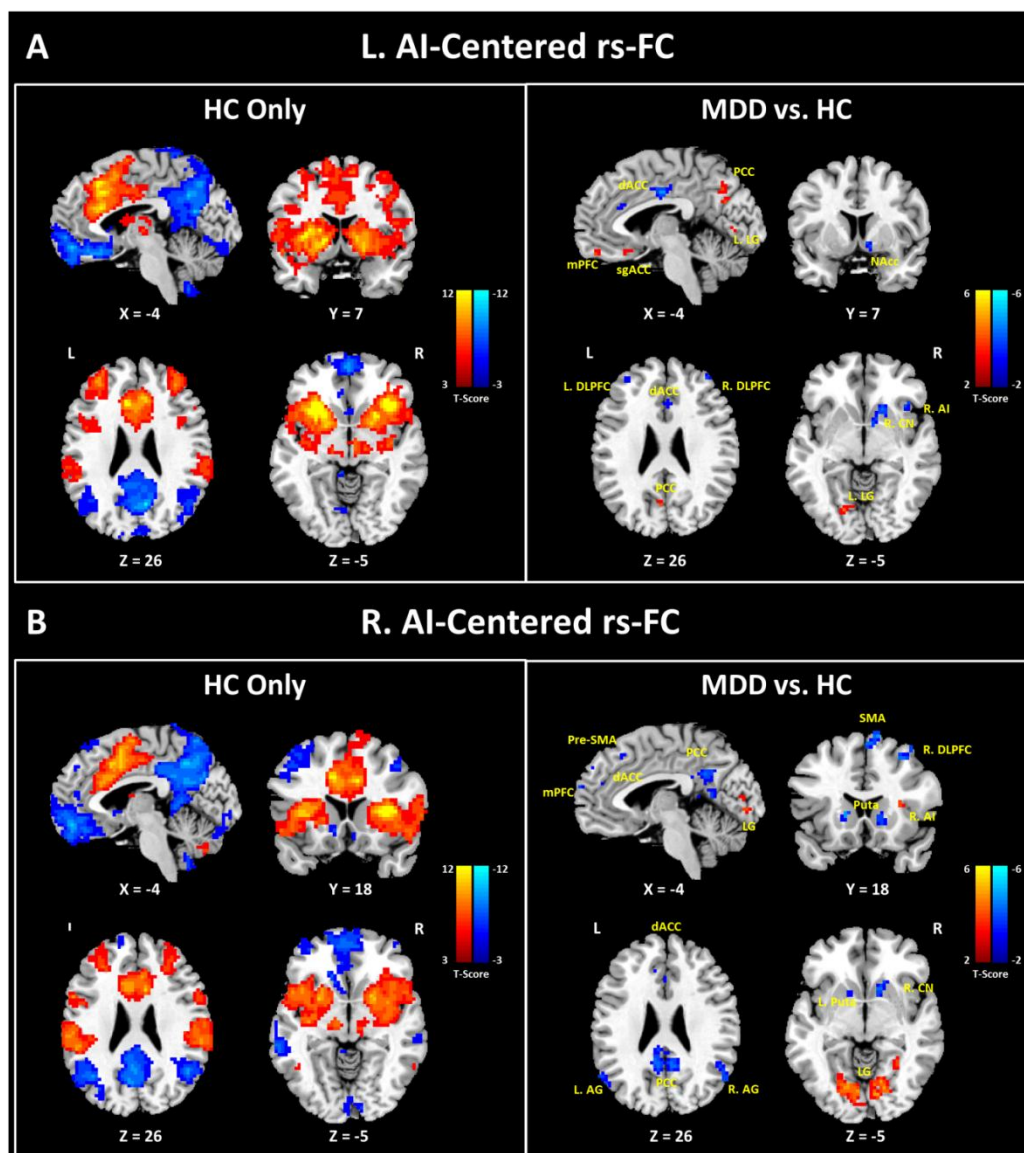
Fig. 6.10: Results of voxel-wise functional connectivity analysis based on resting-state (rs-FC) data. One-sample t-tests were only used for the HC data to show the intact functional connectivity under healthy mental state (left parts of A and B). Two-sample t-tests were used to show the alterations in the functional connectivity caused by MDD via group comparisons (right parts of A and B). (A) Results of L. AI-centered rs-FC analysis. (B) Results of R. AI-centered rs-FC analysis. The color bars indicate t-values from each t-test analysis. Abbreviation: mPFC, medial prefrontal cortex; PCC, posterior cingulate cortex; NAcc, nucleus accumbens; CN, caudate nucleus; pre-SMA, pre-supplementary motor area; SMA, supplementary motor area; Puta, putamen.

Table 6.8: Regions showing significant differences elicited by group comparison of voxel-wise functional connectivity based on resting-state data. Abbreviation: mPFC, medial prefrontal cortex; MCG, middle cingulate gyrus; SMA, supplementary motor area; SPL, superior parietal lobule; STG, superior temporal gyrus; MOG, middle occipital gyrus; PCC, posterior cingulate cortex.

Seed (Contrast)	Region	BA	Cluster	Peak MNI x	y	z	T-score
L. AI							
(MDD > HC)	L. sgACC	25	15	-6	24	-21	3.81
	L. mPFC	10	13	-6	51	-18	3.55
	L. LG	18	20	-18	-75	-9	4.04
	R. Calcarine	18	24	3	-78	3	3.38
	L. Precuneus	7/31	25	-3	-69	27	3.34
(MDD < HC)	R. Insula	47	20	39	18	-9	-4.60
	R. Caudate		34	18	15	-9	-4.03
	R. dACC	24	34	6	30	24	-4.05
	L. DLPFC	10	19	-33	42	24	-3.26
	R. DLPFC	10	15	39	51	30	-3.59
	L. MCG	24	45	-3	-9	36	-4.59
	R. SMA	6	49	12	18	57	-4.94
	R. SPL	7	13	39	-63	60	-4.07
R. AI							
(MDD > HC)	L. LG	18	219	-24	-78	-9	5.00
	R. LG	18	209	18	-75	-9	5.34
	L. STG	41	14	-51	-27	9	3.84
	R. STG	22	16	60	-6	0	3.40
	R. MOG	19	16	30	-84	15	3.42
	R. Insula	13	13	30	15	12	4.07
(MDD < HC)	R. Caudate		26	15	15	-6	-4.34
	L. Putamen		14	-15	18	3	-4.69
	L. mPFC	10	18	-9	57	6	-4.04
	L. dACC	32	15	-9	36	15	-3.82
	R. MCG	31	18	3	-24	39	-3.66
	L. PCC	29	36	-6	-57	9	-3.91
	R. PCC	31	216	6	-54	30	-4.84
	L. AG	39	22	-60	-63	27	-3.78
	R. AG	39	122	51	-54	33	-4.57
	L. DLPFC	8	19	-24	27	57	-3.68
	R. DLPFC	8/6	33	30	15	48	-4.36
	R. SMA	8	64	12	18	66	-4.39

Correlation between fMRI Results and Clinical Data

In the MDD group, the mean percentage BOLD signal change during the positive task exhibited significant negative correlations with the total score of Hamilton Depression Rating Scale 17 Items ($r = -0.48$, $p = 0.038$) and the subscore for feeling down, depressed or hopeless of 9-item Patient Health Questionnaire ($r = -0.58$, $p = 0.009$), suggesting that patients with more severe MDD symptoms show lower BOLD signal change when engaging in positive task. No other significant correlation was found between other fMRI results and clinical data in MDD patients. In the HC group, neither the mean percentage BOLD signal change obtained from task conditions nor averaged zALFF score revealed significant correlation with clinical data. Results of correlations between fMRI results and clinical data are shown in Figure 6.11.
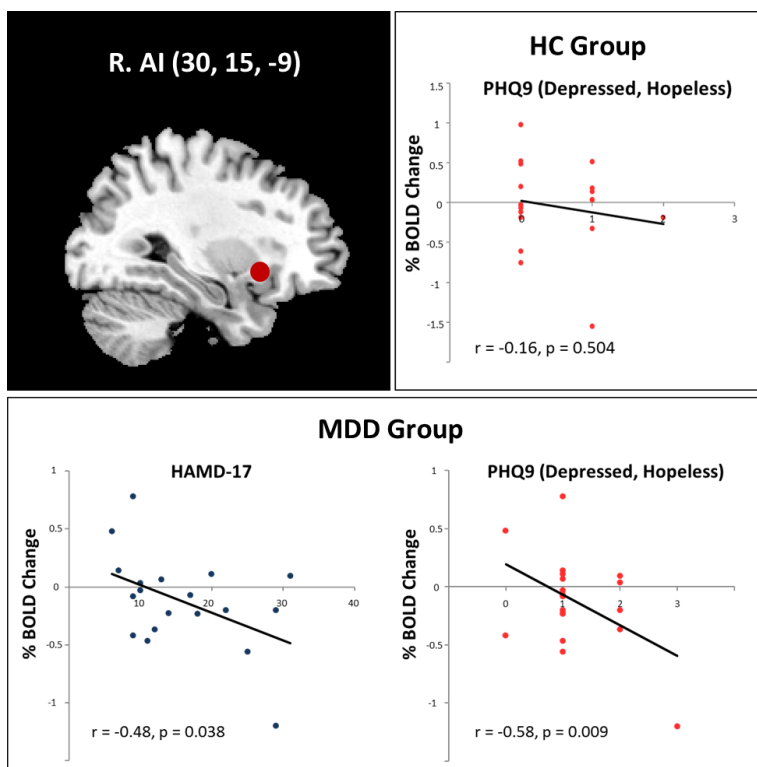

Fig. 6.11: Correlation between percent BOLD change and clinical data. Significant negative correlations with the total score of Hamilton Depression Rating Scale 17 Items and the subscore for feeling down, depressed or hopeless of 9-item Patient Health Questionnaire were identified in only MDD group.

Results of VBA Analysis Based on Diffusion Data

Compared with healthy controls, the MDD patients revealed decreased fractional anisotropy (FA) value in the left unciform fasciculus, with the peak at (-26, -6, -4) in MNI space (see Figure 6.12).
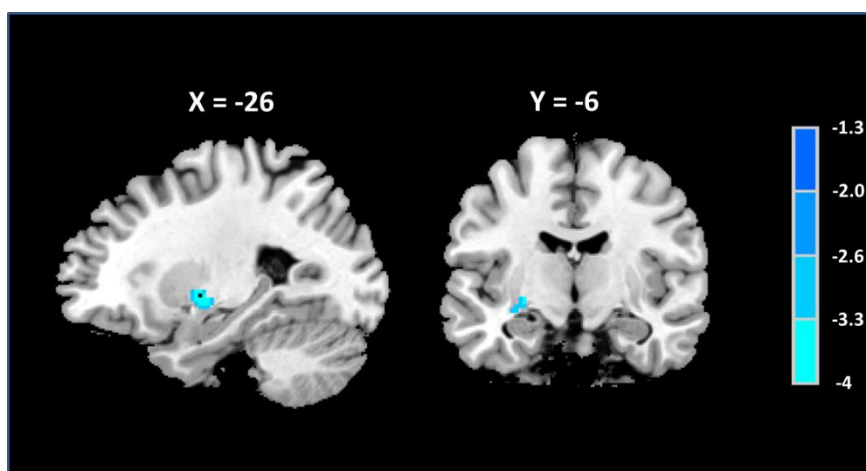
Fig. 6.12: Results of VBA analysis based on diffusion data. MDD patients revealed decreased fractional anisotropy (FA) value in the left unciform fasciculus compared with healthy controls.

6.5.3 Discussion

As a hallmark clinical symptom, anhedonia rates highly in making a diagnosis of depression. Lack of reactivity to pleasurable stimuli within brain is conceived as a cardinal feature of anhedonia, reflected in the dysfunction of midbrain, striatum, and limbic areas (Bracht et al., 2014; Lally et al., 2014; Pizzagalli et al., 2009). Given the prior evidence indicating reduced response to positive stimuli and selective attention to negative stimuli in MDD patients (Asthana et al., 1998; Atchley et al., 2012; Henderson et al., 2014), the abnormalities in the salience detection of positive stimuli is likely to contribute to the diminished pleasure. Therefore, we carried out a distraction experiment, and hypothesized that it would be effortless for MDD patients to shift their foci onto

distractors from viewing positive pictures. On the contrary, drawing attention out from negative pictures would be more difficult and might lead to more increased activation in attention-related regions for patients. Moreover, normalized ALFF values were also calculated for each subject based on their resting-state data to test the consistency of the abnormalities during different states. Resulting brain maps from distraction task and zALFF values obtained from resting-state were overlapped, common regions showing group differences in both states were selected as seeds for guiding subsequent resting-state functional connectivity analyses. Finally, mean percentage BOLD signal change measured during each task condition and averaged zALFF score of each seed were extracted for each subject, and correlated with the symptom scores of depression and anxiety.

Aberrant Executive Control, Ruminative, and Reward Processes in MDD Patients

As post hoc analyses results for the group-level factorial design, only significantly decreased activation was revealed by comparing MDD patients with HC subjects in all the three conditions. Hypoactivity was found in the left DLPFC and precuneus across the three conditions. The left DLPFC is well-known for its role in central executive of working memory (Baddeley, 2003) and top-down voluntary modulation of positive and negative emotions (Beauregard et al., 2001; Phillips et al., 2008). Given that the decreased activation in the left DLPFC was consistent even during neutral task in this study, abnormalities in this region is more likely to associate with difficulties in active cognitive control, i.e., cognitive manipulation in mental calculation. This inference was borne out by the behavioral results which showed significantly lower accuracy in patients relative to healthy subjects in all conditions. The precuneus, as a component of default mode network (DMN) which is always deactivated during goal-oriented

activities, is particularly critical for the facilitation of self-referential cognitive activity and autobiographical memory (Beauregard et al., 2001; Buckner and Carroll, 2007). It has been evidenced that the self-projection related to personal past experience relies closely on the precuneus (Buckner and Carroll, 2007). The deactivation in precuneus might imply the endeavor to suppress depressive rumination while MDD patients attempted to control their attention. The general pattern of the hypoactivity across tasks indicated the poor executive control and maladaptive rumination, especially difficulties in shifting from default mode network activity to task-positive network activity in MDD patients during participating in distraction tasks (Miller et al., 2015a).

Additional regions with decreased activation in only positive task were observed in the bilateral thalamus extending to caudate, putamen, pallidum, and other subcortical areas. These regions are of importance to perception of pleasure and euphoria, owing to the close connection to the dopaminergic mesolimbic pathway (Dreyer, 2010). Reduced activation in the subcortical areas overlapped regions for reward anticipation and receipt (Silverman et al., 2015a; Whitton et al., 2015). This result replicated findings of previous studies. Depressed adults showed reduced putamen activation during reward anticipation as well as reduced caudate, nucleus accumbens (NAcc) and dorsal anterior cingulate (ACC) activation to partially unpredictable rewards (Pizzagalli et al., 2009). The abnormalities in the subcortical areas are likely to be implicated in the impaired unciform fasciculus found by the VBA analysis. Recent findings indicate that ventral striatal blunting might constitute a risk factor for MDD. Specifically, reduced reward-related ventral striatal activation has been described in never-depressed youth at an increased risk for MDD due to a family history of MDD (e.g.,(Gotlib et al., 2010)), is evident even when accounting for (subclinical) depressive symptoms (Olino et al., 2014) and has been found to predict increases in depressive symptoms over 2 years among

adolescents (Morgan et al., 2013). However, differences in subcortical regions did not generalize to neutral or negative conditions, which indicate that reward processing abnormalities are central to the pathophysiology of MDD.

Impaired Salience Responses to Positive Stimuli in MDD Patients

In and only in the positive condition, relatively decreased activation was found in the bilateral orbital insular cortices and dorsal part of ACC which constitute the salience network (Seeley et al., 2007). As we hypothesized, this finding might result from an impaired incentive salience processing, that is, a morbid neglect of positive stimuli in MDD patients. When allocating the attention from viewing pictures to arithmetic problems, multiple salient targets led to more increased activation in the salience-related regions which could be observed across three conditions in HC subjects. However, positive pictures failed to induce activation in the bilateral insula of MDD patients, even when the corresponding activation could be elicited by neutral pictures. It has been built that the insula is situated at the interface of the cognitive, homeostatic, and affective systems of the human brain, providing a link between stimulus-driven processing and brain regions involved in monitoring the internal milieu (Craig, 2009). The dACC underlay interoceptive-autonomic processing and modules for sympathetic efference and interoceptive feedback processing (Critchley, 2005; Critchley et al., 2004). These regions coactivate in response to varied forms of salience, including the emotional dimensions of pain (Peyron et al., 2000), empathy for pain (Singer et al., 2004), metabolic stress, hunger, or pleasurable touch (Craig, 2002), enjoyable "chills" to music (Blood and Zatorre, 2001), faces of loved ones (Bartels and Zeki, 2004), and social rejection (Eisenberger et al., 2003). On the other hand, the co-occurrence of impaired reward processing and reduced activation in the salience network was frequently

identified for MDD patients (Dichter et al., 2012; Henderson et al., 2014). Collectively, it is very likely that the abnormalities in reward processing related to the ahedonia of MDD patients are caused by a morbid salient detection for positive stimuli.

To examine whether the alteration in salience system of MDD patients is dependent on the specific task condition or it is more generalized underlying the depressive pathology, we compared the standardized ALFF values between groups based on their spontaneous neural fluctuations. Interestingly, increased ALFF values seen in MDD patients mirrored the abnormalities revealed by positive task to a large extent, situated at task-related and default mode areas, particularly at the bilateral orbital insular cortices. ALFF has been established as a suggestive marker of regional spontaneous neuronal activity, and been utilized to identify morbid brain alterations (Dutta et al., 2014). The depressive disorder exaggerates the amplitude of spontaneous oscillation in some brain areas, e.g., the anterior insula, and influenced the brain activity during tasks. Although prior evidence has identified abnormalities in insula and dACC, no studies specially investigated changes in the salience network based on resting-state data before (Dutta et al., 2014). The dysfunctions demonstrated in this study occurred consistently across multiple states and supported our hypothesis that neglect of incentive stimuli caused by aberrant salience system underlies the depressive ahedonia.

Other alterations revealed by resting-state data located at the left DLPFC, left precuneus, right AG, bilateral MTG, and left sgACC reflected the maladaptive cognitive control and depressive rumination during task-state. As another DMN component, alterations in the bilateral MTG together with precuneus and AG exhibited a failure to normally regulate activity broadly within the DMN (Sheline et al., 2009). The sgACC is a constantly selected target for deep brain stimulation (DBS) treatment for depression because this region demonstrated abnormal cerebral blood flow (CBF)/metabolism,

tissue volume, and glial cells (Drevets et al., 2008).

Impaired Dynamic Switching in Salience Network of MDD Patients

The salience network is conceived as a toggle system allowing mental switch between DMN and central executive network (CEN) for processing self-referential and environmental information, respectively. The neurobiological basis is that, the AI and ACC which are rich in the von Economo neurons (VENs) are uniquely positioned to initiate control signals that activate the CEN and deactivate the DMN (Menon and Uddin, 2010). In healthy cohorts, the bilateral AI exhibit positive correlations with the CEN and reward circuit, negative correlations with the DMN (see Figure 3). This fixed pattern of interaction between networks regulates the balance between the CEN and DMN when individuals confront different situations. Nevertheless, MDD disintegrates the salience network, and alters the balance between CEN and DMN. In our study, reduced functional connectivity was found between the dACC and bilateral AI which probably induced difficulties during salience processing in monitoring error and conflict associated with the classical function of dACC (Menon et al., 2001; Seeley et al., 2007). Furthermore, decreased connectivity between the left AI and its right counterpart was demonstrated, eliciting functional dissociation between the two nodes. A morbid functional reversion was observed in the left AI which showed increased connectivity with the midline regions of prefrontal and parietal cortices (e.g., mPFC, sgACC, PCC), while exhibited decreased connectivity with regions anchored in CEN and reward circuit (e.g., DLPFC, NAcc). On the other hand, reduced functional connectivity was also found in the right AI, connecting both CEN (e.g., DLPFC, SMA) and DMN (PCC, AG). However, connections between the right AI and bilateral lingual gyri (LG) were strikingly enhanced. The LG has been reported to be within the visual recognition

network and is believed to have a role in the perception of emotions when facial stimuli are presented (Tao et al., 2013). Our findings indicated chaotic spontaneous activity in the left AI and declined activity prone to excessive introspection in the right AIs of MDD patients.

Finally, significant correlations between neural activity and clinical data were only found in the right AI, demonstrating the functional dissociation as well. Although the observed correlation did not line to a subscore of anhedonia directly, "feeling down, depressed, and hopeless" of 9-item Patient Health Questionnaire can also reflect the anhedonia to some extent. Thus, the percentage BOLD signal change in the right AI is likely to predict the severity of anhedonia in depressed patients. Moreover, the association between the total score of HAMD-17 and the mean percentage BOLD signal change in the right AI manifests that the neural changes found in the right AI could be possible state markers for evaluating of depressive severity and effects of anti-depressive treatment at a given time.

6.6   Conclusion

In conclusion, our results indicate that cognition and emotion influence each other, and are likely to compete for the cognitive resources for attention and executive control.

With respect to the MDD patients, the present study applied morphometry analysis and resting-state functional connectivity to examine the structural and functional integrity changes in MDD patients. Our findings provide evidence supporting both morphologic and functional deficits in the limbic-cortical and frontal-parietal areas in MDD patients that can lead to dysfunctions on emotional regulation and cognition. Especially the potential of rACC was revealed as a possible state marker for evaluating

the MDD disease progression, effect of anti-depressive treatment, and even the anxiety level, because of its convergence of gray matter volume abnormality, altered functional connectivity and sensitivity to the symptom severity. Nevertheless, it is unclear whether brain abnormalities in rACC can be also found in other psychiatric patients, such as patients with bipolar disorder. To figure out the specificity of rACC changes to MDD, comparison between MDD and other psychiatric patients will be necessary in the future.

Concurrent deficits in arousing activations were observed in both reward processing-related system and salience network consisting of the dACC and bilateral AI during positive condition in only MDD group. Subsequent ALFF analyses based on resting-state data from each subject showed abnormalities in the bilateral AI as well, demonstrating design-independent, generalized alterations in the salience network of MDD patients. These findings verified our assumption that shifting attention from viewing positive pictures to distractors would be effortless for MDD patients due to selective neglect of positive salience, thus elicit less activation in salience network and reward circuit and present ahedonia when confronting incentive stimili. Resting-state functional connectivity analyses were performed to explore neural mechanisms underpinning the aberrant salience processing, which showed disrupted salience system in MDD patients and indicated their difficulties in regulating the balance between CEN and DMN owing to the altered connectivity among the three networks. Based on the significant correlations between neural activities and the clinical data, the right AI could be a candidate region for evaluating ahedonia severity and effects of anti-depressive treatment.

<div align="right">

Chapter 7

</div>

Epilogue

7.1 Contributions and Discussion

This thesis has investigated the human cognition, emotion, and their interactions. The main contributions of the thesis are as follows:

1. The relationship between mental addition and subtraction and its neural mechanisms have been clarified. Our findings demonstrate that mental subtraction is inherently more complex than mental addition. Auxiliary phonological, visual, and motor processes for representing numbers are needed to complete the calculation of subtraction problems.

As a typical cognitive domain, the mental arithmetic was studied with fMRI in the current thesis. Both common and dissociated cognitive processes were found between addition and subtraction calculations. Relatively lower accuracy when computing subtraction compared with addition indicates the higher complexity and difficulty in subtraction processing. However, the two operations are not totally different as previous studies suggested (Schmithorst and Brown, 2004). The overlapped brain regions with increased activation when processing addition and subtraction in IPS and caudate nuclei demonstrate that addition also depends on magnitude representation and subtraction draws support from retrieving arithmetical fact as well.

However, extra brain regions with significant activation during only subtraction processing confirmed its higher complexity relative to addition calculation. Compared with addition, subtraction induced significantly greater activation in the left inferior frontal gyrus (IFG), middle portion of dorsolateral prefrontal cortex (mDLPFC), and supplementary motor area (SMA), suggesting more reliance on phonological, visual, and motor processes. With help of functional connectivity and dynamic modeling analyses, our results reveal that addition was more likely to engage (numeric) retrieval-based circuits in the left hemisphere, while subtraction tended to draw on (magnitude) processing in bilateral parietal cortex, especially the right intraparietal sulcus (IPS). Our findings endorse previous hypotheses about the differences in strategic implementation, dominant hemisphere, and the neuronal circuits underlying addition and subtraction. Moreover, for simple arithmetic, our connectivity results suggest that subtraction calls on more complex processing than addition: auxiliary phonological, visual, and motor processes, for representing numbers, were needed for subtraction, relative to addition.

2. The self-regulatory processes of aversive emotion induced by affective stimuli have been studied. Our findings show that both the bottom-up suppression and top-down regulation are applied to attenuate the aversive emotion spontaneously. Based on this result, a dual regulation model for controlling aversive emotion has been proposed.

The aversion initially induces responses in VS which endures the emotions by exerting a certain level of inhibition, until the emotions are defused over time. For intense emotions that exceed the magnitude that the VS can bear, the VS will recruit

help from the DLPFC by transmitting signals about the intense emotions along indirect pathways via the VLPFC and dACC. A five-minute observation of the self-regulation on the aversion indicated a tendency during which the bottom-up strategy was dominant in the early phase of the regulation, whereas, subjects switch to the top-down strategy in the latter period.

3. The interactions between mental arithmetic and emotion regulation and their neural substrates have been studied. Furthermore, supplementary investigations were performed on MDD patients. Our results indicate that cognition and emotion influence each other, since some cognitive resources and brain regions are shared by the both brain functions. Abnormal functioning in the joint areas is more likely to lead to impairments in both cognitive and emotional functions simultaneously.

Revealed by a distraction paradigm that combined emotional arousal and processes of mental addition and subtraction, positive stimuli impose less influence on the consequent mental calculation, while aversive stimuli radically hinder the attention for both addition and subtraction calculations. As the distractors, subtraction problems present weaker effects on down-regulating emotions, especially for the aversive emotion, when compared to addition problems. All these findings demonstrate that concurrent emotional regulation and cognitive activities compete for the cognitive resources for attention and executive control. Subtraction processing is characterized by high cognitive demanding, which results in deficiency in the L. DLPFC-centric resources that are necessary for the top-down regulation on aversive emotion. Studies on MDD patients provide new visions for exploring the relationship between cognition and emotion. Both structural and functional alterations can be

found in the cognition-specific, emotion-specific, and cognition-emotion joint brain areas in the MDD group only. Design-independent, generalized abnormalities in the anterior insular cortex of MDD patients, as one of the joint areas, most likely induce the altered salience detection for positive stimuli and contribute to the ahedonia in patients.

7.2 Limitations

Several limitations do exist in this thesis. One possible problem is the representativeness of the mental calculation as it is used to be the important example of human higher cognition. Actually, some other cognitive functions are more essential for human thinking and worth investigating than mental calculation, such as memory in which information is encoded, stored, and retrieved. The reason I chose this topic is that, students in our laboratory have researched on the information processing of mental calculation for a long time, and I continued this topic based on previous studies completed by the graduates. At the beginning of my research, I didn't expect to construct a research frame composed of cognition, emotion, and depression, but concentrated on the neural mechanism underlying mental calculation, and then naturally moved to the interaction between arithmetic and emotion. However, mental calculation is still a critical domain related to cognition. It provides compelling paradigms for investigating fundamental cognitive processes underlying abstract problem solving from a variety of domains, such as magnitude representation, executive control, verbal processes, and sensory-motor-derived concepts. Moreover, further understanding of the mental calculation is helpful to improve mathematical education. Although independent focus on memory was not included in the current thesis, the memory-based retrieval

strategy when performing calculations was indeed discussed. In future study, it is possible for me to explore the role of memory in mathematical study of children, given that individual growth and functional maturation might result in a shift from the memory-based frontal activation to the quantity-specific parietal activation in arithmetic processes.

According to different research purposes, a number of paradigms are available for studying mental calculation. For instance, different tasks can be used for examining exact arithmetic or approximate arithmetic. Methods of feedback collection are also multifarious. Responses can be made by choosing the correct answer out of a few puzzling options, or judging the validity of a proposed solution as adopted in our experiments, or in other forms. However, merits and demerits coexist for each feedback method. In the case of multiple puzzling options, subjects need to control more fingers to manipulate the controller for answering questions, which is likely to elicit more cognitive compounds, and risk pressing wrong buttons. The manipulation will turn to easier if subjects are asked to make a right-or-wrong response, however, the rate of correct answer will increase even if the answers are reliant on guess. We have to evaluate each design. Basically, the more complex an experimental design appears, the more conditions need to be controlled for the experiment. As a (preliminary) main experiment for studying mental arithmetic, we chose the right-or-wrong judgment as described in this thesis. In my opinion, comparison of results from experiments with identical contents but different feedback methods is likely to be an interesting research.

Top-down and bottom-up processes were mentioned in this thesis frequently. Generally speaking, they are two approaches to understand the flow of information in processing within human brain and pervasively utilized in neuroscience and psychology. Typically, sensory input is considered "down", and higher cognitive processes, which

have more information from other sources, are considered "up". In the bottom-up direction, process starts at the sensory input, i.e., the stimulus. Thus, this approach can be described as data-driven. In the top-down direction, process is characterized by a high level processing by more cognition, such as goals or targets. In a micro-scaled perspective, it is known that information about the stimulus is encoded in the pattern of action potentials and transmitted into and around the brain. Neurons are capable of propagating the signals in a remarkable speed over large distances. Thus, switches between top-down and bottom-up transmissions are probably proceeding transitorily. One-way transmission of information during a relatively coarse temporal period is almost impossible. Nevertheless, meso-scaled studies regard human brain as a holistic system, and aim at constructing a cognitive architecture composed by several spatially distributed subsystems (brain regions). The key to achieving such a goal is to conceptualize the trend how information flows are processed. Serving as a main approach dedicated in meso-scaled studies, fMRI is insufficient to disclose the signal transmission at the level of neuron, but is able to offer millimeter-based clues of neural mechanisms to establish cognitive models. In our future work, the observation of brain will be extended to micro scale, and the phrasing must be changed at that time.

In the present thesis, all the experimental results were obtained based on group analyses by averaging results from multiple subjects doing the same task. Apparently, results concluded from one individual subject will be biased by the individual difference extremely. The objective of our researches is to figure out some universal principles to disengage the puzzle of human brain. As a result, we must recruit a group of subjects for representing a population in each experiment to meet the statistical criteria. However, one problem is how to unify the original state of all the subjects before the experiment begins. Our solutions include: (1) recruiting subjects with similar demographic

information and education background (e.g., almost same age, from same college, etc.) to reduce individual differences; (2) performing identical experimental procedures and using same instructions on each subject; (3) training subjects on how to participate in tasks until all the subjects achieve almost same level of proficiency; (4) starting the on-task session of fMRI scanning after the first resting session to ensure that all the subjects have adapted to the environment inside the scanner. Although it is impossible to eliminate differences in the original states between subjects completely, we have done our best to control the differences.

Another problem is how to apply the results generated from group-based analyses to explain or predict an individual subject. Due to the differences in the shape of brains, involved number and even type of neurons confined in a certain brain region that can be specified by coordinates and size may be distinct across different subjects. fMRI has long been expected to play a part in clinic, such as supporting the diagnosis of mental diseases for a single patient. However, this goal is still unreachable at present. Statistics is a core technique supporting analysis of fMRI data. The weakness of fMRI aforementioned is related to the statistics characterized by collecting and analyzing numerical data in large quantities rather than describing each single data in detail. But even if the group-based results cannot be used for personalized service for now, they are still helpful to uncover general mechanisms of brain activities. Furthermore, as the sample size in an experiment increases, the accuracy of the results for predicting each single person will grow as well, as long as the sampling is reasonable. Computer science will accelerate the application of fMRI techniques. Dosenbach et al. (2010) trained a computer to recognize patterns in resting-state data. They collected data from nearly 240 people aged 7–30 years to build up maps of brain connectivity at different ages. By using the maps, they could take a single brain scan from a different person and,

by comparing it with their reference set, work out the owner's brain maturity.

7.3 Future Work

The human brain is highly complex, since it is serving as an information processing system with a hierarchy of different yet tightly integrated levels of organization: from thinking, functional domains, networks, brain regions, to microstructure, synapses, proteins, and genes. The process of understanding the implications of the cognition, emotion, and depression, as well as understanding their functional interactions, is in its infancy. If we can rise to the challenge, we can gain fundamental insights into what it means to human, develop new theories to broaden our horizons, and create new treatments for brain diseases.

As the future work, in addition to the concluded findings, the dissertation gives a direction for the future work. Especially, the following items may be considered as potential, challenging, future research subjects.

7.3.1 Extensions of Systematic Cognitive Experiments

The BI methodology advocates a systematic design of cognitive experiments to direct the top-down investigations on the human brain. Normally, when a specific domain of brain function is selected, a main experiment can be designed at first. One advantage of collecting data by ourselves (not by using shared data) is the availability to customize the experimental design for exploring the objects that have never been studied before. On this occasion, a main experiment will be favorable to serve as a preliminary. A modification of classical theories or paradigms should be a good choice to design the main experiment. In addition to the purpose of uncovering neural mechanisms

underlying a certain aspect of human thinking, another goal of the main experiment is to explore the "realm" of a research topic, for instance, to confirm the feasibility of the research plan, verify the validity of experimental materials, ascertain the minimum but allowable size of subject population, search for promising ideas to implement following experiments, and so forth. In order to support the results of main experiment, simple but solid parallel experiments that concentrate only on a unilateral feature of the main design can be performed. Between the main and parallel experiments, supplementary experiments are helpful to expand the range of the studies and test hypotheses summarized from former experiments. Moreover, deeper experiments should be effective to the investigation of a certain subtle processing that is noticed during the implementation of systematic studies (e.g., functional double-dissociation within a tiny region of the brain). When unscrambling the relationship between the main experiment and multiple parallel experiments, it is likely to think out new design which can be called inspired experiment. Hereby, a coarse frame of a BI-based data set has been established. The systematization makes it easy to find the absent experiments that are important but have not yet been carried out.

The aforementioned method is the principle for the design and practice of the thinking-centric experiments which facilitate the construction of BI brain big datacenter. The overall design of experiments within this thesis followed this principle (see Figure 7.1). At first, a paradigm involving fearful (aversive) picture and arithmetic problems was designed as a main experiment, with the original intention to study how the negative emotion disturbs mental calculation. After that, in order to elaborate the detailed processes of mental calculation and emotional responses, the experiments of arithmetic solving and fearful picture viewing were employed as parallel designs, respectively, to advance the research plan. Later, another use of the main experiment

occurred to us, in which the arithmetic can be utilized as the distractor to modulate the negative emotion. Under this structure, the integration of fearful pictures and numerical reasoning, as well as integration of fearful pictures and Sudoku can be further researched as supplementary or deeper topics.
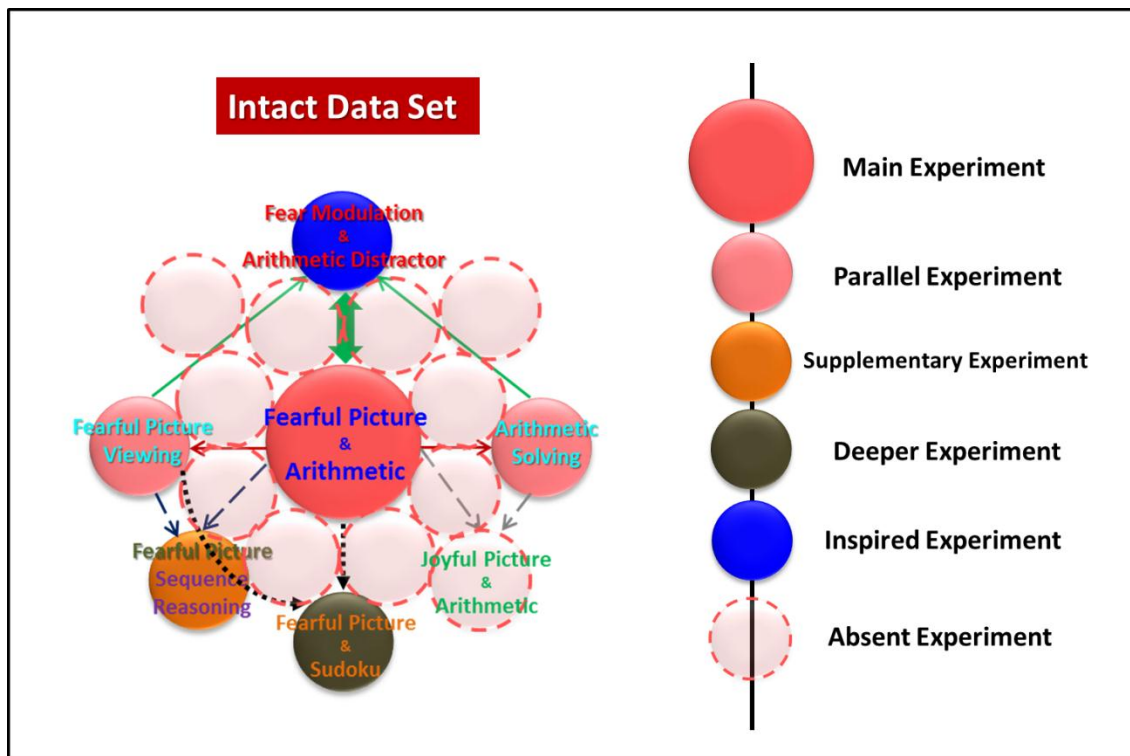

Fig. 7.1: Extensions of systematic cognitive experiments. The BI methodology advocates a systematic design of cognitive experiments to direct the top-down investigations on the human brain, by implementing main experiment, parallel experiment, supplementary experiment, deeper experiment, and inspired experiment.

We have only finished the main parts of this framework. For the collected data, extensions by carrying out supplementary or deeper experiments in the future will make them perfect:

- We analyzed the data of simple addition and subtraction calculations, and concluded that addition calculation is likely to recruit an alterable hybrid

strategy that can switch to the "subtraction mode" when dealing with difficult problems given the feasible neural basis. This result is consistent with the dual-pathway model proposed by Klein and colleagues which suggests a dynamic shift of neural circuits mediated by difficulty levels of the confronted addition problems (Klein et al., 2013). However, in order to verify this theory, only the 2-digit simple arithmetic problems without carrying and borrowing, as the ones adopted in this thesis, is not enough. In our future work, we plan to examine the neural substrates and their possible variations when the brain copes with different arithmetic problems, e.g., 1-digit simple problems without carrying and borrowing, 2-digit hard problems with carrying and borrowing, etc. We will also compare different types of calculations, such as concern on the differences between mental calculation and written calculation, as well as the distinctions between not only addition and subtraction, but also the multiplication and division.

- With respect to the emotion response and regulation, we only focused on the aversive emotion in the current thesis. Neuroimaging data are widely used to provide evidence for a specialization or fractionation of psychological function (Gray et al., 2002). Emotions are also discrete, measurable, and physiologically distinct (Ekman, 1992). Each emotion has unique features: signal, physiology, and antecedent events, as well as characteristics in common with other emotions: rapid onset, short duration, unbidden occurrence, automatic appraisal, and coherence among responses. Thus, couplings between different cognition and emotion types will generate varied neural phenomena that are worth studying. In the future, experiments will also be implemented on both positive and

negative emotions, such as happiness, contentment, excitement, embarrassment, guilt, sadness, etc. In addition, other alternative paradigms can be chosen to investigate the emotion regulation, such as selective inattention to emotional stimuli (Anderson et al., 2003), anticipation-driven emotion (Hsieh et al., 1999), and top-down reappraisal (Ochsner et al., 2002).

- The spectrum concept of mood disorders consists of the components of depression and mania, alone or in combination, on a continuum (Angst et al., 2015). One of the biggest challenges for the psychiatrists and psychologists is to find the biomarkers for telling bipolar and unipolar disorders (i.e., MDD) apart. Accurate diagnosis of bipolar disorder is difficult in clinical practice because onset is most commonly a depressive episode and looks similar to unipolar depression. In the next stage, we plan to compare MDD and bipolar patients based on the results disclosed in this thesis, and try to make it clear how bipolar patients differentiate from MDD patients at the neural level.

7.3.2 Convergence of Data from Different Cognitive Tasks

Interactions between variables may hold the key to understanding complex biological and social systems (Reshef et al., 2011). This is the reason why the current research drew a great emphasis on the relationship between cognition and emotion. We took advantage of the distraction paradigm by combining both the cognition and emotion factors to investigate the interactions between the two brain systems. Some good results are obtained by this approach which allowed the integration in the phase of experimental design and implementation. However, when the number of factors of interest increase, or when the shared open data sets without systematic design are taken

into further analysis, it will become a tough problem to integrate the relevant data. In the last decade, major advances have been made in the availability of shared neuroimaging data, such that there are more than 8,000 shared MRI (magnetic resonance imaging) data sets available online (Poldrack and Gorgolewski, 2014). The large-scale analysis of brain big data that meets the requirement of BI systematic investigations is in its urgent need of new methods. Compared to the brain activation that is normally used as the basic unit of fMRI studies, the functional connectivity eliminated the bias elicited the heterogeneity for different data sets, placing emphasis on pairwise relationships instead. The full correlation can therefore be employed as a stationary method for exploring the brain dynamics among different tasks (Turk-Browne, 2013).
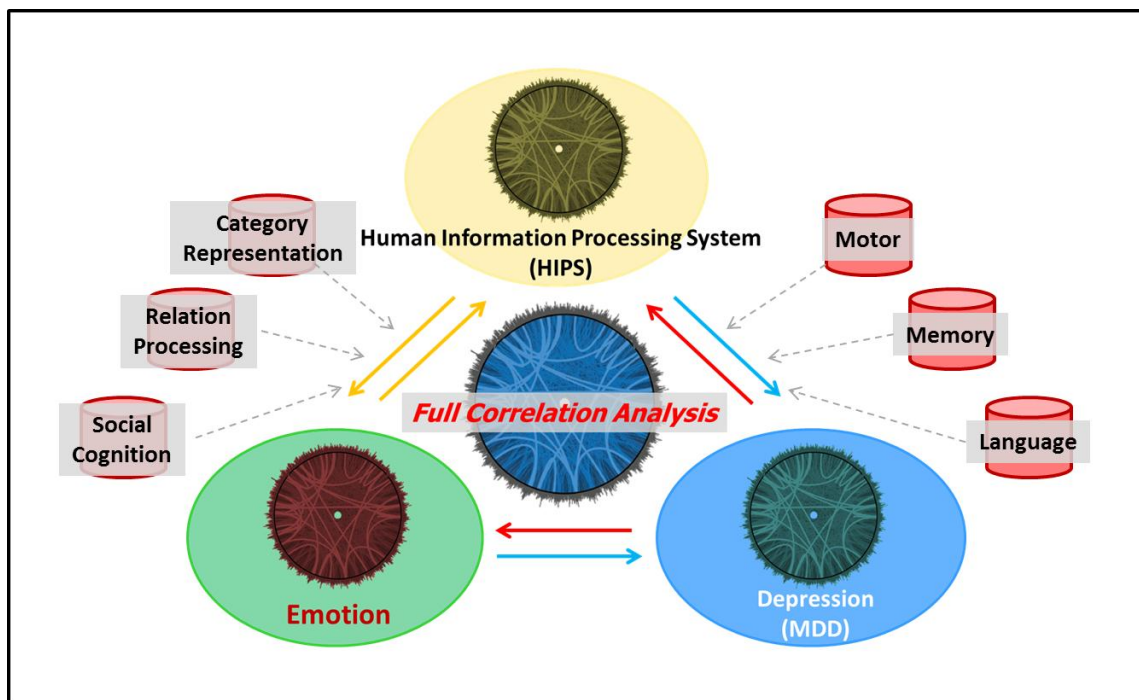

Fig. 7.2: Integrating brain big data with full correlation analysis. The full matrix of coefficients can transform all the brain data into the same scale, so that insights into the topology and dynamics of human brain networks can be generated across data.

For each task, the time course of BOLD activity in every voxel is correlated with every other voxel to produce a full correlation matrix. The full correlation matrix can be represented as a six-dimensional (6-D) autocorrelation field for each 3-D voxel in the brain, since the correlation is pairwise. To enhance the computational speed, matrix multiplication can be used. The full matrix of coefficients can be obtained by the product of a voxels by-time matrix and its transpose (Worsley et al., 2005). In this way, all the brain data can be transformed into the same scale, so that insights into the topology and dynamics of human brain networks can be generated across data (see Figure 7.2). In our future work, we will try the convergence of brain big data from different cognitive tasks by using this method, such unbiased approach provides the greatest flexibility for discovery.

7.3.3 Exploring the Boundary of Brain Big Data

The narrow sense of big data is the data sets with sizes beyond the ability of commonly used software tools to capture, curate, manage, and process data within a tolerable elapsed time. The increasing quantity of neuroimaging data has furthered our understanding on the fundamental principles of cognition and behavior. Meanwhile, the growth of the data also leads to great challenges to collect, transfer, store, and analyze the continuously incoming data (Muller and Hanbury, 2015). In accordance with the generalized concept of big data, the brain big data are also characterized by the volume, variety, velocity, veracity, and value, which indicate the big amount, big range of types, big speed, big accuracy, and big value of the brain data, respectively. However, it seems that too much emphasis has been put on the size only. Criticisms from some researchers have raised concerns about the use of big data in science neglecting principles such as

choosing a representative sample by being too concerned about actually handling the huge amounts of data. Aimless expansion of data size is likely to lead to presence of systematic errors or strong dependence in the data and results bias. A critical consideration about big data sets is whether you need to look at the full data to draw certain conclusions about the properties of the data or is a sample good enough. In this context, BI has put forward a concept about the "utility value" of the brain big data sets. A well-defined framework of thinking-centric brain data set (we call it intact data set) on basis of top-down construction and structured sampling creates higher utility value than a monotonous data set does, even if the monotonous data set contains larger size of data (see Figure 7.3), because interactions among subset data involved in the former are able to propagate new values automatically. Moreover, an intact data set provides more complete options to meet all kinds of needs of users. Hence, we will collect more brain data in view of utility value in future.
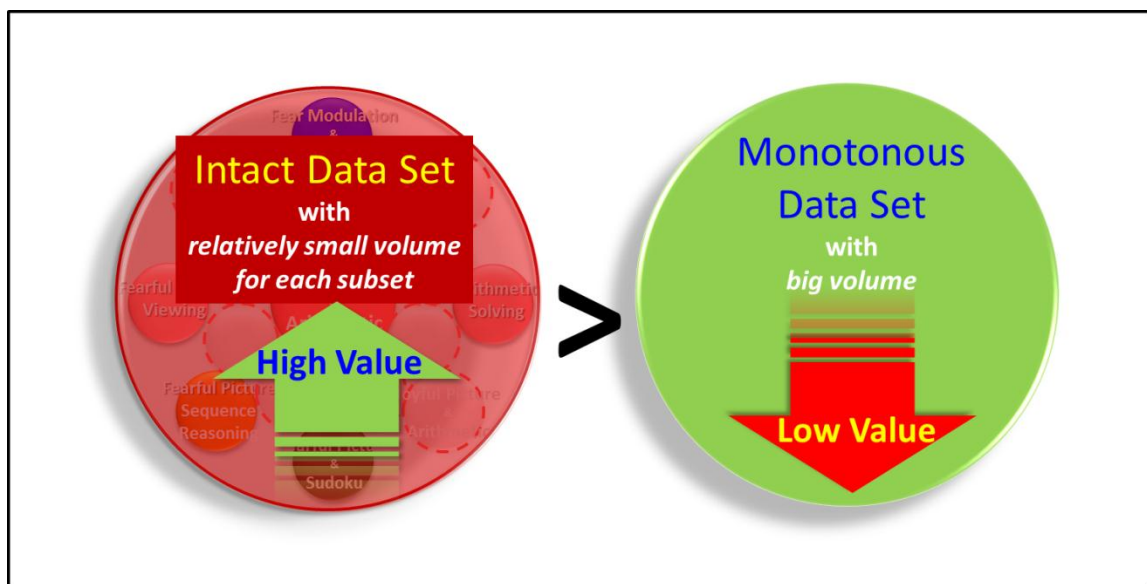

Fig. 7.3: A preliminary discussion about the boundary of brain big data. An intact data set based on top-down construction and structured sampling creates higher utility value than a monotonous data set does.

As the structured sampling will be carried out, a new question has arisen: now that a relatively small amount of subset data is allowable, how many are preferable? It could be predicted that, the available amount of brain data will be infinite if we keep on collecting, while the efficiency of the entire data will peak at a certain amount and then decline, since the hidden information and knowledge within the data is finite. In another word, too much collection of data is a kind of waste. As a result, the minimum of the available data size has become a new challenging scientific problem. In response to this issue, the statistics gives several solutions, one of them is as follows:

$$n \geq \left(\frac{Z_{\alpha/2} * \sigma}{E}\right)^2$$

where the minimum size of a big sample is affected by the population standard deviation σ, Z-value for the desired confidence Level, and the desired margin of error E. In conclusion, determining the optimal size of brain big data will be an important research subject in the future works.

Bibliography

Adler, C.M., DelBello, M.P., Jarvis, K., Levine, A., Adams, J., Strakowski, S.M., 2007. Voxel-based study of structural changes in first-episode patients with bipolar disorder. Biol Psychiatry 61, 776-781.

Alexander, G.E., DeLong, M.R., Strick, P.L., 1986. Parallel organization of functionally segregated circuits linking basal ganglia and cortex. Annu Rev Neurosci 9, 357-381.

Anderson, A.K., Christoff, K., Panitz, D., De Rosa, E., Gabrieli, J.D., 2003. Neural correlates of the automatic processing of threat facial signals. J Neurosci 23, 5627-5633.

Andres, M., Michaux, N., Pesenti, M., 2012. Common substrate for mental arithmetic and finger representation in the parietal cortex. Neuroimage 62, 1520-1528.

Andrews, T.J., Watson, D.M., Rice, G.E., Hartley, T., 2015. Low-level properties of natural images predict topographic patterns of neural response in the ventral visual pathway. J Vis 15, 3.

Angst, J., Ajdacic-Gross, V., Rossler, W., 2015. Classification of mood disorders. Psychiatr Pol 49, 663-671.

Ansari, D., 2008. Effects of development and enculturation on number representation in the brain. Nat Rev Neurosci 9, 278-291.

Anzai, Y., 2013. Human-robot interaction by information sharing. Proceedings of the 8th ACM/IEEE international conference on Human-robot interaction. IEEE Press, Tokyo, Japan, pp. 65-66.

Arsalidou, M., Taylor, M.J., 2011. Is 2+2=4? Meta-analyses of brain areas needed for numbers and calculations. Neuroimage 54, 2382-2393.

Ashburner, J., 2007. A fast diffeomorphic image registration algorithm. Neuroimage 38, 95-113.

Ashburner, J., Friston, K.J., 2000. Voxel-based morphometry--the methods. Neuroimage 11, 805-821.

Asthana, H.S., Mandal, M.K., Khurana, H., Haque-Nizamie, S., 1998. Visuospatial and affect recognition deficit in depression. J Affect Disord 48, 57-62.

Atchley, R.A., Ilardi, S.S., Young, K.M., Stroupe, N.N., O'Hare, A.J., Bistricky, S.L., Collison, E., Gibson, L., Schuster, J., Lepping, R.J., 2012. Depression reduces perceptual sensitivity for positive words and pictures. Cogn Emot 26, 1359-1370.

Baddeley, A., 2003. Working memory: looking back and looking forward. Nat Rev Neurosci 4, 829-839.

Barch, D.M., Burgess, G.C., Harms, M.P., Petersen, S.E., Schlaggar, B.L., Corbetta, M., Glasser, M.F., Curtiss, S., Dixit, S., Feldt, C., Nolan, D., Bryant, E., Hartley, T., Footer, O., Bjork, J.M., Poldrack, R., Smith, S., Johansen-Berg, H., Snyder, A.Z., Van Essen, D.C., 2013. Function in the human connectome: task-fMRI and individual differences in behavior. Neuroimage 80, 169-189.

Barrouillet, P., Mignon, M., Thevenot, C., 2008. Strategies in subtraction problem solving in children. J Exp Child Psychol 99, 233-251.

Bartels, A., Zeki, S., 2004. The neural correlates of maternal and romantic love. Neuroimage 21, 1155-1166.

Beauregard, M., Levesque, J., Bourgouin, P., 2001. Neural correlates of conscious self-regulation of emotion. J Neurosci 21, RC165.

Belleau, E.L., Taubitz, L.E., Larson, C.L., 2015. Imbalance of default mode and regulatory networks during externally focused processing in depression. Soc Cogn Affect Neurosci 10, 744-751.

Berteletti, I., Booth, J.R., 2015. Perceiving fingers in single-digit arithmetic problems. Front Psychol 6, 226.

Binder, J.R., Desai, R.H., Graves, W.W., Conant, L.L., 2009. Where is the semantic system? A critical review and meta-analysis of 120 functional neuroimaging studies. Cereb Cortex 19, 2767-2796.

Blair, K.S., Smith, B.W., Mitchell, D.G., Morton, J., Vythilingam, M., Pessoa, L., Fridberg, D., Zametkin, A., Sturman, D., Nelson, E.E., Drevets, W.C., Pine, D.S., Martin, A., Blair, R.J., 2007. Modulation of emotion by cognition and cognition by emotion. Neuroimage 35, 430-440.

Blankenberger, S., 2001. The arithmetic tie effect is mainly encoding-based. Cognition 82, B15-24.

Blomberg, O., 2011. Conceptions of Cognition for Cognitive Engineering. The International Journal of Aviation Psychology 21, 85-104.

Blood, A.J., Zatorre, R.J., 2001. Intensely pleasurable responses to music correlate with activity in brain regions implicated in reward and emotion. Proc Natl Acad Sci U S A 98, 11818-11823.

Bora, E., Fornito, A., Pantelis, C., Yucel, M., 2012. Gray matter abnormalities in Major Depressive Disorder: a meta-analysis of voxel based morphometry studies. J Affect Disord 138, 9-18.

Bourke, C., Douglas, K., Porter, R., 2010. Processing of facial emotion expression in major depression: a review. Aust N Z J Psychiatry 44, 681-696.

Bracht, T., Horn, H., Strik, W., Federspiel, A., Schnell, S., Hofle, O., Stegmayer, K., Wiest, R., Dierks, T., Muller, T.J., Walther, S., 2014. White matter microstructure alterations of the medial forebrain bundle in melancholic depression. J Affect Disord 155, 186-193.

Buckner, R.L., Andrews-Hanna, J.R., Schacter, D.L., 2008. The brain's default network: anatomy, function, and relevance to disease. Ann N Y Acad Sci 1124, 1-38.

Buckner, R.L., Carroll, D.C., 2007. Self-projection and the brain. Trends Cogn Sci 11, 49-57.

Campbell, J.I., Fuchs-Lacelle, S., Phenix, T.L., 2006. Identical elements model of arithmetic memory: extension to addition and subtraction. Mem Cognit 34, 633-647.

Campbell, J.I., Xue, Q., 2001. Cognitive arithmetic across cultures. J Exp Psychol Gen 130, 299-315.

Cavusoglu, M., Dirik, G., 2011. Fear or disgust? The role of emotions in spider phobia and blood-injection-injury phobia. Turk Psikiyatri Derg 22, 115-122.

Cho, S., Metcalfe, A.W., Young, C.B., Ryali, S., Geary, D.C., Menon, V., 2012. Hippocampal-prefrontal engagement and dynamic causal interactions in the maturation of children's fact retrieval. J Cogn Neurosci 24, 1849-1866.

Chochon, F., Cohen, L., van de Moortele, P.F., Dehaene, S., 1999. Differential contributions of the left and right inferior parietal lobules to number processing. J Cogn Neurosci 11, 617-630.

Cisler, J.M., Olatunji, B.O., Lohr, J.M., 2009. Disgust, fear, and the anxiety disorders: a critical review. Clin Psychol Rev 29, 34-46.

Clower, W.T., Alexander, G.E., 1998. Movement sequence-related activity reflecting numerical order of components in supplementary and presupplementary motor areas. J Neurophysiol 80, 1562-1566.

Collette, F., Van der Linden, M., Delfiore, G., Degueldre, C., Luxen, A., Salmon, E., 2001. The functional anatomy of inhibition processes investigated with the Hayling task. Neuroimage 14, 258-267.

Craig, A.D., 2002. How do you feel? Interoception: the sense of the physiological condition of the body. Nat Rev Neurosci 3, 655-666.

Craig, A.D., 2009. How do you feel--now? The anterior insula and human awareness. Nat Rev Neurosci 10, 59-70.

Critchley, H.D., 2005. Neural mechanisms of autonomic, affective, and cognitive integration. J Comp Neurol 493, 154-166.

Critchley, H.D., Wiens, S., Rotshtein, P., Ohman, A., Dolan, R.J., 2004. Neural systems supporting interoceptive awareness. Nat Neurosci 7, 189-195.

D'Esposito, M., Postle, B.R., Ballard, D., Lease, J., 1999. Maintenance versus manipulation of information held in working memory: an event-related fMRI study. Brain Cogn 41, 66-86.

Damasio, A.R., 1997. Neuropsychology. Towards a neuropathology of emotion and mood. Nature 386, 769-770.

Daunizeau, J., David, O., Stephan, K.E., 2011. Dynamic causal modelling: a critical review of the biophysical and statistical foundations. Neuroimage 58, 312-322.

Davidson, R.J., Putnam, K.M., Larson, C.L., 2000. Dysfunction in the neural circuitry of emotion regulation--a possible prelude to violence. Science 289, 591-594.

de Fockert, J.W., Rees, G., Frith, C.D., Lavie, N., 2001. The role of working memory in visual selective attention. Science 291, 1803-1806.

de Gelder, B., Snyder, J., Greve, D., Gerard, G., Hadjikhani, N., 2004. Fear fosters flight: a mechanism for fear contagion when perceiving emotion expressed by a whole body. Proc Natl Acad Sci U S A 101, 16701-16706.

De Pisapia, N., Slomski, J.A., Braver, T.S., 2007. Functional specializations in lateral prefrontal cortex associated with the integration and segregation of information in working memory. Cereb Cortex 17, 993-1006.

De Smedt, B., Holloway, I.D., Ansari, D., 2011. Effects of problem size and arithmetic operation on brain activation during calculation in children with varying levels of arithmetical fluency. Neuroimage 57, 771-781.

Dehaene S., Cohen L., 1995. Towards an anatomical and functional model of number processing. Math Cogn 1, 82–120.

Dehaene, S., Cohen, L., 1997. Cerebral pathways for calculation: double dissociation between rote verbal and quantitative knowledge of arithmetic. Cortex 33, 219-250.

Dehaene, S., Piazza, M., Pinel, P., Cohen, L., 2003. Three parietal circuits for number processing. Cogn Neuropsychol 20, 487-506.

Demb, J.B., Desmond, J.E., Wagner, A.D., Vaidya, C.J., Glover, G.H., Gabrieli, J.D., 1995. Semantic encoding and retrieval in the left inferior prefrontal cortex: a functional MRI study of task difficulty and process specificity. J Neurosci 15, 5870-5878.

Depping, M.S., Wolf, N.D., Vasic, N., Sambataro, F., Thomann, P.A., Christian Wolf, R., 2015. Specificity of abnormal brain volume in major depressive disorder: a comparison with borderline personality disorder. J Affect Disord 174, 650-657.

Der-Avakian, A., Markou, A., 2012. The neurobiology of anhedonia and other reward-related deficits. Trends Neurosci 35, 68-77.

Dichter, G.S., Kozink, R.V., McClernon, F.J., Smoski, M.J., 2012. Remitted major depression is characterized by reward network hyperactivation during reward anticipation and hypoactivation during reward outcomes. J Affect Disord 136, 1126-1134.

Diedrichsen, J., Wiestler, T., Krakauer, J.W., 2013. Two distinct ipsilateral cortical representations for individuated finger movements. Cereb Cortex 23, 1362-1377.

Diener, C., Kuehner, C., Brusniak, W., Ubl, B., Wessa, M., Flor, H., 2012. A meta-analysis of neurofunctional imaging studies of emotion and cognition in major depression. Neuroimage 61, 677-685.

Dolan, R.J., 2002. Emotion, cognition, and behavior. Science 298, 1191-1194.

Dosenbach, N.U., Nardos, B., Cohen, A.L., Fair, D.A., Power, J.D., Church, J.A., Nelson, S.M., Wig, G.S., Vogel, A.C., Lessov-Schlaggar, C.N., Barnes, K.A., Dubis, J.W., Feczko, E., Coalson, R.S., Pruett, J.R., Jr., Barch, D.M., Petersen, S.E., Schlaggar, B.L., 2010. Prediction of individual brain maturity using fMRI. Science 329, 1358-1361.

Drevets, W.C., Savitz, J., Trimble, M., 2008. The subgenual anterior cingulate cortex in mood disorders. CNS Spectr 13, 663-681.

Dreyer, J.L., 2010. New insights into the roles of microRNAs in drug addiction and neuroplasticity. Genome Med 2, 92.

Duncan, J., 2013. The structure of cognition: attentional episodes in mind and brain. Neuron 80, 35-50.

Durrleman, S., Pennec, X., Trouve, A., Ayache, N., 2009. Statistical models of sets of curves and surfaces based on currents. Med Image Anal 13, 793-808.

Dutta, A., McKie, S., Deakin, J.F., 2014. Resting state networks in major depressive disorder. Psychiatry Res 224, 139-151.

Eftekhari, A., Zoellner, L.A., Vigil, S.A., 2009. Patterns of emotion regulation and psychopathology. Anxiety Stress Coping 22, 571-586.

Eisenberg, N., Fabes, R.A., Guthrie, I.K., Reiser, M., 2000. Dispositional emotionality and regulation: their role in predicting quality of social functioning. J Pers Soc Psychol 78, 136-157.

Eisenberger, N.I., Lieberman, M.D., Williams, K.D., 2003. Does rejection hurt? An FMRI study of social exclusion. Science 302, 290-292.

Ekman, P., 1992. An argument for basic emotions. Cognition and Emotion 6, 169-200.

Fehr, T., Code, C., Herrmann, M., 2007. Common brain regions underlying different arithmetic operations as revealed by conjunct fMRI-BOLD activation. Brain Res 1172, 93-102.

Filler, A., 2009. Magnetic resonance neurography and diffusion tensor imaging: origins, history, and clinical impact of the first 50,000 cases with an assessment of efficacy and utility in a prospective 5000-patient study group. Neurosurgery 65, A29-43.

Fischer, M.H., Shaki, S., 2014. Spatial associations in numerical cognition--from single digits to arithmetic. Q J Exp Psychol (Hove) 67, 1461-1483.

Fox, M.D., 2006. Sleeping with the enemy: Garfield and the National Heart, Lung, and Blood Institute. Pediatrics 118, 1257-1258.

Fox, M.D., Corbetta, M., Snyder, A.Z., Vincent, J.L., Raichle, M.E., 2006. Spontaneous neuronal activity distinguishes human dorsal and ventral attention systems. Proc Natl Acad Sci U S A 103, 10046-10051.

Fox, M.D., Snyder, A.Z., Vincent, J.L., Corbetta, M., Van Essen, D.C., Raichle, M.E., 2005. The human brain is intrinsically organized into dynamic, anticorrelated functional networks. Proc Natl Acad Sci U S A 102, 9673-9678.

Friedrich, R., Friederici, A.D., 2009. Mathematical logic in the human brain: syntax. PLoS One 4, e5599.

Friedrich, R.M., Friederici, A.D., 2013. Mathematical logic in the human brain: semantics. PLoS One 8, e53699.

Friston, K.J., 2011. Functional and effective connectivity: a review. Brain Connect 1, 13-36.

Friston, K.J., Harrison, L., Penny, W., 2003. Dynamic causal modelling. Neuroimage 19, 1273-1302.

Friston, K.J., Li, B., Daunizeau, J., Stephan, K.E., 2011. Network discovery with DCM. Neuroimage 56, 1202-1221.

Fujino, J., Yamasaki, N., Miyata, J., Sasaki, H., Matsukawa, N., Takemura, A., Tei, S., Sugihara, G., Aso, T., Fukuyama, H., Takahashi, H., Inoue, K., Murai, T., 2015. Anterior cingulate volume predicts response to cognitive behavioral therapy in major depressive disorder. J Affect Disord 174, 397-399.

Gabrieli, J.D., Poldrack, R.A., Desmond, J.E., 1998. The role of left prefrontal cortex in language and memory. Proc Natl Acad Sci U S A 95, 906-913.

Gotlib, I.H., Hamilton, J.P., Cooney, R.E., Singh, M.K., Henry, M.L., Joormann, J., 2010. Neural processing of reward and loss in girls at risk for major depression. Arch Gen Psychiatry 67, 380-387.

Grabner, R.H., Ansari, D., Koschutnig, K., Reishofer, G., Ebner, F., 2013. The function of the left angular gyrus in mental arithmetic: evidence from the associative confusion effect. Hum Brain Mapp 34, 1013-1024.

Gradin, V.B., Waiter, G., O'Connor, A., Romaniuk, L., Stickle, C., Matthews, K., Hall, J., Douglas Steele, J., 2013. Salience network-midbrain dysconnectivity and blunted reward signals in schizophrenia. Psychiatry Res 211, 104-111.

Graham, J., Salimi-Khorshidi, G., Hagan, C., Walsh, N., Goodyer, I., Lennox, B., Suckling, J., 2013. Meta-analytic evidence for neuroimaging models of depression: state or trait? J Affect Disord 151, 423-431.

Gray, J.R., Braver, T.S., Raichle, M.E., 2002. Integration of emotion and cognition in the lateral prefrontal cortex. Proc Natl Acad Sci U S A 99, 4115-4120.

Graybiel, A.M., 2005. The basal ganglia: learning new tricks and loving it. Curr Opin Neurobiol 15, 638-644.

Gross, J.J., 1998. Antecedent- and response-focused emotion regulation: divergent consequences for experience, expression, and physiology. J Pers Soc Psychol 74, 224-237.

Gurd, J.M., Amunts, K., Weiss, P.H., Zafiris, O., Zilles, K., Marshall, J.C., Fink, G.R., 2002. Posterior parietal cortex is implicated in continuous switching between verbal fluency tasks: an fMRI study with clinical implications. Brain 125, 1024-1038.

Hagoort, P., 2005. On Broca, brain, and binding: a new framework. Trends Cogn Sci 9, 416-423.

Hamilton, J.P., Etkin, A., Furman, D.J., Lemus, M.G., Johnson, R.F., Gotlib, I.H., 2012. Functional neuroimaging of major depressive disorder: a meta-analysis and new integration of base line activation and neural response data. Am J Psychiatry 169, 693-703.

Hamilton, J.P., Siemer, M., Gotlib, I.H., 2008. Amygdala volume in major depressive disorder: a meta-analysis of magnetic resonance imaging studies. Mol Psychiatry 13, 993-1000.

Hawrylycz, M.J., Lein, E.S., Guillozet-Bongaarts, A.L., Shen, E.H., Ng, L., Miller, J.A., van de Lagemaat, L.N., Smith, K.A., Ebbert, A., Riley, Z.L., Abajian, C., Beckmann, C.F., Bernard, A., Bertagnolli, D., Boe, A.F., Cartagena, P.M., Chakravarty, M.M., Chapin, M., Chong, J., Dalley, R.A., Daly, B.D., Dang, C., Datta, S., Dee, N., Dolbeare, T.A., Faber, V., Feng, D., Fowler, D.R., Goldy, J., Gregor, B.W., Haradon, Z., Haynor, D.R., Hohmann, J.G., Horvath, S., Howard, R.E., Jeromin, A., Jochim, J.M., Kinnunen, M., Lau, C., Lazarz, E.T., Lee, C., Lemon, T.A., Li, L., Li, Y., Morris, J.A., Overly, C.C., Parker, P.D., Parry, S.E., Reding, M., Royall, J.J., Schulkin, J., Sequeira, P.A., Slaughterbeck, C.R., Smith, S.C., Sodt, A.J., Sunkin, S.M., Swanson, B.E., Vawter, M.P., Williams, D., Wohnoutka, P., Zielke, H.R., Geschwind, D.H., Hof, P.R., Smith, S.M., Koch, C., Grant, S.G., Jones, A.R., 2012. An anatomically comprehensive atlas of the adult human brain transcriptome. Nature 489, 391-399.

Hecht, S.A., 2002. Counting on working memory in simple arithmetic when counting is used for problem solving. Mem Cognit 30, 447-455.

Henderson, S.E., Vallejo, A.I., Ely, B.A., Kang, G., Krain Roy, A., Pine, D.S., Stern, E.R., Gabbay, V., 2014. The neural correlates of emotional face-processing in adolescent depression: a dimensional approach focusing on anhedonia and illness severity. Psychiatry Res 224, 234-241.

Herculano-Houzel, S., 2012. The remarkable, yet not extraordinary, human brain as a scaled-up primate brain and its associated cost. Proc Natl Acad Sci U S A 109 Suppl 1, 10661-10668.

Heylighen, F., 2007. Accelerating Socio-Technological Evolution: from ephemeralization and stigmergy to the global brain. CoRR abs/cs/0703004.

Horn, D.I., Yu, C., Steiner, J., Buchmann, J., Kaufmann, J., Osoba, A., Eckert, U., Zierhut, K.C., Schiltz, K., He, H., Biswal, B., Bogerts, B., Walter, M., 2010. Glutamatergic and resting-state functional connectivity correlates of severity in major depression - the role of pregenual anterior cingulate cortex and anterior insula. Front Syst Neurosci 4.

Hou, J., Song, L., Zhang, W., Wu, W., Wang, J., Zhou, D., Qu, W., Guo, J., Gu, S., He, M., Xie, B., Li, H., 2013. Morphologic and functional connectivity alterations of corticostriatal and default mode network in treatment-naive patients with obsessive-compulsive disorder. PLoS One 8, e83931.

Houde, O., Rossi, S., Lubin, A., Joliot, M., 2010. Mapping numerical processing, reading, and executive functions in the developing brain: an fMRI meta-analysis of 52 studies including 842 children. Dev Sci 13, 876-885.

Hsieh, J.C., Meyerson, B.A., Ingvar, M., 1999. PET study on central processing of pain in trigeminal neuropathy. Eur J Pain 3, 51-65.

Hu, Y., Geng, F., Tao, L., Hu, N., Du, F., Fu, K., Chen, F., 2011. Enhanced white matter tracts integrity in children with abacus training. Hum Brain Mapp 32, 10-21.

Hugdahl, K., Thomsen, T., Ersland, L., 2006. Sex differences in visuo-spatial processing: an fMRI study of mental rotation. Neuropsychologia 44, 1575-1583.

Imbo, I., Vandierendonck, A., De Rammelaere, S., 2007a. The role of working memory in the carry operation of mental arithmetic: number and value of the carry. Q J Exp Psychol (Hove) 60, 708-731.

Imbo, I., Vandierendonck, A., Vergauwe, E., 2007b. The role of working memory in carrying and borrowing. Psychol Res 71, 467-483.

Imbo I., Vandierendonck A., 2007c. The role of phonological and executive working memory resources in simple arithmetic strategies. EUR J COGN PSYCHOL 19, 910−933.

Ischebeck, A., Zamarian, L., Siedentopf, C., Koppelstatter, F., Benke, T., Felber, S., Delazer, M., 2006. How specifically do we learn? Imaging the learning of multiplication and subtraction. Neuroimage 30, 1365-1375.

Jabbi, M., Bastiaansen, J., Keysers, C., 2008. A common anterior insula representation of disgust observation, experience and imagination shows divergent functional connectivity pathways. PLoS One 3, e2939.

Jensen, J., McIntosh, A.R., Crawley, A.P., Mikulis, D.J., Remington, G., Kapur, S., 2003. Direct activation of the ventral striatum in anticipation of aversive stimuli. Neuron 40, 1251-1257.

Ma, J., Wen, J., Huang, R., Huang, B., 2011. Cyber-Individual Meets Brain Informatics. Intelligent Systems, IEEE 26, 30-37.

Chen, J., Ma, J., Zhong, N., Yao, Y., Liu, J., Huang, R., Li, W., Huang, Z., Gao, Y., Cao, J., 2014. WaaS: Wisdom as a Service. Intelligent Systems, IEEE 29, 40-47.

Johnstone, T., van Reekum, C.M., Urry, H.L., Kalin, N.H., Davidson, R.J., 2007. Failure to regulate: counterproductive recruitment of top-down prefrontal-subcortical circuitry in major depression. J Neurosci 27, 8877-8884.

Jost, K., Khader, P.H., Burke, M., Bien, S., Rosler, F., 2011. Frontal and parietal contributions to arithmetic fact retrieval: a parametric analysis of the problem-size effect. Hum Brain Mapp 32, 51-59.

Kanske, P., Heissler, J., Schonfelder, S., Bongers, A., Wessa, M., 2011. How to regulate emotion? Neural networks for reappraisal and distraction. Cereb Cortex 21, 1379-1388.

Katzev, M., Tuscher, O., Hennig, J., Weiller, C., Kaller, C.P., 2013. Revisiting the functional specialization of left inferior frontal gyrus in phonological and semantic fluency: the crucial role of task demands and individual ability. J Neurosci 33, 7837-7845.

Kerestes, R., Davey, C.G., Stephanou, K., Whittle, S., Harrison, B.J., 2014. Functional brain imaging studies of youth depression: a systematic review. Neuroimage Clin 4, 209-231.

Kikinis, R., Pieper, S., Vosburgh, K., 2014. 3D Slicer: A Platform for Subject-Specific Image Analysis, Visualization, and Clinical Support. In: Jolesz, F.A. (Ed.), Intraoperative Imaging and Image-Guided Therapy. Springer New York, pp. 277-289.

Klein, E., Huber, S., Nuerk, H.C., Moeller, K., 2014. Operational momentum affects eye fixation behaviour. Q J Exp Psychol (Hove) 67, 1614-1625.

Klein, E., Moeller, K., Glauche, V., Weiller, C., Willmes, K., 2013. Processing pathways in mental arithmetic--evidence from probabilistic fiber tracking. PLoS One 8, e55455.

Klein, E., Willmes, K., Dressel, K., Domahs, F., Wood, G., Nuerk, H.C., Moeller, K., 2010. Categorical and continuous--disentangling the neural correlates of the carry effect in multi-digit addition. Behav Brain Funct 6, 70.

Knutson, B., Fong, G.W., Adams, C.M., Varner, J.L., Hommer, D., 2001. Dissociation of reward anticipation and outcome with event-related fMRI. Neuroreport 12, 3683-3687.

Kohn, N., Eickhoff, S.B., Scheller, M., Laird, A.R., Fox, P.T., Habel, U., 2014. Neural network of cognitive emotion regulation--an ALE meta-analysis and MACM analysis. Neuroimage 87, 345-355.

Koolschijn, P.C., van Haren, N.E., Lensvelt-Mulders, G.J., Hulshoff Pol, H.E., Kahn, R.S., 2009. Brain volume abnormalities in major depressive disorder: a meta-analysis of magnetic resonance imaging studies. Hum Brain Mapp 30, 3719-3735.

Koster, R., Guitart-Masip, M., Dolan, R.J., Duzel, E., 2015. Basal Ganglia Activity Mirrors a Benefit of Action and Reward on Long-Lasting Event Memory. Cereb Cortex.

Kumar, P., Berghorst, L.H., Nickerson, L.D., Dutra, S.J., Goer, F.K., Greve, D.N., Pizzagalli, D.A., 2014. Differential effects of acute stress on anticipatory and consummatory phases of reward processing. Neuroscience 266, 1-12.

Lally, N., Nugent, A.C., Luckenbaugh, D.A., Ameli, R., Roiser, J.P., Zarate, C.A., 2014. Anti-anhedonic effect of ketamine and its neural correlates in treatment-resistant bipolar depression. Transl Psychiatry 4, e469.

Lancaster, J.L., Woldorff, M.G., Parsons, L.M., Liotti, M., Freitas, C.S., Rainey, L., Kochunov, P.V., Nickerson, D., Mikiten, S.A., Fox, P.T., 2000. Automated Talairach atlas labels for functional brain mapping. Hum Brain Mapp 10, 120-131.

Lang, P.J., Bradley, M.M., Cuthbert, B.N., 1998. Emotion and motivation: measuring affective perception. J Clin Neurophysiol 15, 397-408.

Le Bihan, D., Mangin, J.F., Poupon, C., Clark, C.A., Pappata, S., Molko, N., Chabriat, H., 2001. Diffusion tensor imaging: concepts and applications. J Magn Reson Imaging 13, 534-546.

LeDoux, J., 1998. Fear and the brain: where have we been, and where are we going? Biol Psychiatry 44, 1229-1238.

Lener, M.S., Iosifescu, D.V., 2015. In pursuit of neuroimaging biomarkers to guide treatment selection in major depressive disorder: a review of the literature. Ann N Y Acad Sci 1344, 50-65.

Liddell, B.J., Brown, K.J., Kemp, A.H., Barton, M.J., Das, P., Peduto, A., Gordon, E., Williams, L.M., 2005. A direct brainstem-amygdala-cortical 'alarm' system for subliminal signals of fear. Neuroimage 24, 235-243.

Liu, S., Cai, W., Liu, S., Zhang, F., Fulham, M., Feng, D., Pujol, S., Kikinis, R., 2015a. Multimodal neuroimaging computing: a review of the applications in neuropsychiatric disorders. Brain Informatics 2, 167-180.

Liu, S., Cai, W., Liu, S., Zhang, F., Fulham, M., Feng, D., Pujol, S., Kikinis, R., 2015b. Multimodal neuroimaging computing: the workflows, methods, and platforms. Brain Informatics 2, 181-195.

Liu, X., Hairston, J., Schrier, M., Fan, J., 2011. Common and distinct networks underlying reward valence and processing stages: a meta-analysis of functional neuroimaging studies. Neurosci Biobehav Rev 35, 1219-1236.

Lucchelli, F., De Renzi, E., 1993. Primary dyscalculia after a medial frontal lesion of the left hemisphere. J Neurol Neurosurg Psychiatry 56, 304-307.

Luo, J., Yu, R., 2015. Follow the heart or the head? The interactive influence model of emotion and cognition. Front Psychol 6, 573.

Ma, L., Steinberg, J.L., Cunningham, K.A., Lane, S.D., Kramer, L.A., Narayana, P.A., Kosten, T.R., Bechara, A., Moeller, F.G., 2015. Inhibitory behavioral control: a stochastic dynamic causal modeling study using network discovery analysis. Brain Connect 5, 177-186.

Mainy, N., Kahane, P., Minotti, L., Hoffmann, D., Bertrand, O., Lachaux, J.P., 2007. Neural correlates of consolidation in working memory. Hum Brain Mapp 28, 183-193.

Maldjian, J.A., Laurienti, P.J., Kraft, R.A., Burdette, J.H., 2003. An automated method for neuroanatomic and cytoarchitectonic atlas-based interrogation of fMRI data sets. Neuroimage 19, 1233-1239.

Maruyama, M., Pallier, C., Jobert, A., Sigman, M., Dehaene, S., 2012. The cortical representation of simple mathematical expressions. Neuroimage 61, 1444-1460.

McKiernan, K.A., Kaufman, J.N., Kucera-Thompson, J., Binder, J.R., 2003. A parametric manipulation of factors affecting task-induced deactivation in functional neuroimaging. J Cogn Neurosci 15, 394-408.

Menon, V., Adleman, N.E., White, C.D., Glover, G.H., Reiss, A.L., 2001. Error-related brain activation during a Go/NoGo response inhibition task. Hum Brain Mapp 12, 131-143.

Menon, V., Glover, G.H., Pfefferbaum, A., 1998. Differential activation of dorsal basal ganglia during externally and self paced sequences of arm movements. Neuroreport 9, 1567-1573.

Menon, V., Uddin, L.Q., 2010. Saliency, switching, attention and control: a network model of insula function. Brain Struct Funct 214, 655-667.

Miller, C.H., Hamilton, J.P., Sacchet, M.D., Gotlib, I.H., 2015a. Meta-analysis of Functional Neuroimaging of Major Depressive Disorder in Youth. JAMA Psychiatry 72, 1045-1053.

Miller, C.H., Hamilton, J.P., Sacchet, M.D., Gotlib, I.H., 2015b. Meta-analysis of Functional Neuroimaging of Major Depressive Disorder in Youth. JAMA Psychiatry.

Miskowiak, K.W., Carvalho, A.F., 2014. 'Hot' cognition in major depressive disorder: a systematic review. CNS Neurol Disord Drug Targets 13, 1787-1803.

Morgan, J.K., Olino, T.M., McMakin, D.L., Ryan, N.D., Forbes, E.E., 2013. Neural response to reward as a predictor of increases in depressive symptoms in adolescence. Neurobiol Dis 52, 66-74.

Muhlberger, A., Wieser, M.J., Gerdes, A.B., Frey, M.C., Weyers, P., Pauli, P., 2011. Stop looking angry and smile, please: start and stop of the very same facial expression differentially activate threat- and reward-related brain networks. Soc Cogn Affect Neurosci 6, 321-329.

Muller, H., Hanbury, A., 2015. [Research applications in digital radiology : Big data and co]. Radiologe.

Nieder, A., Dehaene, S., 2009. Representation of number in the brain. Annu Rev Neurosci 32, 185-208.

Nomura, E.M., Reber, P.J., 2008. A review of medial temporal lobe and caudate contributions to visual category learning. Neurosci Biobehav Rev 32, 279-291.

Northoff, G., Sibille, E., 2014. Why are cortical GABA neurons relevant to internal focus in depression? A cross-level model linking cellular, biochemical and neural network findings. Mol Psychiatry 19, 966-977.

Nuerk, H.C., Weger, U., Willmes, K., 2001. Decade breaks in the mental number line? Putting the tens and units back in different bins. Cognition 82, B25-33.

Nuerk, H.C., Weger, U., Willmes, K., 2004. On the perceptual generality of the unit-decade compatibility effect. Exp Psychol 51, 72-79.

Ochsner, K.N., Bunge, S.A., Gross, J.J., Gabrieli, J.D., 2002. Rethinking feelings: an FMRI study of the cognitive regulation of emotion. J Cogn Neurosci 14, 1215-1229.

Ochsner, K.N., Gross, J.J., 2005. The cognitive control of emotion. Trends Cogn Sci 9, 242-249.

Ochsner, K.N., Silvers, J.A., Buhle, J.T., 2012. Functional imaging studies of emotion regulation: a synthetic review and evolving model of the cognitive control of emotion. Ann N Y Acad Sci 1251, E1-24.

Oh, S.W., Harris, J.A., Ng, L., Winslow, B., Cain, N., Mihalas, S., Wang, Q., Lau, C., Kuan, L., Henry, A.M., Mortrud, M.T., Ouellette, B., Nguyen, T.N., Sorensen, S.A., Slaughterbeck, C.R., Wakeman, W., Li, Y., Feng, D., Ho, A., Nicholas, E., Hirokawa, K.E., Bohn, P., Joines, K.M., Peng, H., Hawrylycz, M.J., Phillips, J.W., Hohmann, J.G., Wohnoutka, P., Gerfen, C.R., Koch, C., Bernard, A., Dang, C., Jones, A.R., Zeng, H., 2014. A mesoscale connectome of the mouse brain. Nature 508, 207-214.

Olino, T.M., McMakin, D.L., Morgan, J.K., Silk, J.S., Birmaher, B., Axelson, D.A., Williamson, D.E., Dahl, R.E., Ryan, N.D., Forbes, E.E., 2014. Reduced reward anticipation in youth at high-risk for unipolar depression: a preliminary study. Dev Cogn Neurosci 8, 55-64.

Owen, A.M., Evans, A.C., Petrides, M., 1996. Evidence for a two-stage model of spatial working memory processing within the lateral frontal cortex: a positron emission tomography study. Cereb Cortex 6, 31-38.

Palaniyappan, L., Liddle, P.F., 2012. Does the salience network play a cardinal role in psychosis? An emerging hypothesis of insular dysfunction. J Psychiatry Neurosci 37, 17-27.

Pannekoek, J.N., Veer, I.M., van Tol, M.J., van der Werff, S.J., Demenescu, L.R., Aleman, A., Veltman, D.J., Zitman, F.G., Rombouts, S.A., van der Wee, N.J., 2013. Resting-state functional connectivity abnormalities in limbic and salience networks in social anxiety disorder without comorbidity. Eur Neuropsychopharmacol 23, 186-195.

Patel, A.D., 2003. Language, music, syntax and the brain. Nat Neurosci 6, 674-681.

Penny, W.D., Stephan, K.E., Mechelli, A., Friston, K.J., 2004. Comparing dynamic causal models. Neuroimage 22, 1157-1172.

Pessoa, L., 2008. On the relationship between emotion and cognition. Nat Rev Neurosci 9, 148-158.

Pessoa, L., McKenna, M., Gutierrez, E., Ungerleider, L.G., 2002. Neural processing of emotional faces requires attention. Proc Natl Acad Sci U S A 99, 11458-11463.

Petrides, M., 2000. Dissociable roles of mid-dorsolateral prefrontal and anterior inferotemporal cortex in visual working memory. J Neurosci 20, 7496-7503.

Petrides, M., Alivisatos, B., Evans, A.C., Meyer, E., 1993. Dissociation of human mid-dorsolateral from posterior dorsolateral frontal cortex in memory processing. Proc Natl Acad Sci U S A 90, 873-877.

Peyron, R., Laurent, B., Garcia-Larrea, L., 2000. Functional imaging of brain responses to pain. A review and meta-analysis (2000). Neurophysiol Clin 30, 263-288.

Phillips, M.L., Chase, H.W., Sheline, Y.I., Etkin, A., Almeida, J.R., Deckersbach, T., Trivedi, M.H., 2015. Identifying predictors, moderators, and mediators of antidepressant response in major depressive disorder: neuroimaging approaches. Am J Psychiatry 172, 124-138.

Phillips, M.L., Ladouceur, C.D., Drevets, W.C., 2008. A neural model of voluntary and automatic emotion regulation: implications for understanding the pathophysiology and neurodevelopment of bipolar disorder. Mol Psychiatry 13, 829, 833-857.

Pizzagalli, D.A., Holmes, A.J., Dillon, D.G., Goetz, E.L., Birk, J.L., Bogdan, R., Dougherty, D.D., Iosifescu, D.V., Rauch, S.L., Fava, M., 2009. Reduced caudate and nucleus accumbens response to rewards in unmedicated individuals with major depressive disorder. Am J Psychiatry 166, 702-710.

Pizzagalli, D.A., Iosifescu, D., Hallett, L.A., Ratner, K.G., Fava, M., 2008. Reduced hedonic capacity in major depressive disorder: evidence from a probabilistic reward task. J Psychiatr Res 43, 76-87.

Poldrack, R.A., Gorgolewski, K.J., 2014. Making big data open: data sharing in neuroimaging. Nat Neurosci 17, 1510-1517.

Poldrack, R.A., Wagner, A.D., Prull, M.W., Desmond, J.E., Glover, G.H., Gabrieli, J.D., 1999. Functional specialization for semantic and phonological processing in the left inferior prefrontal cortex. Neuroimage 10, 15-35.

Price, C.J., Moore, C.J., Friston, K.J., 1997. Subtractions, conjunctions, and interactions in experimental design of activation studies. Hum Brain Mapp 5, 264-272.

Price, C.J., Mummery, C.J., Moore, C.J., Frakowiak, R.S., Friston, K.J., 1999. Delineating necessary and sufficient neural systems with functional imaging studies of neuropsychological patients. J Cogn Neurosci 11, 371-382.

Price, C.J., Wise, R.J., Warburton, E.A., Moore, C.J., Howard, D., Patterson, K., Frackowiak, R.S., Friston, K.J., 1996. Hearing and saying. The functional neuro-anatomy of auditory word processing. Brain 119 (Pt 3), 919-931.

Rama, P., Courtney, S.M., 2005. Functional topography of working memory for face or voice identity. Neuroimage 24, 224-234.

Ratinckx, E., Nuerk, H.C., van Dijck, J.P., Klaus, W., 2006. Effects of interhemispheric communication on two-digit arabic number processing. Cortex 42, 1128-1137.

Reshef, D.N., Reshef, Y.A., Finucane, H.K., Grossman, S.R., McVean, G., Turnbaugh, P.J., Lander, E.S., Mitzenmacher, M., Sabeti, P.C., 2011. Detecting novel associations in large data sets. Science 334, 1518-1524.

Ressler, K.J., Mayberg, H.S., 2007. Targeting abnormal neural circuits in mood and anxiety disorders: from the laboratory to the clinic. Nat Neurosci 10, 1116-1124.

Rickard, T.C., Romero, S.G., Basso, G., Wharton, C., Flitman, S., Grafman, J., 2000. The calculating brain: an fMRI study. Neuropsychologia 38, 325-335.

Rigoux, L., Stephan, K.E., Friston, K.J., Daunizeau, J., 2014. Bayesian model selection for group studies - revisited. Neuroimage 84, 971-985.

Rivera, S.M., Reiss, A.L., Eckert, M.A., Menon, V., 2005. Developmental changes in mental arithmetic: evidence for increased functional specialization in the left inferior parietal cortex. Cereb Cortex 15, 1779-1790.

Robinson, D., 2008. Brain function, emotional experience and personality. Netherlands Journal of Psychology 64, 152-168.

Rodd, J.M., Davis, M.H., Johnsrude, I.S., 2005. The neural mechanisms of speech comprehension: fMRI studies of semantic ambiguity. Cereb Cortex 15, 1261-1269.

Rosenberg-Lee, M., Chang, T.T., Young, C.B., Wu, S., Menon, V., 2011. Functional dissociations between four basic arithmetic operations in the human posterior parietal cortex: a cytoarchitectonic mapping study. Neuropsychologia 49, 2592-2608.

Rydberg, J.N., Hammond, C.A., Grimm, R.C., Erickson, B.J., Jack, C.R., Jr., Huston, J., 3rd, Riederer, S.J., 1994. Initial clinical experience in MR imaging of the brain with a fast fluid-attenuated inversion-recovery pulse sequence. Radiology 193, 173-180.

Schmithorst, V.J., Brown, R.D., 2004. Empirical validation of the triple-code model of numerical processing for complex math operations using functional MRI and group Independent Component Analysis of the mental addition and subtraction of fractions. Neuroimage 22, 1414-1420.

Schultz, W., Tremblay, L., Hollerman, J.R., 1998. Reward prediction in primate basal ganglia and frontal cortex. Neuropharmacology 37, 421-429.

Seeley, W.W., Menon, V., Schatzberg, A.F., Keller, J., Glover, G.H., Kenna, H., Reiss, A.L., Greicius, M.D., 2007. Dissociable intrinsic connectivity networks for salience processing and executive control. J Neurosci 27, 2349-2356.

Sehlmeyer, C., Schoning, S., Zwitserlood, P., Pfleiderer, B., Kircher, T., Arolt, V., Konrad, C., 2009. Human fear conditioning and extinction in neuroimaging: a systematic review. PLoS One 4, e5865.

Sekiyama, K., Kanno, I., Miura, S., Sugita, Y., 2003. Auditory-visual speech perception examined by fMRI and PET. Neurosci Res 47, 277-287.

Shackman, A.J., Sarinopoulos, I., Maxwell, J.S., Pizzagalli, D.A., Lavric, A., Davidson, R.J., 2006. Anxiety selectively disrupts visuospatial working memory. Emotion 6, 40-61.

Shah, A., Jhawar, S.S., Goel, A., 2012. Analysis of the anatomy of the Papez circuit and adjoining limbic system by fiber dissection techniques. J Clin Neurosci 19, 289-298.

Shah, N.J., Oros-Peusquens, A.M., Arrubla, J., Zhang, K., Warbrick, T., Mauler, J., Vahedipour, K., Romanzetti, S., Felder, J., Celik, A., Rota-Kops, E., Iida, H., Langen, K.J., Herzog, H., Neuner, I., 2013. Advances in multimodal neuroimaging: hybrid MR-PET and MR-PET-EEG at 3 T and 9.4 T. J Magn Reson 229, 101-115.

Shaver, P., Schwartz, J., Kirson, D., O'Connor, C., 1987. Emotion knowledge: further exploration of a prototype approach. J Pers Soc Psychol 52, 1061-1086.

Sheehan, D.V., Sheehan, K.H., Shytle, R.D., Janavs, J., Bannon, Y., Rogers, J.E., Milo, K.M., Stock, S.L., Wilkinson, B., 2010. Reliability and validity of the Mini International Neuropsychiatric Interview for Children and Adolescents (MINI-KID). J Clin Psychiatry 71, 313-326.

Sheline, Y.I., Barch, D.M., Price, J.L., Rundle, M.M., Vaishnavi, S.N., Snyder, A.Z., Mintun, M.A., Wang, S., Coalson, R.S., Raichle, M.E., 2009. The default mode network and self-referential processes in depression. Proc Natl Acad Sci U S A 106, 1942-1947.

Shmuel, A., Leopold, D.A., 2008. Neuronal correlates of spontaneous fluctuations in fMRI signals in monkey visual cortex: Implications for functional connectivity at rest. Hum Brain Mapp 29, 751-761.

Shmuel, A., Yacoub, E., Pfeuffer, J., Van de Moortele, P.F., Adriany, G., Hu, X., Ugurbil, K., 2002. Sustained negative BOLD, blood flow and oxygen consumption response and its coupling to the positive response in the human brain. Neuron 36, 1195-1210.

Shokouhi, M., Barnes, A., Suckling, J., Moorhead, T.W., Brennan, D., Job, D., Lymer, K., Dazzan, P., Reis Marques, T., Mackay, C., McKie, S., Williams, S.C., Lawrie, S.M., Deakin, B., Williams, S.R., Condon, B., 2011. Assessment of the impact of the scanner-related factors on brain morphometry analysis with Brainvisa. BMC Med Imaging 11, 23.

Silverman, M.H., Jedd, K., Luciana, M., 2015a. Neural networks involved in adolescent reward processing: An activation likelihood estimation meta-analysis of functional neuroimaging studies. Neuroimage 122, 427-439.

Silverman, M.H., Jedd, K., Luciana, M., 2015b. Neural networks involved in adolescent reward processing: An activation likelihood estimation meta-analysis of functional neuroimaging studies. Neuroimage.

Simmhan, Y.L., Plale, B., Gannon, D., 2005. A survey of data provenance in e-science. SIGMOD Rec. 34, 31-36.

Singer, T., Seymour, B., O'Doherty, J., Kaube, H., Dolan, R.J., Frith, C.D., 2004. Empathy for pain involves the affective but not sensory components of pain. Science 303, 1157-1162.

Smith, E.E., Jonides, J., Marshuetz, C., Koeppe, R.A., 1998. Components of verbal working memory: evidence from neuroimaging. Proc Natl Acad Sci U S A 95, 876-882.

Smith, S.M., Fox, P.T., Miller, K.L., Glahn, D.C., Fox, P.M., Mackay, C.E., Filippini, N., Watkins, K.E., Toro, R., Laird, A.R., Beckmann, C.F., 2009. Correspondence of the brain's functional architecture during activation and rest. Proc Natl Acad Sci U S A 106, 13040-13045.

Song, X.W., Dong, Z.Y., Long, X.Y., Li, S.F., Zuo, X.N., Zhu, C.Z., He, Y., Yan, C.G., Zang, Y.F., 2011. REST: a toolkit for resting-state functional magnetic resonance imaging data processing. PLoS One 6, e25031.

Sridharan, D., Levitin, D.J., Menon, V., 2008. A critical role for the right fronto-insular cortex in switching between central-executive and default-mode networks. Proc Natl Acad Sci U S A 105, 12569-12574.

Stanescu-Cosson, R., Pinel, P., van De Moortele, P.F., Le Bihan, D., Cohen, L., Dehaene, S., 2000. Understanding dissociations in dyscalculia: a brain imaging study of the impact of number size on the cerebral networks for exact and approximate calculation. Brain 123 (Pt 11), 2240-2255.

Stephan, K.E., Penny, W.D., Moran, R.J., den Ouden, H.E., Daunizeau, J., Friston, K.J., 2010. Ten simple rules for dynamic causal modeling. Neuroimage 49, 3099-3109.

Stern, C.E., Owen, A.M., Tracey, I., Look, R.B., Rosen, B.R., Petrides, M., 2000. Activity in ventrolateral and mid-dorsolateral prefrontal cortex during nonspatial visual working memory processing: evidence from functional magnetic resonance imaging. Neuroimage 11, 392-399.

Stocco, A., Lebiere, C., Anderson, J.R., 2010. Conditional routing of information to the cortex: a model of the basal ganglia's role in cognitive coordination. Psychol Rev 117, 541-574.

Tahmasian, M., Knight, D.C., Manoliu, A., Schwerthoffer, D., Scherr, M., Meng, C., Shao, J., Peters, H., Doll, A., Khazaie, H., Drzezga, A., Bauml, J., Zimmer, C., Forstl, H., Wohlschlager, A.M., Riedl, V., Sorg, C., 2013. Aberrant intrinsic connectivity of hippocampus and amygdala overlap in the fronto-insular and dorsomedial-prefrontal cortex in major depressive disorder. Front Hum Neurosci 7, 639.

Tao, H., Guo, S., Ge, T., Kendrick, K.M., Xue, Z., Liu, Z., Feng, J., 2013. Depression uncouples brain hate circuit. Mol Psychiatry 18, 101-111.

Tatsuno, Y., Sakai, K.L., 2005. Language-related activations in the left prefrontal regions are differentially modulated by age, proficiency, and task demands. J Neurosci 25, 1637-1644.

Thayer, R.E., Newman, J.R., McClain, T.M., 1994. Self-regulation of mood: strategies for changing a bad mood, raising energy, and reducing tension. J Pers Soc Psychol 67, 910-925.

Tschentscher, N., Hauk, O., 2014. How are things adding up? Neural differences between arithmetic operations are due to general problem solving strategies. Neuroimage 92, 369-380.

Turk-Browne, N.B., 2013. Functional interactions as big data in the human brain. Science 342, 580-584.

Turkheimer, F., Pettigrew, K., Sokoloff, L., Smith, C.B., Schmidt, K., 2000. Selection of an adaptive test statistic for use with multiple comparison analyses of neuroimaging data. Neuroimage 12, 219-229.

Uddin, L.Q., 2015. Salience processing and insular cortical function and dysfunction. Nat Rev Neurosci 16, 55-61.

Uddin, L.Q., Supekar, K., Lynch, C.J., Cheng, K.M., Odriozola, P., Barth, M.E., Phillips, J., Feinstein, C., Abrams, D.A., Menon, V., 2014. Brain State Differentiation and Behavioral Inflexibility in Autismdagger. Cereb Cortex.

Van Beek, L., Ghesquiere, P., Lagae, L., De Smedt, B., 2014. Left fronto-parietal white matter correlates with individual differences in children's ability to solve additions and multiplications: a tractography study. Neuroimage 90, 117-127.

van den Heuvel, M.P., Hulshoff Pol, H.E., 2010. Exploring the brain network: a review on resting-state fMRI functional connectivity. Eur Neuropsychopharmacol 20, 519-534.

Van Dillen, L.F., Heslenfeld, D.J., Koole, S.L., 2009. Tuning down the emotional brain: an fMRI study of the effects of cognitive load on the processing of affective images. Neuroimage 45, 1212-1219.

Vandenberghe, R., Price, C., Wise, R., Josephs, O., Frackowiak, R.S., 1996. Functional anatomy of a common semantic system for words and pictures. Nature 383, 254-256.

Vrieze, E., Pizzagalli, D.A., Demyttenaere, K., Hompes, T., Sienaert, P., de Boer, P., Schmidt, M., Claes, S., 2013. Reduced reward learning predicts outcome in major depressive disorder. Biol Psychiatry 73, 639-645.

Wager, T.D., Phan, K.L., Liberzon, I., Taylor, S.F., 2003. Valence, gender, and lateralization of functional brain anatomy in emotion: a meta-analysis of findings from neuroimaging. Neuroimage 19, 513-531.

Wagner, G., Schachtzabel, C., Peikert, G., Bar, K.J., 2015. The neural basis of the abnormal self-referential processing and its impact on cognitive control in depressed patients. Hum Brain Mapp.

Wang, Z., Liu, J., Zhong, N., Qin, Y., Zhou, H., Li, K., 2012. Changes in the brain intrinsic organization in both on-task state and post-task resting state. Neuroimage 62, 394-407.

Warner-Schmidt, J.L., Duman, R.S., 2006. Hippocampal neurogenesis: opposing effects of stress and antidepressant treatment. Hippocampus 16, 239-249.

Webb, T.L., Miles, E., Sheeran, P., 2012. Dealing with feeling: a meta-analysis of the effectiveness of strategies derived from the process model of emotion regulation. Psychol Bull 138, 775-808.

Whalen, J., McCloskey, M., Lesser, R.P., Gordon, B., 1997. Localizing arithmetic processes in the brain: evidence from a transient deficit during cortical stimulation. J Cogn Neurosci 9, 409-417.

White, N.M., Salinas, J.A., 2003. Mnemonic functions of dorsal striatum and hippocampus in aversive conditioning. Behav Brain Res 142, 99-107.

Whitton, A.E., Treadway, M.T., Pizzagalli, D.A., 2015. Reward processing dysfunction in major depression, bipolar disorder and schizophrenia. Curr Opin Psychiatry 28, 7-12.

Wise, T., Cleare, A.J., Herane, A., Young, A.H., Arnone, D., 2014. Diagnostic and therapeutic utility of neuroimaging in depression: an overview. Neuropsychiatr Dis Treat 10, 1509-1522.

Worsley, K.J., Chen, J.I., Lerch, J., Evans, A.C., 2005. Comparing functional connectivity via thresholding correlations and singular value decomposition. Philos Trans R Soc Lond B Biol Sci 360, 913-920.

Yi-Rong, N., Si-Yun, S., Zhou-Yi, G., Si-Run, L., Yun, B., Song-Hao, L., Chan, W.Y., 2011. Dissociated brain organization for two-digit addition and subtraction: an fMRI investigation. Brain Res Bull 86, 395-402.

Yu, X., Chen, C., Pu, S., Wu, C., Li, Y., Jiang, T., Zhou, X., 2011. Dissociation of subtraction and multiplication in the right parietal cortex: evidence from intraoperative cortical electrostimulation. Neuropsychologia 49, 2889-2895.

Zhang, J., Wang, J., Wu, Q., Kuang, W., Huang, X., He, Y., Gong, Q., 2011. Disrupted brain connectivity networks in drug-naive, first-episode major depressive disorder. Biol Psychiatry 70, 334-342.

Zhao, Y.J., Du, M.Y., Huang, X.Q., Lui, S., Chen, Z.Q., Liu, J., Luo, Y., Wang, X.L., Kemp, G.J., Gong, Q.Y., 2014. Brain grey matter abnormalities in medication-free patients with major depressive disorder: a meta-analysis. Psychol Med 44, 2927-2937.

Zhong, N., Liu, J., Yao, Y., 2002. In search of the wisdom web. Computer 35, 27-31.

Zhong, N., International WIC Institute., Web Intelligence Consortium., 2007a. Web intelligence meets brain informatics : first WICI international workshop, WImBI 2006, Beijing, China, December 15-16, 2006 : revised selected and invited papers. Springer, Berlin.

Zhong, N., Liu, J., Yao, Y., 2007b. Envisioning intelligent information technologies through the prism of web intelligence. Commun. ACM 50, 89-94.

Zhong, N., Liu, J., Yao, Y., Wu, J., Lu, S., Qin, Y., Li, K., Wah, B., 2007c. Web Intelligence Meets Brain Informatics. In: Zhong, N., Liu, J., Yao, Y., Wu, J., Lu, S., Li, K. (Eds.), Web Intelligence Meets Brain Informatics. Springer Berlin Heidelberg, pp. 1-31.

Zhong, N., Motomura, S., 2009. Agent-Enriched Data Mining: A Case Study in Brain Informatics. Intelligent Systems, IEEE 24, 38-45.

Zhong, N., Bradshaw, J.M., Liu, J., Taylor, J.G., 2011. Brain Informatics. Intelligent Systems, IEEE 26, 16-21.

Zhong, N., J. M., B., Jiming, L., J. G., T., 2011. Brain Informatics. Intelligent Systems, IEEE 26, 16-21.

Zhong, N., Chen, J., 2012. Constructing a New-Style Conceptual Model of Brain Data for Systematic Brain Informatics. Knowledge and Data Engineering, IEEE Transactions on 24, 2127-2142.

Zhong, N., Ma, J., Huang, R., Liu, J., Yao, Y., Zhang, Y., Chen, J., 2013. Research challenges and perspectives on Wisdom Web of Things (W2T). The Journal of Supercomputing 64, 862-882.

Zhong, N., S. S., Y., Ma, J., S., S., M., J., Hu, B., Wang, G., K., O., Y., A., 2015. Brain Informatics-Based Big Data and the Wisdom Web of Things. Intelligent Systems, IEEE 30, 2-7.

Zhou, X., Chen, C., Dong, Q., Zhang, H., Zhou, R., Zhao, H., Qiao, S., Jiang, T., Guo, Y., 2006. Event-related potentials of single-digit addition, subtraction, and multiplication. Neuropsychologia 44, 2500-2507.

Zhou, X., Chen, C., Zang, Y., Dong, Q., Qiao, S., Gong, Q., 2007. Dissociated brain organization for single-digit addition and multiplication. Neuroimage 35, 871-880.

Publications

Research Interests

Brain Informatics, Web Intelligence, Cognitive Psychology, Neuroimaging, Neuropsychiatry, Clinical Psychology

The Title of the Ph.D. Thesis

A Brain Informatics-Based Study on Human Cognition, Emotion, and Their Relationship

Publications in the Ph.D. Program

Scientific International Journals

Ning Zhong[*], **Yang Yang**[*], Kazuyuki Imamura, Shengfu Lu, Mi Li, Haiyan Zhou, Gang Wang, and Kuncheng Li, Self-regulation of Aversive Emotion: A Dynamic Causal Model, Advances in Computational Psychophysiology, Science Supplement, 350 (6256, Supple):25-27, 2015 ([*]Contributed equally to this work).

Yang Yang, Ning Zhong, Kazuyuki Imamura, Shengfu Lu, Mi Li, Haiyan Zhou, Huaizhou Li, Xiaojing Yang, Zhijiang Wan, Gang Wang, Bin Hu, and Kuncheng Li, Task and Resting-State fMRI Reveal Altered Salience Responses to Positive Stimuli in Patients with Major Depressive Disorder, PloS One (Accepted).

Yang Yang, Ning Zhong, Karl Friston, Kazuyuki Imamura, Shengfu Lu, Mi Li, Haiyan Zhou, Bin Hu, and Kuncheng Li, The Functional Architectures of Addition and Subtraction: Network Discovery Using fMRI and DCM, Human Brain Mapping (Revision for 2nd round review).

Proceedings of International Conferences

Yang Yang, Changqing Hu, Kazuyuki Imamura, Xiaojing Yang, Huaizhou Li, Gang Wang, Lei Feng, Bin Hu, Shengfu Lu, and Ning Zhong, Morphologic and Functional Connectivity Alterations in Patients with Major Depressive Disorder, Springer LNAI 9250, 33-42, 2015.

Yang Yang, Emi Tosaka, Xiaojing Yang, Kazuyuki Imamura, Xiuya Lei, Gang Wang, Bin Hu, Shengfu Lu, and Ning Zhong, Shift of Brain-State during Recovery from Discomfort Induced by Aversive Pictures, Springer LNAI 8609, 45-56, 2014.

Yang Yang, Ning Zhong, Kazuyuki Imamura, Xiuya Lei, Common and Dissociable Neural Substrates for 2-Digit Simple Addition and Subtraction, Springer LNAI 8211, 92-102, 2013.

Conference Presentations

Yang Yang, Changqing Hu, et al., Morphologic and Functional Connectivity Alterations in Patients with Major Depressive Disorder. The 2015 International Conference on Brain Informatics & Health (BIH' 15), London, UK, 2015.

Yang Yang, Emi Tosaka, et al., Shift of Brain-State during Recovery from Discomfort Induced by Aversive Pictures. The 2014 International Conference on Brain Informatics & Health (BIH' 14), Warsaw, Poland, 2014.

Yang Yang, Ning Zhong, et al., Common and Dissociable Neural Substrates for 2-Digit Simple Addition and Subtraction. The 2013 International Conference on Brain & Health Informatics (BHI' 13), Maebashi, Japan, 2013.

Yang Yang, Ning Zhong, et al., An fMRI/ DTI Study on Arithmetic Problem-Solving of Patients with Depression. The 2012 Web Intelligence Congress (WIC 2012), Macau, China, 2012.

Award

Best Paper Award in the 2014 International Conference on Brain Informatics & Health (BIH'14), Warsaw, Poland.